2018-06-01

Biomarker Analysis and Clinical Relevance of Thymidine Kinase 1 in Solid and Hematological Malignancies

Evita Giraldez Weagel
Brigham Young University

Biomarker Analysis and Clinical Significance of Thymidine Kinase 1 in Solid and Hematological Malignancies

Evita Giraldez Weagel

A dissertation submitted to the faculty of
Brigham Young University
in partial fulfillment of the requirements for the degree of

Doctor of Philosophy

Kim L. O'Neill, Chair
Julianne H. Grose
K. Scott Weber
Richard A. Robison
Juan Arroyo

Department of Microbiology and Molecular Biology

Brigham Young University

ABSTRACT

Biomarker Analysis and Clinical Significance of Thymidine Kinase 1 in Solid and Hematological Malignancies

Evita Giraldez Weagel
Department of Microbiology and Molecular Biology, BYU
Doctor of Philosophy

Despite the global effort to discover and improve ways to detect, treat, and monitor cancer, it still remains the second leading cause of death in the United States and poses a major health and economic burden worldwide. While traditional treatments like surgery, chemotherapy, radiation therapy, and hormone therapy have been successful and have decreased cancer mortality, cancer incidence in all sites continues to rise. Consequently, there is an immediate need to find new therapeutics for the treatment of cancer. In recent years, and with the continuing push towards personalized medicine, cancer biomarkers have become crucial to detect, treat, and monitor cancer. Thymidine kinase 1 (TK1) has been identified as a cancer biomarker with diagnostic, prognostic, and therapeutic potential. TK1 is a nucleotide salvage pathway enzyme responsible for maintaining a balance in the cell nucleotide pool and providing the cell with thymidine monophosphate, which upon further phosphorylation is incorporated into DNA during cell replication. TK1 has been found to be upregulated in the serum of cancer patients. Serum TK1 (sTK1) has been used as an early diagnostic and prognostic biomarker in many types of cancer and has been shown to be a better proliferation biomarker than Ki67.

In this dissertation, we described the characterization of TK1 as a cancer biomarker that associates with the plasma membrane of hematological malignancies such as Burkitt's lymphoma, acute lymphoblastic leukemia, acute promyelocytic leukemia, acute T cell lymphoma, and solid malignancies such as lung, breast, and colon cancer. We also describe the different oligomeric TK1 forms that are found on the cell membrane and show that membrane TK1 has activity. We assess the clinical relevance of TK1 in all these malignancies, looking at tissue expression as well as gene expression from patients from The Cancer Genome Atlas database. We find that TK1 is not expressed on the surface of normal cells, whether they are proliferating or not, making TK1 a unique cancer biomarker, with the potential to be used in targeted therapy. We also find that TK1 expressed on the surface may be involved in the invasion potential of cancer cells. The knowledge gained from this study will help researchers working in clinical research and cancer immunotherapeutics to potentially use TK1 as a biomarker and cancer target, and thus providing another weapon against cancer.

Keywords: thymidine kinase 1, TK1, cancer biomarker

ACKNOWLEDGMENTS

I would like to express my gratitude to God for all the guidance I have received during all my formal education, especially during graduate school. He has blessed me and my family in many ways and in every step of this experience.

I would like to thank my mentor and friend Kim O'Neill. His words of encouragement, his advice, his jokes, his pranks, and his constant support have made this experience an incredible one. I will forever be grateful to him for taking me into his lab as an undergraduate and for encouraging me to pursue my research goals and for believing in my potential to obtain a PhD. I am grateful to him for providing me with all the necessary tools to develop critical thinking and intellectual freedom. This achievement would not have been possible without his tremendous support.

I also would like to thank the other members of my committee Julianne Grose, Scott Weber, Richard Robison, and Juan Arroyo for their excellent advice, insights, and suggestions, which have been invaluable in my academic experience. They have been rigorous and supporting, and always rooting for my success. I appreciate the time they have taken to make themselves available for research and personal advice.

This work could not have been possible without the help of many students in the O'Neill lab. I would like to thank Madison Ramsden for her friendship and support, and for always encouraging me to become a better scientist. I would like to thank Wei Meng for always being by my side at the bench, learning and helping, and going above and beyond his research duties. I would also like to thank Melissa Alegre, Michelle Townsend, Edwin Velazquez for their friendship and for the many intellectual and non-intellectual conversations. I would like to thank Pin Guo Liu, Nick Anderson, Joshua Davies, Rachel Brog, Roman Kovtun, Rachel Morris,

Weston Burrup, Humberto Giraldez, Joshua Keller, and Brie Kingery for all their help at the bench. It has been a pleasure to train and work alongside with all of them.

I would also like to thank my parents José Miguel and Martha Giraldez for always encouraging me to pursue higher education and for sacrificing so much so that I could move to the United States and pursue an education in my field of interest. I will forever be grateful to them for never limiting my thinking and always showing me ways to develop my talents and interests. I would like to thank my brothers José Miguel "Jota" Giraldez and Humberto Giraldez for their support in and out of the lab, and for finding ways to serve me and my family throughout graduate school. I would like to thank my in-laws for their support, encouragement, and words of wisdom. I would like to specifically thank my mother-in-law, Deborah, for her example and support, and for even travelling with me to conferences to watch Charles while I attended meetings, and my sister-in-law, Elisabeth, for her extraordinary example of a woman of faith and letters, and for her help watching Charles and cooking for us for many months while I was in graduate school.

Finally, I would like to dedicate this work to my eternal companion, Arthur, and my son, Charles. I thank Arthur for his love, constant encouragement and motivation, for always supporting my crazy research goals, for putting up with my long hours and weekends in the lab, and for watching Charles day and night on top of working full time so that I can do what I love. I thank Charles for his sweet personality and love, and for his patience as I have sacrificed time with him to show him that hard work and education are important.

TABLE OF CONTENTS

TITLE PAGE i

ABSTRACT ii

ACKNOWLEDGMENTS iii

TABLE OF CONTENTS v

LIST OF TABLES xiii

LIST OF FIGURES xiv

ABBREVIATIONS xvii

CHAPTER 1: The Biology of Thymidine Kinase 1 1

Introduction 1

Summary of research chapters 4

Summary of appendices 6

CHAPTER 2: Biomarker Analysis and Clinical Relevance of Thymidine Kinase 1 on the Cell Membrane of Burkitt's Lymphoma and Acute Lymphoblastic Leukemia 8

Abstract 8

Introduction 8

Materials and Methods 11

Tissue collection, cell lines, and ALL samples 11

Mononuclear cell separation 11

B cell magnetic sorting 11

B cell proliferation 12

Antibodies 12

Flow cytometry 13

Fluorescent microscopy 13

Scanning electron microscopy 14

Plasma membrane and cytoplasmic protein isolation and Western blotting 15

Membrane separation and TK1 activity radioisotype assay 17

Statistical analysis 18

Results 18

Flow cytometry shows a significant fluorescent shift in Raji, HL60, and Jurkat cells bound to anti-TK1 antibodies suggesting TK1 is localized on the plasma membrane of these cells 18

Fluorescent microscopy suggests TK1 is associated with the plasma membrane 22

TK1 is absent on the plasma membrane of normal lymphocytes 23

Scanning Electron Microscopy (SEM) shows further confirmation of TK1 localization on the surface of cancer cells 25

ALL clinical samples also express TK1 on their plasma membrane 28

TK1 on the membrane is found in different oligomeric 29

TK1 on the membrane shows activity 30

Discussion 31

Conclusion 32

Acknowledgments 32

CHAPTER 3: Membrane Expression of Thymidine Kinase 1 and Potential Clinical Relevance in Lung, Breast, and Colorectal Malignancies 33
Abstract 33
Introduction 34
Materials and Methods 35
Cell lines and cell culture conditions 35
Antibodies 36
Flow cytometry 36
Confocal microscopy 37
Cell surface protein isolation and Western blotting 37
Tissue dissociation and analysis 39
TK1 gene expression bioinformatics analysis 40
Immunohistochemistry 40
Statistical analysis 42
Results 42
TK1 expression is elevated on the surface of NCI-H460, A549, MCF7, MDA-MB-231, SW620, and HT-29 cells 42
TK1 is strongly associated with the membrane of NCI-H460, MDA-MB-231, and HT-29 cells 45
Membrane TK1 expression is significantly lower in normal colon than malignant colon clinical samples 48

TK1 levels are significantly higher in malignant vs. normal healthy tissue 50

TK1 gene expression levels are upregulated in malignant lung adenocarcinoma, lung squamous carcinoma, breast invasive carcinoma, and colorectal adenocarcinoma 55

Triple negative breast cancer patients show higher levels of TK1 than HER2+ cancer patients 56

TK1 expression levels in triple negative breast cancer show positive correlation with stem cell and EMT markers 58

Discussion 60

Declarations 62

Ethics approval and consent to participate 62

Funding 62

Acknowledgments 62

CHAPTER 4: TK1 Membrane Expression May Play a Role in the Invasion Potential of A549 Lung Cancer Cells 63

Abstract 63

Introduction 64

Materials and methods 65

Cell line and cell culture 65

siRNA library 65

Transfection 65

Flow cytometry 66

Invasion Assay 67
Statistical analysis 67
Results 67
Flow cytometry 67
Invasion study 69
Discussion 70
CHAPTER 5: Macrophage Polarization and its Role in Cancer 72
Abstract 72
Introduction 72
M1 Phenotype 74
M2 Phenotype 76
Macrophage polarization 77
Tumor Associated Macrophages (TAMs) 78
Metabolism and activation pathways 80
Conclusion 88
APPENDIX 1: How Does the Tumor Microenvironment Affect Macrophage Aggressiveness? 90
Abstract 90
Materials and Methods 91
Cell lines and culture 91
Preparation of Macrophages 92

Engulfment Assay 92
Flow Cytometry Analysis 93
Gene expression analysis 94
Results 95
U937-derived macrophage engulfment is decreased when they are exposed to cancer cell spent media and cancer cells 95
Total macrophage engulfment was reduced when we exposed U937-derived macrophages to HT-29 spent media and cells, to MCF7 and MDA-MB-231 spent media and cells, Raji spent media and cells, PC3 cells, and normal lymphocyte spent media (Figure A1-3). 95
3+ Bead engulfment population decreases when U937-derived are exposed to cancer cell spent media and cancer cells 95
U937-derived macrophages gene expression profile mimics M2 macrophages 99
Conclusion 99
APPENDIX 2: Prostate Cancer Microenvironment Modulates Macrophage Phagocytosis 101
Abstract 101
Materials and Methods 102
Results 103
Flow cytometry analysis of the engulfment assay 103
Macrophage engulfment decreases when exposed to either DU145 or PC3 cells but not when exposed to spent media 103

Macrophage engulfment decreases after 5 hours of treatment with prostate cancer-derived exosomes 104

Aggressive engulfment (3+Bead population) significantly decreases after 4-6 hour treatment with prostate cancer-derived exosomes 105

Gene expression shows an upregulation of IL-10 and a decrease of IL-12 in macrophages exposed to DU145-derived exosomes 106

Conclusions 107

APPENDIX 3: Oxidants and Antioxidants: A Question of Balance 109

Abstract 109

Introduction 110

Materials and Methods 115

Chemicals 115

Materials 116

Equipment 116

Lymphocyte separation 116

Sample preparation 117

Simulation of Oxidative Stress assay 117

ORAC assay 118

Standard curve data 118

Cytotoxicity 118

Results 119

Conclusion 127

APPENDIX 4: Yeast Two-Hybrid Reveals Novel Proteins Interacting with TK1 131

Yeast two-hybrid assay 131

Vectors 132

TK1 Sequence 133

Primers 134

Results and analysis 134

Dependency assays 134

Novel proteins interacting with TK1 135

REFERENCES 136

LIST OF TABLES

Table 3- 1. TK1 staining in normal and malignant tissue. 50

Table 4- 1. Summary of Spearman's correlation coefficients between TK1 and cell stemness or EMT markers in HER2+ and TNBC patients. 71

Table 5- 1. Cancer immunotherapy approaches using macrophages 87

Table A3- 1. Antioxidant activity in normal lymphocytes after incubation with L-ascorbic acid (vitamin C), α-tocopherol (vitamin E), glutathione, lipoic acid, resveratrol, or PBS and after oxidative treatment and followed by incubation with the mentioned antioxidants 120

Table A3- 2. Antioxidant activity measured in Raji cells after incubation with L-ascorbic acid (vitamin C), α-tocopherol (vitamin E), glutathione, lipoic acid, resveratrol, or PBS. Values are shown in Trolox Equivalents per liter per $1x10^6$ cells (TE/L per $1x10^6$ cells). 121

LIST OF FIGURES

Figure 1- 1. Structure of human thymidine kinase 1. 2

Figure 1- 2. TK1 protein-protein interaction network predicted by STRING. 3

Figure 2- 1. Flow cytometry quantification analysis of normal lymphocytes. 20

Figure 2- 2. Flow cytometry analysis of HL60 and Jurkat cells. 21

Figure 2- 3. Fluorescent microscopy images of viable Raji, Jurkat, HL-60, and normal lymphocytes cells stained with CB1-FITC (anti-TK1 antibody), isotype control, anti-Na+K+ ATPase antibody, and DAPI at 20X. 22

Figure 2- 4. Flow cytometry quantification analysis of normal lymphocytes. 24

Figure 2- 5. Scanning Electron Microscopy of Raji cells. 26

Figure 2- 6. Scanning Electron Microscopy of normal lymphocytes. 27

Figure 2- 7. Flow cytometry analysis of ALL clinical samples. 28

Figure 2- 8. Western blot of membrane and cytosolic fractions in Raji cells and normal lymphocytes and blotted with anti-TK1 antibody. 29

Figure 2- 9. TK1 activity in membrane fractions. 30

Figure 3- 1. Flow cytometry analysis of TK1 expression on the cell membrane of colon, breast, and lung cancer cell lines. 44

Figure 3- 2. TK1 co-localizes with the plasma membrane of lung, breast, and colon cancer cell lines. 46

Figure 3- 3. Western blot of membrane proteins isolated from HT-29 cells probed with anti-TK1 antibody ab91651. 47

Figure 3- 4. Flow cytometry evaluation of TK1 expression on the surface of colorectal patient tissue. 49

Figure 3- 5. Immunohistochemistry analysis of lung cancer tissue. 52
Figure 3- 6. Immunohistochemistry analysis of TK1 expression in breast cancer tissue. 53
Figure 3- 7. Immunohistochemistry analysis of TK1 expression in colon cancer tissue. 54
Figure 3- 8. Histograms of RNA-Sequencing data from The Cancer Genome Atlas showing increased TK1 gene expression in lung, breast, and colorectal cancer patients when compared to normal patients. 56
Figure 4- 1. Membrane expression of TK1 at 60 hours post siRNA transfection by flow cytometry. 68
Figure 4- 2. Invasion assay with A549 cells transfected with TK1 siRNA. 69
Figure 5- 1. Macrophage polarization is a spectrum. 83
Figure A1- 1. Diagram of the macrophage engulfment assay. 93
Figure A1- 2. Flow cytometry analysis of the engulfment assay. 94
Figure A1- 3. Quantification of U937-derived macrophage engulfment after treatment with conditioned media or cells. 96
Figure A1- 4. Quantification of bead population engulfment among treatments. 98
Figure A1- 5. Gene expression profile of U937-derived macrophages after exposure conditioned media or cell treatment. 100
Figure A2- 1. Flow cytometry analysis of the engulfment assay. 103
Figure A2- 2. Engulfment quantification of macrophages exposed to either PC3 or DU145 spent media or cells. 104
Figure A2- 3. Macrophages exposed to PC3 or DU145-derived exosomes over a period of time. 105

Figure A2- 4. The population of aggressive macrophages (3+Beads) exposed to PC3 or DU145-derived exosomes over a period of time. 106

Figure A2- 5. qPCR gene expression analysis of macrophages exposed to DU145-derived exosomes at 2 and 4 hours showing an increase of IL-10 and IL-12 at 4 hours. 107

Figure A3- 1. Differences in cellular antioxidant activity in Raji cells followed antioxidant incubation and oxidative treatment + antioxidant incubation. 123

Figure A3- 2. Differences in cellular antioxidant activity in Raji cells followed antioxidant incubation and oxidative treatment + antioxidant incubation. 125

Figure A4- 1. Diagram of the Matchmaker Gold Yeast Two-Hybrid system. 131

Figure A4- 2. Vector information from the Normalized Yeast Two-Hybrid cDNA Library from Clonetech. 132

ABBREVIATIONS

ALL- Acute lymphoblastic leukemia

BSA- Bovine serum albumin

BL- Burkitt’s lymphoma

DPBS- Dulbecco's phosphate-buffered saline

FBS- Fetal bovine serum

LSM- Lymphocyte Separation Medium

SEM- Scanning electron microscopy

STR- short tandem repeat

TK1- thymidine kinase 1

CHAPTER 1: The Biology of Thymidine Kinase 1

Introduction

Cancer is a group of complex diseases that are characterized by unregulated cell proliferation and cell death, tumor-promoting inflammation, genome instability and mutations, induction of angiogenesis, evasion of the immune system, dysregulation of metabolic pathways, immortal cell replication, and activation of metastasis and invasion.[1] Despite efforts to improve prevention methods, early detection, and treatments, cancer continues to be the second leading cause of death in the United States and a major economic burden to both developed and underdeveloped countries, indicating a critical need to identify clinically relevant cancer-specific biomarkers.[2] Thymidine kinase 1 (TK1) has been identified as a cancer biomarker that has diagnostic, prognostic, and therapeutic potential.[3,4]

Cells undergoing normal proliferation must maintain a balanced supply of deoxyribonucleotides to avoid replication stress, a common source of genome instability.[5] Mammalian cells synthesize deoxyribonucleotide triphosphates (NTPs) either *de novo* or through the nucleoside salvage pathway. TK1 belongs to the deoxyribonucleoside kinase family, a group of four enzymes that catalyze the first phosphorylation step of deoxyribonucleosides in the salvage pathway.[6] TK1's main function is to phosphorylate deoxythymidine to deoxythymidine monophosphate (dTMP) using ATP as the phosphate source.[3,7] Further phosphorylation of dTMP yields deoxythymidine triphosphate (dTTP), which is then incorporated into DNA. While most deooxyribunucleoside kinases are dimers, TK1 is unique because its most active form is a tetramer (Figure 1-1).[6]

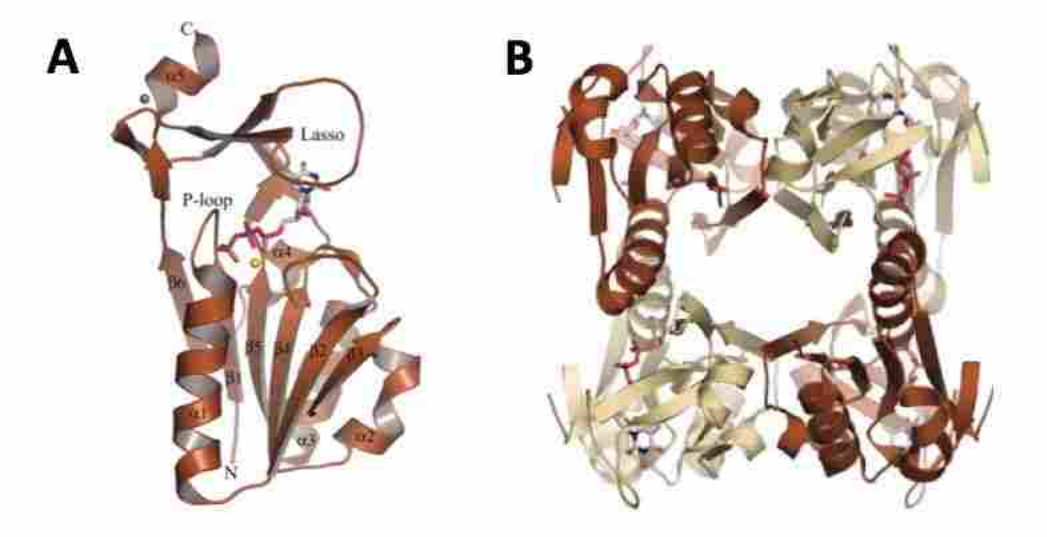

Figure 1- 1. Structure of human thymidine kinase 1.

A) Monomer subunit structure of human TK1 with dTTP colored according to atom type. Mg2+ is shown in yellow, and Zn2+ is shown in gray. B) Tetrameric structure of human TK1. Adapted from Welin M, Kosinska U, Mikkelsen N-E, et al. Structures of thymidine kinase 1 of human and mycoplasmic origin. Proc Natl Acad Sci U S A. 2004;101(52):17970-17975. doi:10.1073/pnas.0406332102.

There are two major enzymes responsible for maintaining the cellular nucleotide pool, TK1 and dCK. TK1 is the only one whose expression is tightly regulated by the cell cycle.[7] TK1's levels are low or undetectable during G1 phase, rising during late G1 phages, peaking during S phase, and again decreasing during the G2 phase.[8] The increased levels of TK1 during the S phase are due to a 3-fold increase in TK1 mRNA transcription and 12-fold increase in translation efficiency of that mRNA.[8] During the G2 phase, TK1 levels decrease as a result of a C-terminal dependent degradation of the enzyme through the APC/C-Cdh-1 pathway.[9] The other salvage pathway enzyme responsible for maintaining the cellular nucleotide pool is deoxycytidine kinase (dCK), which phosphorylates deocycytidine, deoxyadenoside and deoxyguanosine.[10] TK1 interacts with dCK, helping counteract dCK inactivation, which results

in restoring dCTP, dATP, and dGTP levels. The interaction between dCK and TK1 demonstrates the complex and redundant functions of TK1 (Figure 1-2).[5]

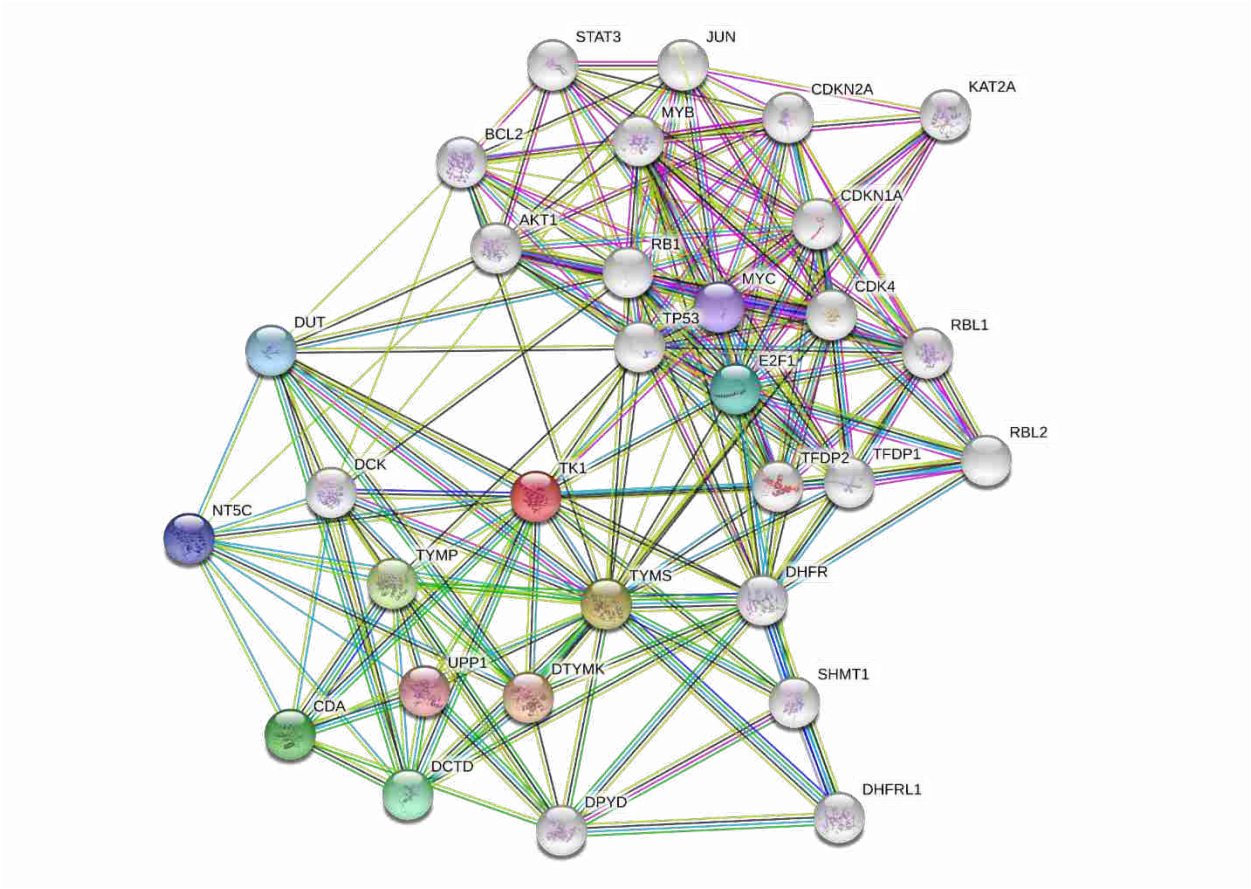

Figure 1- 2**.** TK1 protein-protein interaction network predicted by STRING.
Colored lines represented different interactions: black (co-expression), pink (experimental), green (text mining), blue (homology).

Studies have also shown that TK1 is involved in DNA repair. Chen et al. (2010) showed that $p53^{-/-}$ tumor cells upregulate TK1 as a response to DNA damage.[7] Other groups have shown that p53 is essential for TK1 controlled expression and upon loss of p53, TK1 levels increase.[11–13] This increase of TK1 seems to be essential for tumor cells seeking DNA repair. McKenna et al. showed that increased TK1 levels and increased dTTP levels are necessary for DNA repair in

tumor cells following treatment with radiation.[14] Thus, TK1 functions as a mechanism of resistance for the survival of cancer cells.[3]

TK1 has been widely studied as a cancer serum biomarker. TK1 has been found upregulated in the serum and in tissues of cancer patients. Serum TK1 (sTK1) can be used as early detection and diagnostic biomarker because the presence of TK1 in serum results from tumor cell death and correlates with tumor size.[15–17] Higher serum TK1 concentration levels correlate with a more advance stage and grade in many cancer types.[14,18–20] Moreover, sTK1 levels show prognostic potential and can help predict relapse after primary diagnosis in both solid and hematological malignancies.[21–25]

Summary of research chapters

Chapter 2 outlines our efforts to characterize TK1 as a cancer biomarker and its clinical relevance in multiple hematological malignancies including Burkitt's lymphoma (Raji), acute promyelocytic leukemia (HL60), and acute T cell leukemia (Jurkat) cell lines, and acute lymphoblastic lymphoma (ALL) clinical samples. We show that TK1 localizes on the cell membrane of malignant cells and is absent on the membrane of normal resting and normal proliferating lymphocytes, suggesting that TK1's membrane localization is independent from proliferation. These findings were confirmed through flow cytometry, confocal microscopy, and scanning electron microscopy. We also show that membrane TK1 is found in monomeric and dimeric forms. Moreover, we show that TK1 isolated from the membrane has enzymatic activity, suggesting a function for TK1 on the membrane.

In Chapter 3, we characterize TK1's potential as a tumor biomarker and immunotherapeutic target and clinical relevance in the major cancer killers: lung, breast, and colorectal cancers. We showed that TK1 localizes on the membrane of lung (NCI-H460, A549),

breast (MDA-MB-231, MCF7), and colorectal (HT-29, SW620) cancer cell lines. We also compared TK1 expression levels in normal and malignant tissue through flow cytometry and immunohistochemistry, showing that TK1 is upregulated exclusively in malignant cells, independently of proliferation. We also analyzed *in-silico* RNA-Seq patient data from The Cancer Genome Atlas (TCGA), where we show differential expression of the TK1 gene in lung, breast, and colorectal cancer patients. We also show that TK1 is expressed in both HER2+ and triple negative breast cancer, suggesting that TK1 is a membrane biomarker in hormone-independent breast cancer. We also show that as breast cancer progresses, TK1 levels positively correlate with epithelial-mesenchymal transition (EMT). This suggests that TK1 may have a role in invasion and metastasis in breast cancer. These results suggest TK1's relevance as a potential immunotherapeutic target.

In Chapter 4, we explore the role of TK1 on the membrane. Using siRNA, we silenced TK1 expression on the membrane of A549 cells, a lung cancer cell line known to express TK1 on its membrane. We show that TK1 membrane expression is significantly downregulated after 60 hours post-transfection. Using a Matrigel-based quantitative invasion assay, we measured cell invasion potential in cells either expressing or lacking TK1 on their membrane. We found that cells that lack TK1 on their membrane exhibit a significantly decreased invasion potential compared to cells expressing TK1. These results suggest that TK1's presence on the membrane may play a role in invasion and cell migration in cancer.

Chapter 5 is a review paper where we describe macrophage polarization and its role in cancer. We define macrophage polarizations M1 and M2 and their subsets, their functions and gene expression, and what molecules induce polarization to their respective subsets, as well as their activation pathways and metabolism. We also describe tumor associated macrophages

(TAMs) and their role in the cancer microenvironment and potential approaches to cancer immunotherapy using macrophages.

Summary of appendices

Appendix 1 contains data that accompanies a published abstract in Cancer Research entitled "How does the tumor microenvironment affect macrophage aggressiveness?" In this study, we show that U937-derived macrophages decrease their phagocytic capacity when exposed to cells and conditioned media from breast, lung, colon, and Burkitt's lymphoma cell lines. We also observed that these U937-derived macrophages show an M2-like gene expression profile, upregulating IL-10 and downregulating IL-12.

Appendix 2 contains data that accompanies a published abstract in Cancer Research entitled "Prostate cancer exosomes and their effects on macrophage engulfment and polarization." In this study, we researched the effects of prostate cancer-derived exosomes on macrophage engulfment and polarization. We found that phagocytosis was affected around 5 hours post-exposure to exosomes. Macrophage gene expression macrophages exposed to exosomes change around 4 hours, where we see an upregulation of IL-10 and downregulation of IL-12, mimicking a M2 macrophage polarization.

Appendix 3 contains unpublished data from a study done on the role of antioxidants in cell response against oxidative stress and reactive oxidative species (ROS). The abstract from this study was published in Cancer Research as "Differences in cellular antioxidant activity in Burkitt's lymphoma and normal human lymphocytes." We explored the cellular antioxidant capacity in normal lymphocytes and Raji cells before and after exposure to a radical oxygen initiator followed by exposure to L-Ascorbic, resveratrol, α-Tocopherol, glutathione, and α-Lipoic acid for 10, 20, 45, and 60 minutes. Our study shows that cancer cells cannot maintain

balance after oxidative stress, as we see that they increase and keep increasing antioxidant capacity over time. Normal cells stop increasing their antioxidant capacity when they sense that the oxidative stress has been reduced. Our study also shows that the differences we see between Raji cells and normal lymphocytes with this oxidative treatment may suggest that cancer cells can increase their antioxidant capacity when they are exposed to oxidative stress, a mechanism that may be employed to protect themselves from the damaging effects of chemotherapy drugs.

Appendix 4 contains data from a yeast-2-hybrid assay where we evaluate protein-protein interactions using a human cDNA library in a prey plasmid and the TK1 gene in a bait plasmid. We report 4 novel proteins that interact with TK1.

CHAPTER 2: Biomarker Analysis and Clinical Relevance of Thymidine Kinase 1 on the Cell Membrane of Burkitt's Lymphoma and Acute Lymphoblastic Leukemia

The following chapter is taken from an article published in OncoTargets and Therapy Journal. All content and figures have been formatted for this dissertation but it is otherwise unchanged.

Abstract

Thymidine kinase 1 (TK1) is an enzyme involved in DNA synthesis and repair. TK1 is elevated in cancer patients' serum, making it a useful tumor proliferation biomarker that strongly correlates with cancer stage, metastatic capabilities, and recurrence risk. In this study, we show TK1 is upregulated and localizes on the plasma membrane of Burkitt's lymphoma, acute lymphoblastic leukemia (ALL), and other hematological malignancies. Using flow cytometry, we confirmed that TK1 localizes on the surface of Raji, HL60, Jurkat cell lines, and on ALL clinical samples. Using fluorescent microscopy, we found a strong association of TK1 with the plasma membrane in Raji, HL60, and Jurkat cell lines. These findings were also confirmed by electron microscopy. Also, our study demonstrates this phenomenon does not occur on normal resting or proliferating lymphocytes. Interestingly, membrane TK1 is found in all oligomeric forms ranging from monomer to tetramer and exhibit enzymatic activity. These findings suggest TK1as a possible target for immunotherapy with the potential to be utilized in the treatment of hematological cancers.

Introduction

Thymidine kinase 1 (TK1) is a nucleotide salvage pathway enzyme primarily responsible for phosphorylating deoxythymidine to deoxythymidine monophosphate.[7] Under normal

conditions, TK1 is tightly regulated by the cell cycle. Usually, TK1 levels are low in G1, peak in S phase, and low during late G2/M phase.[8] The low levels of TK1 during the late G2/M phase occur because degradation, which is thought to be regulated by polyubiquitination that targets degradation via the APC/C pathway.[3] The rapid increase in TK1 levels during S phase is thought to be partly mediated by a TK1 regulatory switch, which happens when TK1 switches from a dimer (inactive enzyme) to a tetramer (active enzyme).[3,26,27]

In cancer events and upon loss of p53 regulation, TK1's cell cycle regulation is lost and TK1 levels are upregulated.[12] TK1 has been found upregulated in tissue and serum in both solid tumors and hematological malignances, which is why TK1 has been extensively studied as a cancer proliferation biomarker.[15,17] The diagnostic and prognostic potential of TK1 has been demonstrated using the traditional TK activity radioassay for hematological malignancies and solid tumors.[26,28] Moreover, TK1 levels in serum have been shown to have diagnostic potential in other cancers such as bladder, cervical carcinoma, gastric, non-small cell lung, renal and colorectal cancers.[14,18,21,22,24,28–30] Early events in carcinogenesis show an upregulation of TK1 in the serum as well so TK1 has also been studied as a prognostic marker in many cancer types.[15,17,20,31] In summary, high TK1 serum levels correlate with tumor aggressiveness and can be indicative of early events in carcinogenesis.[15,28]

Burkitt's lymphoma (BL) and acute lymphoblastic leukemia (ALL) are some of the most highly proliferative hematological malignancies and primarily affect children, with a small incidence in adults too.[32,33] BL is an aggressive non-Hodgkin lymphoma that affects B cells. BL is the most common type of pediatric cancer in malaria-endemic regions, such as equatorial Africa, Brazil, and Papua New Guinea, affecting over 40 million children every year.[34] While the current available multi-agent chemotherapy treatment (cyclophosphamide, vincristine,

prednisolone, and doxorubicin) has a 5-year event-free survival rate of over 90% in high-income countries, the survival rate is much lower in low-income countries (50% for 1-year event-free survival rate).[35,36] ALL is the most common hematological malignancy diagnosed in children in the United States with over 6000 cases every year.[37,38] The highest peak of incidence occurs between the ages of 3-9 years and it is the number one cause of death from cancer in people under 20 years old.[37,38] One of the major complications with ALL in children is the infiltration of leukemic cells in the central nervous system (CNS), which usually occurs in relapse. In the past few decades, there has been major improvements in ALL treatments including an intensive 8-week chemotherapy regimen that has increased ALL 5 year-remission rates to up to 85% and overall survival rates from 10% to 90%.[39] These new treatments include a combination chemotherapy regimen during the 6-8 months after remission designed to prevent relapse and CNS leukemic infiltration. Unfortunately, 15-20% of children with ALL will relapse and their survival rates drop to 20-30%.[37] More research is needed to understand the unique characteristics of BL and ALL and to find new targets that could help increase survival.

Due to the proliferative nature of BL and ALL, we hypothesized that TK1 was highly expressed in BL and ALL cells. While researching this hypothesis, we found TK1 to be overexpressed on the membrane of BL, acute promyelocytic leukemia, acute T cell leukemia, and ALL clinical samples. Of note, TK1 is not readily detectable on the membrane of normal resting or proliferating lymphocytes, and thus TK1 membrane localization appears to be an event exclusive in malignant cells. Moreover, membrane TK1 is found in all oligomeric forms and exhibits enzymatic activity. These findings suggest TK1 is a tumor specific antigen on the cell surface and therefore a potential immunotherapy target for BL and ALL.

Materials and Methods

Tissue collection, cell lines, and ALL samples

Raji (Burkitt's lymphoma), HL60 (acute promyelocytic leukemia), and Jurkat (acute T cell leukemia) cell lines were purchased from ATCC (Manassas, VA). All cell lines were authenticated by short tandem repeat (STR) analysis at the University of Arizona Genetics Core Facility prior to our study. All cells were grown in RPMI 1640 supplemented with 10% FBS and 2mM L-glutamine and incubated at 37°C with 5% CO_2. ALL samples were obtained from patients at diagnosis or relapse after informed consent on a biobank protocol at the Huntsman Cancer Institute (Salt Lake City, UT) and frozen with DMSO and albumin in aliquots. ALL samples were thawed at 37ºC and washed with Dulbecco's phosphate-buffered saline (DPBS) immediately before use.

Mononuclear cell separation

Whole blood was collected from healthy young volunteers ages 18-30 under IRB approval from the Office of Research and Creative Activities at Brigham Young University (BYU X090281). All healthy blood volunteers provided informed consent. Blood was diluted 1:1 with DPBS layered on top of Lymphocyte Separation Medium (LSM) (Cellgro, Corning Life Sciences, VWR International, Radnor, PA) and centrifuged at 400 x g for 30 mins without brake or acceleration. The mononuclear cell layer was aspirated and rinsed with DPBS. The cells were treated with red blood cell lysis buffer and resuspended in RPMI 1640 supplemented with 10% FBS and 20% human serum from the original blood donor. After a further incubation for 24 hours at 37°C with 5% CO_2, the lymphocytes were aspirated and washed with DPBS and prepared for flow cytometry and scanning electron microscopy.

B cell magnetic sorting

Lymphocytes (B and T cells) were obtained by mononuclear cell separation from whole blood with LSM. Cells were then washed with MACS buffer and stained with anti-CD19 antibody conjugated to biotin. We incubated these cells with streptavidin-gold magnetic MACS beads (Miltenyi Biotech) and $CD19^+$ cells were sorted via magnetic selection. Cells were resuspended in MACS buffer and then washed and resuspended in DPBS for downstream application.

B cell proliferation

B cells obtained through magnetic selection were seeded at $2x10^5$ cells/mL in a 6 well plate in RPMI 1640 supplemented with 10% FBS. We used the CellXVivo Human B Cell Expansion Kit (R&D Systems) to induce proliferation. We counted the B cells and incubated them following the kit's instructions for 5 days. After 5 days, we observed the cells under a microscope to assess proliferation and counted them again to quantify division. Cells were washed and resuspended in DPBS and used in flow cytometry.

Antibodies

We used 3 custom mouse monoclonal antibodies developed in our lab against TK1 (CB1, A72, and A74) and a commercially available rabbit monoclonal antibody against TK1 (ab91651) (Abcam). CB1 binds to a region in the C-terminal domain of TK1, specifically to the active domain.[40–42] A72 and A74 are against an immunodominant region besides the TK1 C-terminal domain.[28] The three custom antibodies were conjugated to FITC using a conjugation kit (EasyLink, Abcam, ab102884) and stored in the dark at 4°C. The custom antibodies were used for most assays and the commercially available antibody (Commercial) was used for immunohistochemistry. The ALL samples were stained with CD34-APC-Cy7, HLA-DR-

AlexaFluor488, and Commercial-APC for staining of ALL samples. CD34 and HLA-DR antibodies were purchased from BioLegend (San Diego, CA).

Flow cytometry

Raji, Jurkat, HL60, normal lymphocytes, and B cells were washed 3X in DPBS. All cells were resuspended in DPBS at $5x10^5$ cells/mL and were placed in individual microcentrifuge tubes and incubated with Fc block (Human TruStain FcX, BioLegend, San Diego, CA) for 10 minutes at room temperature. Cells were then stained with CB1, A72, and A74 conjugated to FITC. Negative controls include unstained cells and cells stained with an isotype antibody. ALL samples were resuspended in Cell Staining Buffer (BioLegend, San Diego, CA), incubated with Fc Block for 10 minutes at room temperature and then stained with isotype control, CD34 (APC-Cy7), HLA-DR (AlexaFluor488) to confirm ALL phenotype and with Commercial (APC) to check for TK1 expression. For lymphocytes treated with TK1, we incubated $5x10^6$ cells per well in a 6-well plate and added DPBS or concentrations of yeast recombinant TK1 at 0.25uM, 0.5uM or 0.75uM. Cells were incubated at 37ºC and 5% CO_2 for 24 hours, then the cells were washed 3X in DPBS and incubated in Fc block for 10 minutes, after which cells were stained with anti-TK1 antibody ab91651 and then with an anti-rabbit secondary FITC antibody. Negative controls include unstained sample, (rabbit) anti-NFKB, and anti-rabbit secondary FITC antibody. We also performed dead cell discrimination using a PI solution (2mg/mL) immediately before analysis. We collected $10x10^4$ events per sample in a flow cytometer (Attune, Life Technologies) and data was analyzed using the FlowJo software (FlowJo, Inc., Ashland, OR).

Fluorescent microscopy

Raji, HL60, Jurkat, and normal lymphocytes were stained with FITC-conjugated antibodies, namely isotype control, anti-NaK antibody, or anti-TK1 antibody (CB1) for 30

minutes on ice and in the dark. Cells were washed with cold DPBS and then were resuspended at $5x10^5$ cells/mL. 20uL of cell solution were placed on a glass slide, after which a drop of mounting medium containing DAPI was added to the sample (Vectashield Antifade Mounting Medium with DAPI, Vectashield, Burlingame, CA), and a coverslip was placed on top. Cells were visualized in a light microscope (Zeiss Imager A.1 Fluorescence Microscope, Carl Zeiss, Oberkochen, Germany) using different channels to detect fluorescence. Blue represents DAPI fluorescence and green represents FITC fluorescence.

Scanning electron microscopy

Raji and normal lymphocytes were washed 3X in DPBS for 5 minutes to remove medium and cellular debris. The cells were then resuspended in flow cytometry staining buffer (eBioscience) for 15 minutes and then blocked with 1% Bovine serum albumin (BSA) in DPBS (BSA/DPBS) for 5 minutes. We then added anti-TK1 antibody (A72) conjugated to biotin at a concentration of 0.005ug/uL and incubated the cells for 15 mins on ice. After incubation with primary antibody, we washed the cells with BSA/DPBS twice. We then stained the cells with anti-biotin conjugated to 2nm gold nanoparticles (Nanoprobes, Yaphank, NY) at a concentration of 1:500 in BSA/DPBS and incubated for 30 minutes on ice. We then washed the cells with BSA/DPBS for 5 minutes and twice with DPBS to remove any block. After staining, we fixed the cells in 0.2 % glutaraldehyde for 15 minutes followed by a wash in 0.02M glycine for 10 minutes to quench the fixative. We then rinsed the cells 3X in DPBS and used a Cytocentrifuge (Cytospin, Thermo Scientific, Waltham, MA) to spread the cells onto coverslips. Cells were then rinsed 3X with ddH_2O and gold particles, if present, were enhanced for 3 minutes using the GoldEnhance™ EM Plus kit (Nanoprobes). The cells were then rinsed 3X with ddH2O and dehydrated via sequential washes of 70%, 80%, 90%, and 100% EtOH for 5 min each. After the

coverslips were dry, we imaged them using an XL-30 ESEM (Philips, Amsterdam, Netherlands). Pictures provided were taken using a GSE detector. Raw images are provided next to enhanced images showing red dots as gold. Energy Dispersive Analysis X-ray (EDAX) was performed on all samples to quantify the levels of gold present. EDAX analysis will provide a k-ratio, a Z value, an A value, and an F value. The k-ratio represents the element's peak height compared to a sample of the pure element collected under the same conditions. The Z value represents a correction in the atomic number taking backscattered election yield of the pure element and the sample. The A value represents a compensation for X-rays generated in the sample that are cannot emit energy. The F value represents a correction for the generation of X-rays. We used these EDAX output values to normalize our samples gold weight percentages using the following equation:

$$Normalized\ Weight\ Percentage = \frac{k - ratio * 100}{Z * A * F}$$

Plasma membrane and cytoplasmic protein isolation and Western blotting

To separate the plasma membrane and cytoplasmic proteins, we used the Pierce™ Cell Surface Protein Isolation Kit (Thermo Fisher Scientific, Waltham, MA, Cat # 89881). For this procedure, we used $4x10^7$ Raji cells or normal lymphocytes per test. Normal lymphocytes were isolated as described in the "Mononuclear cell separation" section. To label the cells with biotin, cells were incubated with a 40 mL of biotin solution in a T75 flask. Biotin solution was made by dissolving the contents of one vial of Sulfo-NHS-SS_Biotin (provided in the kit) in 48mL of ice-cold PBS. The flask was incubated on a rocking platform with gentle agitation for 30 mins at

4°C. After incubation, 500uL of quenching solution were added to the flask to quench the reaction. Then, cells were transferred to a conical tube and pelleted at 500 x g for 3 minutes, after which the supernatant was discarded. Cells were then washed with 5mL of TBS by pipetting up and down twice with a serological pipette and pelleted at 500 x g for 3 minutes. A cocktail of protease inhibitors was added to 500uL of lysis buffer (provided in the kit) and added to the cell pellet. The cells in lysis buffer were transferred to a microcentrifuge tube and resuspended in the fluid by pipetting up and down. The cells were then disrupted using a cell disruptor (Sonicator 3000, Misonix, Inc., Farmingdale, NY) at low power (1.5) on ice using five 1-second bursts. Cells were incubated for 30 minutes on ice, vortexed every 5 minutes for 5 seconds, and sonicated for 1 second at low power (1.5) every 10 minutes. The cell lysate was centrifuged at 10,000 x g for 2 minutes at 4°C and the clarified supernatant transferred to a new microcentrifuge tube. To isolate the biotin-labeled proteins, the clarified supernatant was added to a column that contained 500uL of NeutrAvidin Agarose that had been previously washed with 500uL of wash buffer and centrifuged for 1 minute at 1000 x g. The column was capped and incubated for 60 minutes at room temperature with end-over-end mixing using a rotator. Then, the column was centrifuged for 1 minute at 1000 x g and the flow-through kept for cytoplasmic protein analysis. The column was washed 3 times with 500uL of wash buffer containing a cocktail of protein inhibitors to remove any other cytoplasmic proteins. To elute the membrane proteins, a 50mM DTT solution was made by adding 23.7uL of 1M DTT to 450uL SDS-PAGE sample buffer. 450uL of DTT solution were added to the column and incubated for 60 minutes at room temperature with an end-over-end mixing on a rotator. The column was then centrifuged for 2 minutes at 100 x g and the flow-through collected and stored at -20°C. For Western blot analysis, samples were thawed on ice after which they were boiled for 5 minutes and then run on

a 12% acrylamide SDS gel at 90 V for 2-3 hours. The proteins on the gel were transferred onto a nitrocellulose membrane at 90 V for 50 minutes. The membrane was blocked with 5% non-fat milk in DPBS for 1 hour at 4°C in a rotating platform and then incubated in anti-TK1 commercial antibody (ab91651) in a 1:1000 dilution in milk overnight at 4°C in a rotating platform. Membrane was washed 3 times in DPBS for 3 minutes each in a rotating platform and then incubated with a IRDye 800 donkey anti-rabbit secondary antibody for 1 hour at 4°C in a rotating platform (LI-COR, Lincoln, NE). Finally, the membrane was washed 3 times with DPBS and imaged in an Odyssey CLx Imaging System (LI-COR, Lincoln, NE).

Membrane separation and TK1 activity radioisotype assay

Plasma membranes were separated using a sucrose gradient. First, Raji, Jurkat, and HL60 cell line were grown to an exponential growth phase. $17x10^7$ cells were pelleted at 210 x g for 20 minutes and the pellets were resuspended in 6mL of a buffer consisting on 20% (v/w) sucrose-Tris buffer (pH 6.8). The cell suspension was freeze-thawed in liquid nitrogen and then at 37°C 3X and centrifuged at 600 x g for 10 mins at 4°C to collect cell membranes. The supernatant was discarded and the pellet, containing the membranes, was washed with Tris buffer (pH 6.8) and then resuspended in 9mL of 20% (w/v) sucrose-Tris buffer. A two-step sucrose gradient was prepared in a Beckman open-top tube (Beckman Coulter, Brea, CA, catalog number 337922) by adding 13 mL of 70% (w/v) sucrose-Tris buffer, followed by 12 mL of 50% (w/v) sucrose-Tris buffer, followed by 9mL of 20% (w/v) sucrose-Tris buffer containing the membranes. The gradients were centrifuged at 25,000 rpm for 14 hours in a Beckman L8-60M ultracentrifuge (Beckman Coulter, Brea, CA). The plasma membranes are found at the 50-70% (w/v) sucrose-Tris buffer interface. The membranes were collected by the bottom drip method, which consists on using a hot needle to create a hole at the bottom of the tube and collect each layer separately

drop-by-drop. The 50-70% (w/v) sucrose-Tris buffer interface was diluted to below 20% (w/v) sucrose-Tris buffer using Tris buffer (pH 6.8). The diluted interface was centrifuged at 47,000 rpm for 1hr and the pellet resuspended in 1mL Tris buffer (pH 6.8). This solution containing the membranes was used in the TK radioisotype assay. The TK radioisotype assay was previously described by O'Neill et al was performed.[43] Briefly, reactions were set up with 100 uL of the solution containing the membranes and 100 uL of a solution containing 2 μM [^{3}H]-Thymidine, 0.02 M Tris, 20 uM $MgCl_2$, 0.2 M KCl, 0.1 M NH_4Cl, 5 mM β-mercaptoethanol or dithiothreitol (DTT), and 4 mM ATP or 4 mM CTP for 1 hr at 37°C. After incubation, four 25 uL of each sample were applied to 2.5 cm DE-81 paper discs (Sigma-Aldrich, St. Louis, MO, catalog # Whatman Article No., 28419431) and the discs were washed 3X in 20mM ammonium formate (Sigma- Aldrich, St. Louis, MO, catalog # 156264), followed by a wash in 95% ethanol and a wash in distilled water. The discs were placed in scintillation vials with 3m of CytoScint (MP Biomedicals, Santa Ana, CA, catalog # 0188245301) and radioactivity was measured using a wet scintillation counter (Beckman Coulter, Brea, CA, model number LS6500).

Statistical analysis

Flow cytometry and TK1 activity data were analyzed using an unpaired t-test comparing the isotype control to each of the samples. Error bars represent the standard error of the mean. EDAX data were analyzed using a Kruskal-Wallis One-way ANOVA test. 2-tailed P-values ≤ 0.05 were determined to be significant.

Results

Flow cytometry shows a significant fluorescent shift in Raji, HL60, and Jurkat cells bound to anti-TK1 antibodies suggesting TK1 is localized on the plasma membrane of these cells

Using standard surface staining and flow cytometry, we discovered that Raji cells have a significant fluorescent shift compared to controls when bound to TK1 antibodies, suggesting TK1 is found on the outer cell membrane of Raji cells (Figure 2-1 A-C). We used an anti- NF-κB antibody as a control to confirm the integrity of the cell membrane since TK1 is also a cytoplasmic protein. The cells were NF-κB negative, which suggests our anti-TK1 antibodies were indeed bound to the surface of the cell and not internalized. (Figure 2-1 A). We also used a CD19 as positive surface staining control. This finding that TK1 is on the surface of Raji cells was confirmed using three different monoclonal antibodies against different TK1 epitopes (Figure 2-1 B). Quantification and statistical analysis of the fluorescent shifts show a significant difference in the percentage of Raji cells positive for TK1 compared to isotype control (Figure 2-1 C).

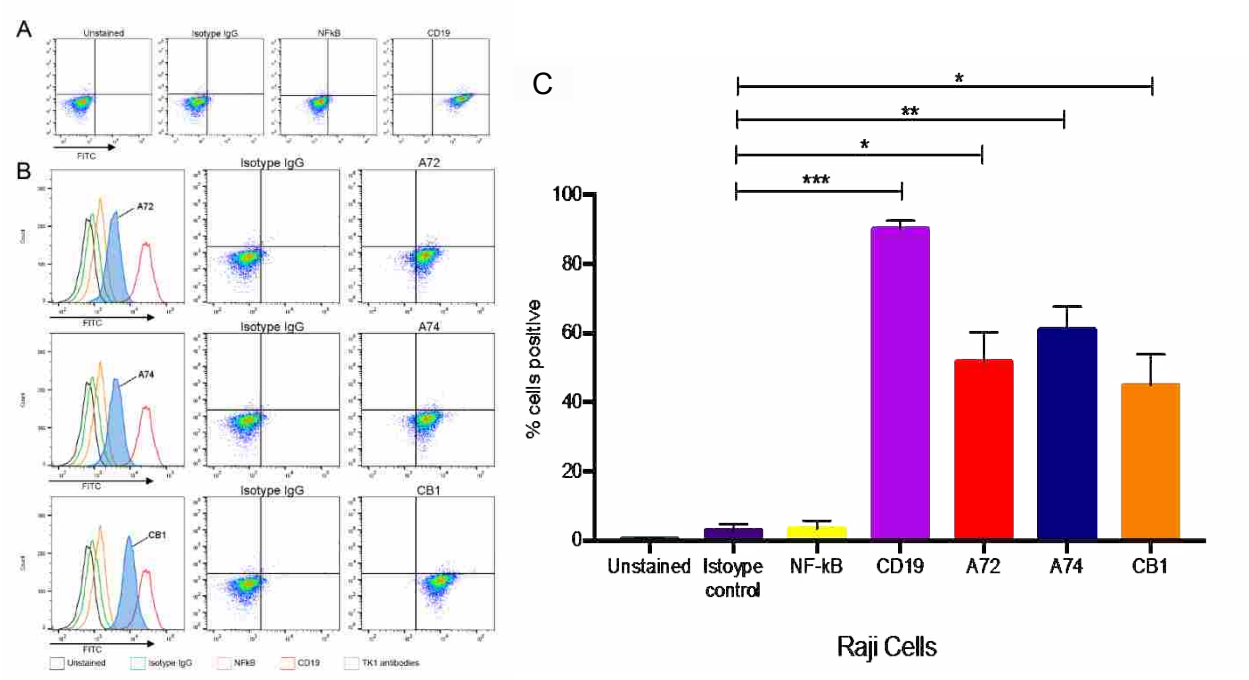

Figure 2- 1. Flow cytometry quantification analysis of normal lymphocytes.

A) Lymphocytes were isolated from whole blood and stained with anti-TK1 antibodies A72, A74, and CB1, anti-CD45 (positive control), isotype control, and anti-NFkB antibodies. Lymphocytes were also stimulated to proliferate and then stained with anti-TK1 antibodies A72, A74, and CB1, anti-CD45 (positive control), isotype control, and anti-NFkB antibodies. Normal resting lymphocytes show absence of TK1 on their surface even under proliferating conditions. B) Lymphocytes were treated with supraphysiological levels of purified TK1 (0.25uM, 0.5uM, and 0.75uM TK1). Lymphocytes were stained with anti-TK1 antibody (ab91651) and CD52 (positive control). Lymphocytes show non-significant amounts of TK1 on their surface, suggesting that extracellular sources of TK1 don't interact with the membrane. P-value ≤0.001= ***, P-value ≤0.0001= ****.

To confirm these findings, we also stained other hematological cancer cell lines such as HL60 (acute promyelocytic leukemia) and Jurkat (acute T cell leukemia) with CB1 conjugated to FITC and a commercially available anti-TK1 antibody conjugated to FITC. We used CD45 and Na+/K+ ATPase as positive controls, as both cells express them highly on their membrane. Both HL60 and Jurkat cells showed a significant fluorescent shift when bound to TK1 antibody (Figure 2-2).

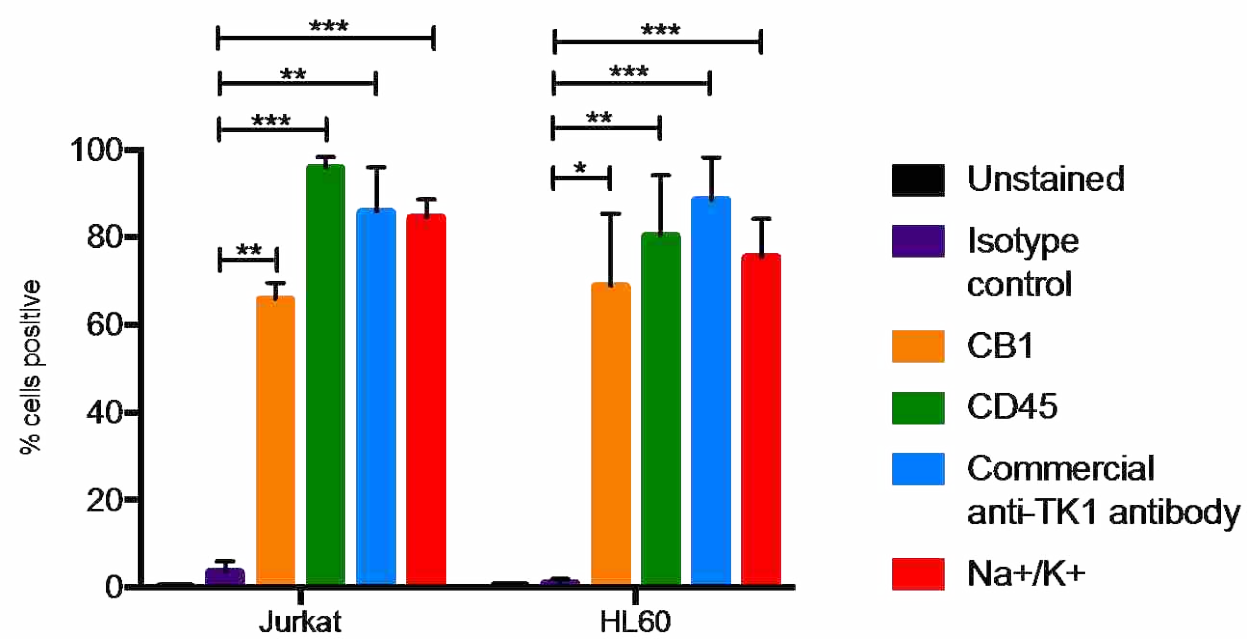

Figure 2- 2**.** Flow cytometry analysis of HL60 and Jurkat cells.

Here we show the quantification of the percentage of cells showing a positive fluorescent shift when bound to conjugated antibodies. The percentage of HL60 cells that are positive for TK1 (CB1 and commercially available anti- TK1 antibodies) is similar to that of CD45 and Na+K+ ATPase (positive controls) and significantly higher than the isotype control. Similarly, Jurkat cells show a significantly higher percentage of TK1+ cells than isotype controls with both CB1 and commercially available anti-TK1 antibodies. P-value ≤0.05= *, P-value ≤0.01= **, P-value ≤0.001= ***.

Fluorescent microscopy suggests TK1 is associated with the plasma membrane

To confirm that TK1 was associated with the membrane, we produced images using a fluorescent microscope to visualize this membrane localization phenomenon. We stained Raji, Jurkat, HL60, and normal lymphocytes with CB1 antibody conjugated to FITC (Figure 2-3). Our isotype control shows minimal fluorescent background while the samples treated with antibodies against $Na^{+}K^{+}$ ATPase and TK1 showed strong FITC signals on the cell membranes, suggesting a strong association of TK1 with the cell membranes. Normal lymphocytes show minimal FITC signal associated with TK1, indicating minimal presence of TK1 on their surface.

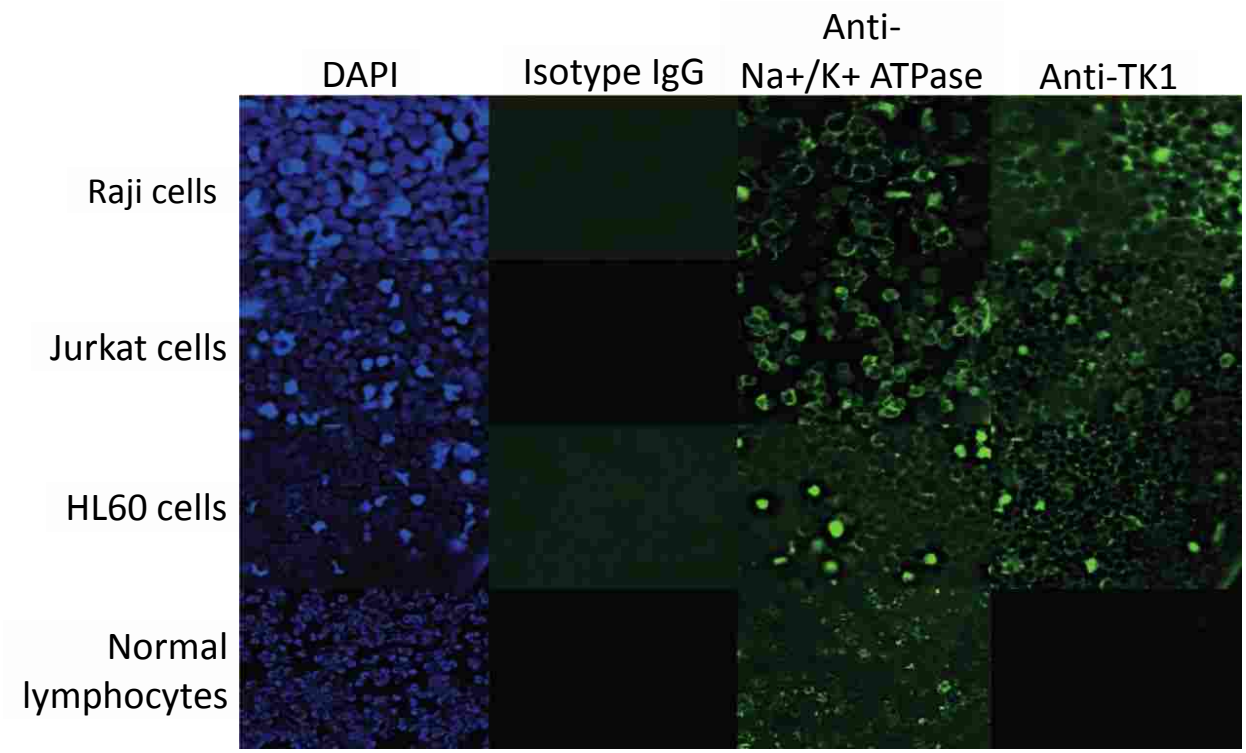

Figure 2- 3. Fluorescent microscopy images of viable Raji, Jurkat, HL-60, and normal lymphocytes cells stained with CB1-FITC (anti-TK1 antibody), isotype control, anti-Na+K+ ATPase antibody, and DAPI at 20X. Hematological cell lines stain positive for TK1 and Na+K+ ATPase. Normal lymphocytes do not stain positive for TK1. All cells are negative for isotype control. We can observe an association of the fluorescence of FITC with the membrane. These images suggest TK1 associates and localizes on the cell membrane.

TK1 is absent on the plasma membrane of normal lymphocytes

To test whether TK1 membrane localization was exclusive to malignant cells, we stained normal resting lymphocytes from whole blood with our antibodies. We isolated mononuclear cells from whole blood using Lymphocyte Separation Medium. We analyzed these cells immediately using flow cytometry. These normal lymphocytes were $CD45^+$ and $TK1^-$. We also tested whether the localization of TK1 on the surface was due to proliferation. We magnetically sorted $CD19^+$ cells from mononuclear lymphocytes isolated from whole blood by using an anti-CD19 antibody conjugated to biotin which we bound to streptavidin-magnetic beads. We stimulated these cells to proliferate using the CellXVivo Human B Cell Expansion Kit (R&D Systems). We then stained the cells with the same antibodies used with the resting lymphocytes using CD45 as positive control and analyzed the cells through flow cytometry. Flow cytometry analysis confirmed that normal lymphocytes do not significantly upregulate TK1 on their surface even when undergoing cell division (Figure 2- 4 A). These results indicate that the localization of TK1 on the outside layer of the plasma membrane may be an event exclusive to malignant cells.

Additionally, to test whether extracellular TK1 interacts with membrane, we incubated normal lymphocytes with 0.25uM, 0.50uM, 0.75uM, and 1uM of purified TK1 for 24 hours and then probed the cells with anti-TK1 antibody. Flow cytometry analysis showed that there is no significant expression of TK1 on the surface of these lymphocytes when exposed to supraphysiological levels of TK1 (Figure 2-4 B). These results suggest that there is no interaction of membrane with extracellular TK1.

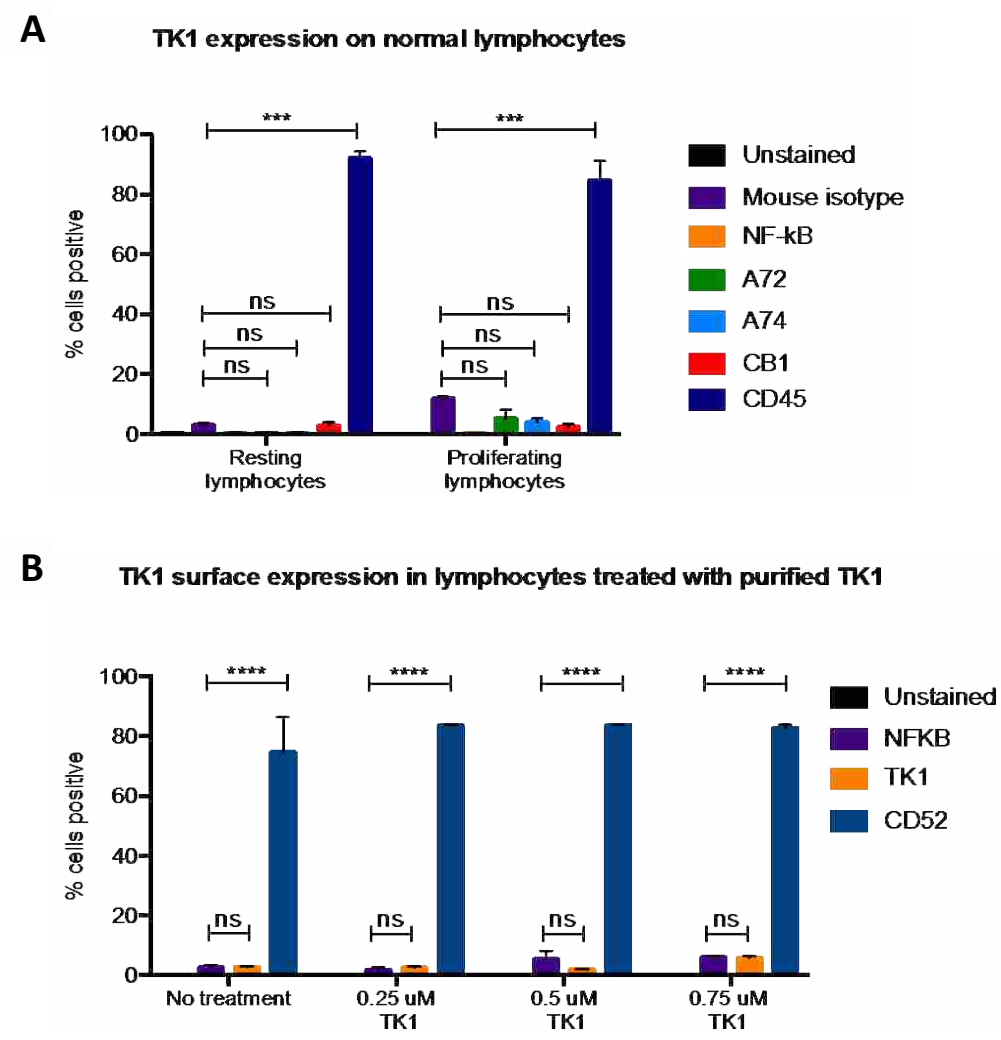

Figure 2- 4. Flow cytometry quantification analysis of normal lymphocytes.

A) Lymphocytes were isolated from whole blood and stained with anti-TK1 antibodies A72, A74, and CB1, anti-CD45 (positive control), isotype control, and anti-NFkB antibodies. Lymphocytes were also stimulated to proliferate and then stained with anti-TK1 antibodies A72, A74, and CB1, anti-CD45 (positive control), isotype control, and anti-NFkB antibodies. Normal resting lymphocytes show absence of TK1 on their surface even under proliferating conditions. B) Lymphocytes were treated with supraphysiological levels of purified TK1 (0.25uM, 0.5uM, and 0.75uM TK1). Lymphocytes were stained with anti-TK1 antibody (ab91651) and CD52 (positive control). Lymphocytes show non-significant amounts of TK1 on their surface, suggesting that extracellular sources of TK1 don't interact with the membrane. P-value ≤0.001= ***, P-value ≤0.0001= ****.

Scanning Electron Microscopy (SEM) shows further confirmation of TK1 localization on the surface of cancer cells

To further confirm the location of TK1 on the surface of cancer cells, we developed a scanning electron microscopy (SEM) protocol and used gold nanoparticles to visualize TK1. For this procedure, we used our A72 antibody. TK1 is shown to be expressed on the surface of Raji cells (Figure 2-5 A-B) and is absent in normal resting lymphocytes (Figure 2-6 A-B). EDAX analysis helped us quantify the amounts of gold present on the cell surface. The Raji cells probed with A72 antibody show significantly higher amounts of gold bound to their membrane than Raji cells probed isotype control. Raji cells probed with A72 antibody show similar amounts of gold to Raji cells probed with Na^+/K^+ antibody (Figure 2-5 C). In normal lymphocytes, the amounts of gold in Raji cells probed with A72 are similar to those probed with isotype control, suggesting TK1 is absent on the surface of normal lymphocytes (Figure 2-6 C).

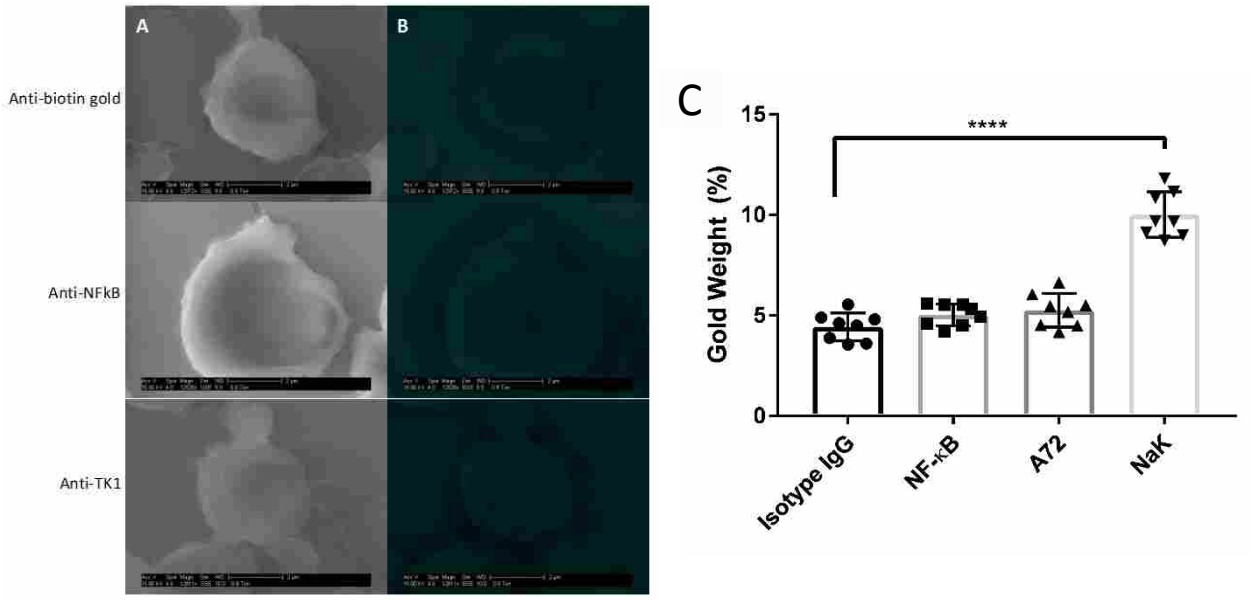

Figure 2- 5. Scanning Electron Microscopy of Raji cells.

A) Cells were stained with anti-biotin gold, anti-NFkB-biotin + anti-biotin gold, and anti-TK1 (A72)-biotin + anti-biotin gold visualized through a GSE detector. White spots represent gold bound to the membrane of the cells. B) Images were filtered so the white spots (gold) could be shown in red for better visualization. C) EDAX analysis quantification of gold weight percentages in Raji cells stained with anti-biotin gold, anti-NFkB-biotin + anti-biotin gold, A72-biotin + anti-biotin gold, and a positive control Na+/K+ ATPase-biotin + anti-biotin gold. The amount of gold particles found on the surface of Raji cells when stained with anti-TK1 A72 antibody are significantly higher than background. P-value ≤0.05= *, P-value ≤0.01= **.

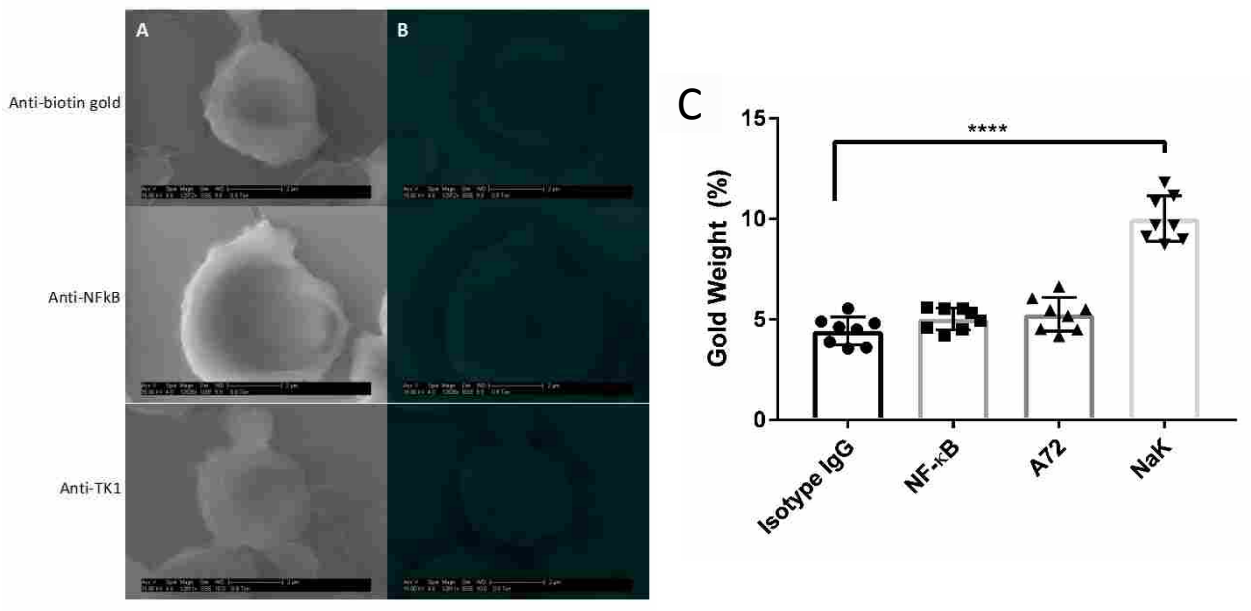

Figure 2- 6. Scanning Electron Microscopy of normal lymphocytes.

A) Cells were stained with anti-biotin gold, anti-NFkB-biotin + anti-biotin gold, and anti-TK1 (A72)-biotin + anti-biotin gold visualized through a GSE detector. White spots represent gold bound to the membrane of the cells. B) Images were filtered so the white spots (gold) could be represented in red for better visualization. No gold is can be visualized in these samples. C) EDAX analysis quantification of gold weight percentages in normal lymphocytes stained with anti-biotin gold, anti-NFkB-biotin + anti-biotin gold, A72-biotin + anti-biotin gold, and a positive control Na+/K+ ATPase-biotin + anti-biotin gold. The amount of gold particles found on the surface of normal lymphocytes when stained with anti-TK1 A72 antibody are the same as the background indicating the absence of TK1 in these cells. P-value ≤0.0001= ****.

ALL clinical samples also express TK1 on their plasma membrane

To ensure TK1's relevance in clinical samples, we tested ALL samples (n=9) obtained from the Huntsman Cancer Institute. These samples were $CD34^+$ and $HLA\text{-}DR^+$ as expected (Figure 2-7 A). We performed alive/dead cell discrimination to prevent any false positives in these samples. All ALL samples tested were positive for TK1. Cell viability impacted the analysis as we got lower event counts when we discriminated dead cells. However, even in samples with low viable cell count TK1 was expressed on the cell membrane. Percentage of cells positive for TK1 varied from 8% to 43.5%, averaging 28.01% (Figure 2-7 B). We believe we see this big range due to disease progression and grade.

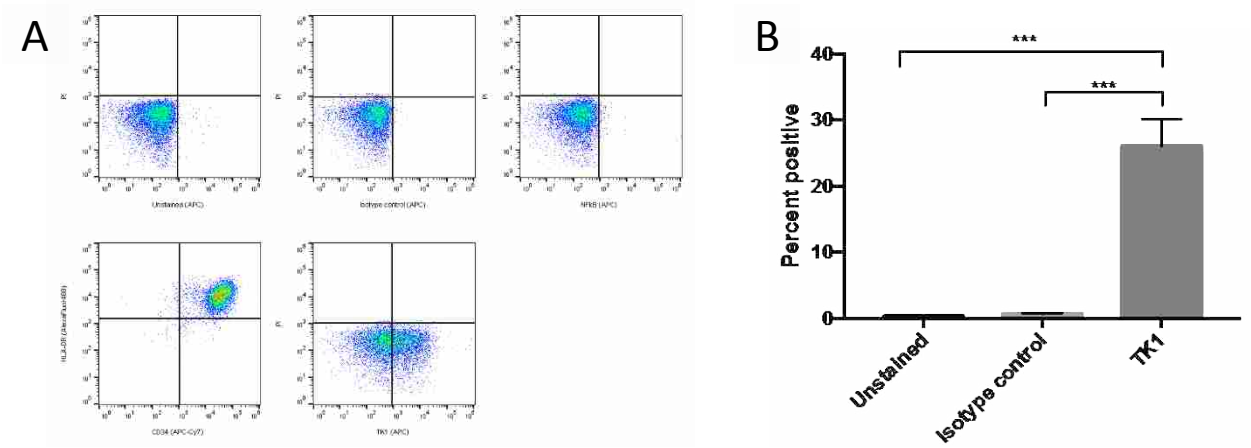

Figure 2- 7. Flow cytometry analysis of ALL clinical samples.

A) Density plots of flow cytometry controls used in the analysis of ALL samples. Cells are CD45+ and HLA-DR+. Controls indicate an insignificant fluorescent shift in cells stained with isotype IgG control and anti-NFkB antibody. Cells appear to shift in fluorescence when bound to anti-TK1 antibody. B) Quantification of cells shifting towards a greater fluorescence in ALL samples. ALL samples have a significant percent of cells with a greater fluorescent shift compared to controls. P-value ≤0.01= **.

TK1 on the membrane is found in different oligomeric

To further characterize TK1 on the membrane, plasma membrane and cytoplasmic proteins were isolated from Raji cells and normal lymphocytes. Both the membrane and the cytosolic proteins were run on a 12% acrylamide SDS gel and then transferred to a nitrocellulose membrane and probed with anti-TK1 antibody ab91651. Results show that the Raji cell membrane protein fraction contains mostly monomers and dimers of TK1 (Figure 2-8 A). On the other hand, the normal lymphocyte membrane protein fraction contains minimal traces of TK1 (Figure 2-8 B).

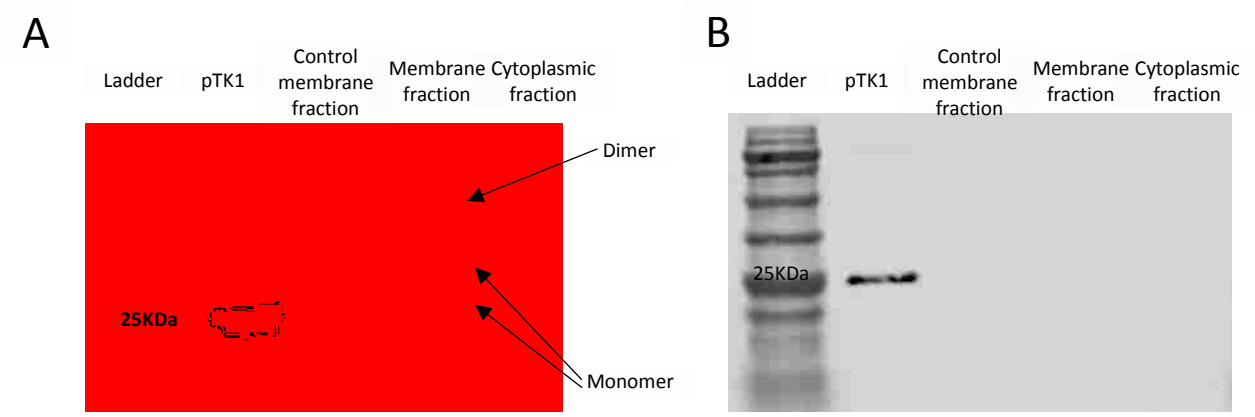

Figure 2- 8. Western blot of membrane and cytosolic fractions in Raji cells and normal lymphocytes and blotted with anti-TK1 antibody.

A) Membrane proteins on viable Raji cells membranes were biotinylated or not (control) and then bound to streptavidin beads. Membrane proteins bound to the beads were eluted and used as samples in a Western blot. Samples were probed against TK1. We observe that TK1 found on Raji cells' membranes adopts many oligomeric forms as pointed by the arrows. B) Membrane proteins on viable normal lymphocytes were biotinylated or not (control) and then bound to streptavidin beads. Membrane proteins bound to the beads were eluted and used as samples in a Western blot. Samples were probed against TK1. We observe that normal lymphocytes do not show any detectable TK1 on their membrane fraction.

TK1 on the membrane shows activity

Membrane fractions of Raji, Jurkat, and HL-60 cell lines and normal lymphocytes were used in a radioassay to measure TK1 activity. TK1 activity was measured by subtracting the enzymatic activity with CTP as the phosphate donor from the total enzymatic activity with ATP as the phosphate donor. The reasoning behind this is that TK2, an isozyme form of TK1 found in mitochondria, favors CTP as the phosphate donor. By subtracting the enzymatic activity with CTP as the phosphate donor, we ensure the remaining enzymatic activity is purely due to TK1 activity, as described by Lee and Cheng.[44] Our data shows that the membrane fractions of Raji, Jurkat, and HL-60 cell lines show TK1 enzymatic activity (Figure 2-9). Moreover, these membrane fractions show higher TK1 activity levels than those in normal lymphocytes. This could be due to minimal presence of TK1 on the surface of normal lymphocytes.

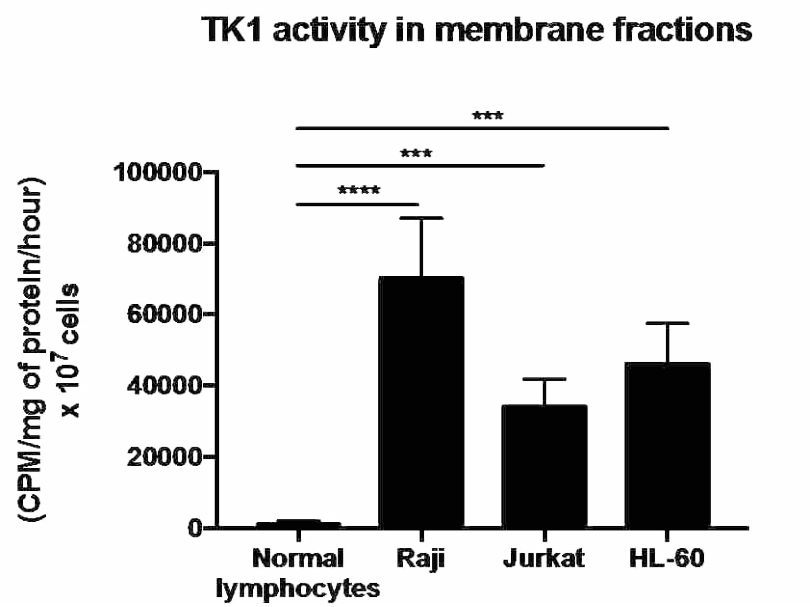

Figure 2- 9. TK1 activity in membrane fractions.

Membrane fractions were isolated from normal lymphocytes, Raji, Jurkat, and HL-60 cells and then used as samples in the TK1 radioassay. Normal lymphocytes show minimal TK1 activity. However, Raji, Jurkat, and HL-60 membrane fractions show significantly higher TK1 activity than normal lymphocytes. P-value ≤0.001= ***, P-value ≤0.0001= ****.

Discussion

Burkitt's lymphoma and acute lymphoblastic leukemia are complex diseases that affect millions of children worldwide. They are also two of the fastest proliferating tumors in humans.[32,33] Rapid cellular proliferation and resisting apoptosis are two of the hallmarks of cancer that we can clearly see in hematological malignancies, especially in BL and ALL.[1,34,37,38,45] Early events in the deregulation of the cell cycle can lead to rapid proliferation and possible cancer. Current treatments for BL and ALL include combination chemotherapy drugs that cause debilitating side effects in children, therefore, there is an immediate need to identify new targets to treat BL and ALL through immunotherapy. This study provides a potential novel target against these malignancies.

Our study shows that upregulation of TK1 can also be found on the membrane of hematological malignancies. This upregulation can be due to increased levels of TK1 in the cell during cellular division, an event that happens very frequently in most cancer, especially in BL and ALL.[32,33] Here we show the novel finding that multiple hematological cancer cell lines and ALL clinical samples express high levels of TK1 on their surface. Interestingly, this is not seen in resting or proliferating normal lymphocytes. TK1's expression appears to be similar to that of CD229 in multiple myelomas, where CD229 is upregulated only in malignant cells and remains low/absent in normal lymphocytes.[46]

Additionally, our data suggest membrane TK1 is found in monomeric and dimer form and has enzymatic activity suggesting that TK1 has a function on the membrane. The actual function of membrane TK1 and the mechanism/pathway by which TK1 reaches the membrane remain unknown. However, our data suggests that the origins of membrane TK1 are endogenous and do not come from serum TK1. We believe that during rapid proliferation events in

malignancy, as TK1 protein levels increase, TK1 interacts with one or several membrane proteins in the ER. For example, SELZ6 and COPS6 are membrane proteins known to interact with TK1.[47–49] Both of these proteins also upregulate during malignancy events and are found in greater quantities on the cellular membrane. Perhaps their interaction results in TK1 being transported to the membrane, remaining there, or perhaps being released into the bloodstream to be later found in the serum.

The findings presented in this study are important for the field as they represent the discovery of a novel antigen on the surface of some cancer cells, which if used in conjunction with current immunotherapeutic treatments, such as CAR T cells, has the potential to improve treatments for different hematological malignancies.

Conclusion

TK1 is localized on the surface of Raji (Burkitt's lymphoma), HL60 (acute promyelocytic leukemia), and Jurkat (acute T cell leukemia) cell lines and ALL clinical samples, and not on the surface of normal resting or proliferating lymphocytes and may be used as a target to treat hematological malignancies.

Acknowledgments

This research was supported by funding from the Brigham Young University Department of Microbiology and Molecular Biology, the Brigham Young University College of Life Sciences, and the Simmons Center for Cancer Research. We thank Dr. Juan Arroyo for his technical assistance in microscopy imaging/processing, and Jaden Evans for his assistance with the radioactive assays.

CHAPTER 3: Membrane Expression of Thymidine Kinase 1 and Potential Clinical Relevance in Lung, Breast, and Colorectal Malignancies

The following chapter is taken from an article published in Cancer Cell International. All content and figures have been formatted for this dissertation but it is otherwise unchanged.

Abstract

Lung, breast, and colorectal malignancies are the leading cause of cancer-related deaths in the world causing over 2.8 million cancer-related deaths yearly. Despite efforts to improve prevention methods, early detection, and treatments, survival rates for advanced stage lung, breast, and colon cancer remain low, indicating a critical need to identify cancer-specific biomarkers for early detection and treatment. Thymidine kinase 1 (TK1) is a nucleotide salvage pathway enzyme involved in cellular proliferation and considered an important tumor proliferation biomarker in the serum. In this study, we further characterized TK1's potential as a tumor biomarker and immunotherapeutic target and clinical relevance. We assessed surface localization by flow cytometry and confocal microscopy in lung (NCI-H460, A549), breast (MDA-MB-231, MCF7), and colorectal (HT-29, SW620) cancer cell lines. To evaluate TK1's clinical relevance, we compared TK1 expression levels in normal and malignant tissue through flow cytometry and immunohistochemistry. We also analyzed RNA-Seq data from The Cancer Genome Atlas (TCGA) to assess differential expression of the TK1 gene in lung, breast, and colorectal cancer patients. We found significant expression of TK1 on the surface of NCI-H460, A549, MDA-MB-231, MCF7, and HT-29 cell lines and a strong association between TK1's localization with the membrane through confocal microscopy. We found negligible TK1 surface expression in normal healthy tissue and significantly higher TK1 expression in malignant tissues.

Patient data from TCGA revealed that the TK1 gene expression is upregulated in cancer patients compared to normal healthy patients. Our results show that TK1 localizes on the surface of lung, breast, and colorectal cell lines and is upregulated in malignant tissues and patients compared to healthy tissues and patients. We conclude that TK1 is a potential clinical biomarker for the treatment of lung, breast, and colorectal cancer.

Introduction

Lung, breast, and colorectal malignancies are the leading causes of cancer-related deaths in the world. These three cancers account for over 4.86 million cases diagnosed and over 2.8 million cancer-related deaths worldwide every year [50]. Thus, lung, breast, and colorectal cancers are a major health concern as over 11.7 million people are currently diagnosed and living with these diseases worldwide and represent a substantial economic burden in countries of all incomes [50,51].

Despite efforts to improve methods of prevention, early detection, and treatments, survival rates for advanced stage lung, breast, and colon cancer remain low at 4%, 26%, and 13%, respectively [52]. Therefore, there is an urgent need to identify cancer-specific biomarkers for early detection and treatment of the leading cause of cancer-related deaths such as lung, breast, and colorectal cancers [53,54].

Thymidine kinase 1 (TK1) is a nucleotide salvage pathway enzyme involved in cellular proliferation and considered an important tumor proliferation biomarker [4,19,28,55]. In serum, TK1 has been shown to be elevated in early events of malignancy, and thus, TK1 can serve as an early detection biomarker [4,56,57]. Moreover, serum TK1 has been found to be elevated in several hematological and solid tumors including breast, lung, colorectal cancer, among others, and high serum TK1 levels usually correlate with cancer grade and stage, increased T-values, and

increased tumor size [4,17–19,22,55]. Serum TK1 can be also used as a prognostic tool to monitor responses to chemotherapy or surgery [3,22].

To further characterize TK1's potential as a tumor biomarker, we evaluate TK1 as a potential immunotherapeutic target. In this study, we evaluate the expression levels of membrane TK1 on lung, breast, and colorectal cell lines using flow cytometry. We also show evidence that TK1 is localized on the surface of lung, breast, and colorectal cell lines. In addition, we evaluate TK1 expression levels in normal and malignant tissue to determine TK1's clinical relevance. These results suggest TK1 as a potential immunotherapeutic target.

Materials and Methods

Cell lines and cell culture conditions

Lung cancer cell lines NCI-H460 (ATCC® HTB-1770 ™) and A549 (ATCC® CCL-185 ™), breast cancer cell lines MCF7 (ATCC® HTB-22™) and MDA-MB-231 (ATCC® HTB-26™), and colon carcinoma cell lines SW620 (ATCC® CCL-227™) and HT-29 (ATCC® HTB-38™) were purchased from ATCC (Rockville, MD). NCI-H460 and HT-29 cell lines were grown in RPMI 1640 medium (Corning Life Sciences, VWR International, Radnor, PA) supplemented with 2mM L-glutamine and 10% fetal bovine serum. MDA-MB-231, MCF7, and SW620 cell lines were grown in DMEM medium (Gibco, Thermo Fisher, Waltham, MA) supplemented with 4mM L-glutamine and 10% fetal bovine serum. A549 cells were grown in DMEM/F-12 medium (Gibco, Thermo Fisher, Waltham, MA) supplemented with 4mM L-glutamine and 10% fetal bovine serum. L-glutamine and fetal bovine serum were purchased from Thermo Fisher (Waltham, MA). The media was renewed every 2-3 days. For subculturing, cells were detached using Accutase (Stem Cell Technology, Vancouver, Canada) and seeded in 1:3 or 1:6 ratios. All cells were cultured at 37°C with 5% CO_2. All cell lines were authenticated

by short tandem repeat (STR) analysis at the University of Arizona Genetics Core Facility during our study.

Antibodies

We used 3 custom mouse monoclonal antibodies developed in our lab against TK1 (CB1, A72, and A74) and a commercially available rabbit monoclonal antibody against TK1 (ab91651) (Abcam, Cambridge, United Kingdom). CB1 binds to the C-terminal domain of TK1, specifically to the active domain. A72 and A74 are against an immunodominant region not on the TK1 C-terminal domain. These antibodies have been previously tested to work in ELISA, immunohistochemistry, and Western blots to confirm their specificity [28,40,41]. The three custom antibodies were conjugated to FITC using a conjugation kit (EasyLink, Abcam, ab102884) and stored in the dark at 4°C. The commercially available antibody (ab91651) was conjugated to FITC or APC using a conjugation kit (EasyLink, Abcam, ab102884) and stored in the dark at 4°C. We used FITC-conjugated CB1, A72, A74, and APC-conjugated ab91651 for flow cytometry, FITC-conjugated A72 for confocal microscopy, and unconjugated ab91651 was used for Western blotting and immunohistochemistry.

Flow cytometry

Cells were rinsed with Dulbecco's phosphate-buffered saline (DPBS) and treated with Accutase (Stem Cell Technology, Vancouver, Canada) at 37°C for 5-10 mins to allow for detachment and then rinsed with their respective complete medium. Cells were pelleted and resuspended at $1x10^6$ cells/mL in Cell Staining Buffer (BioLegend, San Diego, CA) and 200uL of cells were placed in individual microcentrifuge tubes and stained with 1 ug of FITC-conjugated CB1, A72, A74, or APC-conjugated ab91651 for 30 minutes on ice in the dark. Negative controls used were unstained cells, cells stained with isotype mouse and rabbit

antibodies, and NFkB to confirm the integrity of the cell membrane. Cells were then washed with Cell Staining Buffer and resuspended in 500uL of FACS buffer. FACS buffer was made with phosphate-buffered saline (PBS), 2% calf serum (Thermo Fisher, Waltham, MA), 1 mM EDTA (Thermo Fisher, Waltham, MA, CAS 6381-92-6), and 0.1% sodium azide (Sigma Aldrich, St. Louis, MO, CAS 26628-22-8). We collected $1x10^4$ events per sample in a flow cytometer (Attune, Life Technologies, Carlsbad, CA) and data was analyzed using the FlowJo software (FlowJo, Ashland, OR).

Confocal microscopy

Cells were grown on glass coverslips for 48 hours. Coverslips containing cells were washed in DPBS and then incubated with either isotype control, NFkB, or A72-FITC for 30 minutes at 4°C on a rocking platform. Coverslips were then washed 3 times with DPBS for 10 minutes on a rocking platform. We then dipped the coverslips in 1X CellMask™ Deep Red Plasma membrane stain (Thermo Fisher Scientific, Waltham, MA) for 10 mins at 37°C. The cells were rinsed in DPBS and imaged immediately using an Olympus FluoView FV1000 confocal laser scanning microscope (Olympus, Tokyo, Japan). Images were obtained using the Laser Sharp Computer Software (Bio Rad Laboratories, Hercules, CA) and later processed in Photoshop (Adobe Systems, San Jose, CA).

Cell surface protein isolation and Western blotting

To isolate the cell surface proteins, we used the Pierce™ Cell Surface Protein Isolation Kit (Thermo Fisher Scientific, Waltham, MA, Cat # 89881). Briefly, the HT-29 cell line was grown to 90% confluency in T75 flasks and their media was removed. The cells were washed with ice-cold PBS (provided in the kit) and then the PBS was removed within 5 seconds. To label the cells with biotin, cells were incubated with a biotin solution made by dissolving the

contents of one vial of Sulfo-NHS-SS_Biotin (provided in the kit) in 48mL of ice-cold PBS. 10mL of the biotin solution were added to each flask of cells and the flasks were incubated on a rocking platform with gentle agitation for 30 mins at 4°C. After incubation, 500uL of quenching solution (provided in the kit) were added to each flask to quench the reaction. Then, cells were gently scraped and transferred to a conical tube and pelleted at 500 x g for 3 minutes, after which the supernatant was discarded. Cells were then washed with 5mL of Tris-buffered saline (TBS, provided in the kit) by pipetting up and down twice with a serological pipette and pelleted at 500 x g for 3 minutes. A cocktail of protease inhibitors (Halt™ Protease & Phosphatase Inhibitor Cocktail, Thermo Fisher, Waltham, MA, product # 78440) was added to 500uL of lysis buffer (provided in the kit) and added to the cell pellet. The cells in lysis buffer were transferred to a microcentrifuge tube and resuspended in the fluid by pipetting up and down. The cells were then disrupted using a cell disruptor (Sonicator 3000, Misonix, Inc., Farmingdale, NY) at low power (1.5) on ice using five 1-second bursts. Cells were incubated for 30 minutes on ice, vortexed every 5 minutes for 5 seconds, and sonicated for 1 second at low power (1.5) every 10 minutes. The cell lysate was centrifuged at 10,000 x g for 2 minutes at 4°C and the clarified supernatant transferred to a new microcentrifuge tube. To isolate the biotin-labeled proteins, the clarified supernatant was added to a column that contained 500uL of NeutrAvidin Agarose that had been previously washed with 500uL of wash buffer and centrifuged for 1 minute at 1000 x g. The column was capped and incubated for 60 minutes at room temperature with end-over-end mixing using a rotator. Then, the column was centrifuged for 1 minute at 1000 x g and the flow-through was discarded. The column was washed 3 times with 500uL of wash buffer containing a cocktail of protein inhibitors to remove any other cytoplasmic proteins. To elute the membrane proteins, a 50mM DTT solution was made by adding 23.7uL of 1M DTT (provided in the kit) to 450uL

SDS-PAGE sample buffer. 450uL of DTT solution were added to the column and incubated for 60 minutes at room temperature with an end-over-end mixing on a rotator. The column was then centrifuged for 2 minutes at 100 x g and the flow-through collected and stored at -20°C. For Western blot analysis, samples were thawed on ice after which they were boiled for 5 minutes and then run on a 12% acrylamide SDS gel at 90 V for 2-3 hours. The proteins on the gel were transferred onto a nitrocellulose membrane at 90 V for 50 minutes in a cold room. The nitrocellulose membrane was blocked with 5% non-fat milk in DPBS for 1 hour at 4°C in a rotating platform and then incubated in anti-TK1 commercial antibody (ab91651) in a 1:1000 dilution in milk overnight at 4°C in a rotating platform. The nitrocellulose membrane was washed 3 times in DPBS for 3 minutes each in a rotating platform and then incubated with a IRDye 800 donkey anti-rabbit secondary antibody for 1 hour at 4°C in a rotating platform (LI-COR, Lincoln, NE). Finally, the membrane was washed 3 times with DPBS and imaged in an Odyssey CLx Imaging System (LI-COR, Lincoln, NE).

Tissue dissociation and analysis

Healthy and malignant colon tissues were obtained from Utah Valley Regional Medical Center in Provo, UT under informed consent and following a protocol established by Utah Valley Regional Medical Center. Tissues were minced into 3-4 mm pieces with a sterile scalpel. Minced tissue was washed with 1X Hank's Balanced Salt Solution (HBSS) (Thermo Fisher, Waltham, MA) containing 5% FBS. Collagenase type II or type IV (both from Thermo Fisher, Waltham, MA, product # 17101015 and # 17104019, respectively) was added to the minced tissue and incubated at 37°C for 4-8 hours to allow for cell dissociation. To obtain a cell suspension and separate dispersed cells from larger tissue pieces, cells were filtered through a 100um nylon mesh cell strainer (BD Biosciences, San Jose, CA). To prepare cells for flow

cytometry analysis, cells were washed twice with HBSS and then resuspended in Cell Staining Buffer. Cells were treated with Fc block (Human TruStain FcX™, BioLegend, San Diego, CA), anti-human CD45 antibody (clone 2D1, eBioscience, San Diego, CA) and PI to gate out resident lymphocytes and dead cells. We collected $2x10^4$ events per sample in a flow cytometer (Attune, Life Technologies, Carlsbad, CA) and data was analyzed using the FlowJo software (FlowJo, Ashland, OR).

TK1 gene expression bioinformatics analysis

First, we evaluated differences in expression levels of the TK1 gene in 2,645 tumor samples and 264 normal samples from The Cancer Genome Atlas.[58] We used RNA-Sequencing data that had been summarized at the gene level to transcripts-per-million units and processed using the *featureCounts* algorithm.[59,60] We also log-transformed the data values. These data included expression values from tumor-adjacent and blood samples; these samples were often, but not necessarily, matched to the tumor samples. Second, we evaluated breast-cancer samples from The Cancer Genome Atlas for which hormone-receptor status had been determined via immunohistochemistry; we limited this analysis to tumors that either were 1) positive for HER2 expression or 2) negative for HER2, ER, and PR expression. In calculating differences in expression between these groups, we used a two-sided, Mann-Whitney U Test. We also evaluated the level of correlation between TK1 and six stemness and EMT genes (CD44, SNAI1, SNAI2, TWIST1, ZEB1, TGFB1) using Spearman's method. We wrote scripts in the Python programming language (https://python.org, v.3.6.1) to parse and prepare the data. We used the R (v.3.2.2) statistical software and the ggplot2 software package (v.2.2.1) to generate graphs illustrating these expression levels.[61,62]

Immunohistochemistry

Lung, breast, and colorectal tissue microarrays were purchased from US Biomax (Rockville, MD, catalog # LC2084, #BR721, and #CO1002b). Each slide contains at least 40 tissue cores with tissues varying in grade and stage and, and normal healthy tissues. The slides were incubated in Histo-Clear (National Diagnostic, Atlanta, GA) for 10 mins for 3 changes to remove paraffin. The slides were then incubated in 100% EtOH for 2 changes for 3 min each, then in 90% EtOH for 2 changes for 1 min each, then in 70% EtOH for 1 change for 1 min. The slides were then washed in ddH_2O for 5 mins. To perform antigen retrieval, the slides were incubated in DIVA Decloaker (Biocare Medical, Pacheco, CA) at 80- 95 °F for 30 mins and let them cool for 10 mins. We then washed 2X in ddH_20 for 5 mins. To perform peroxidase quenching, the slides were washed in Tris-buffered saline (TBS) containing 3% hydrogen peroxide for 20 mins and then washed 2X with TBS-T for 3 mins. The slides were blocked for 15 mins using a Background Sniper Block (Biocare Medical) to reduce background and then washed with TBS twice for 3 mins. We incubated the slides with a 1:200 dilution of anti-TK1 (Abcam, ab91651) anti-GAPDH (positive control, mouse monoclonal, Cell Signaling Technologies), and universal negative control serum (negative control, Biocare Medical) and put them in a humidity chamber to prevent drying. After primary antibody staining, the slides were washed 3X for 5 mins with TBS and incubated with MACH 4 Universal Horseradish Peroxidase (HRP) Polymer (universal for rabbit/mouse secondary, Biocare Medical) for 30 mins in a humidity chamber and then washed again 2X for 3 mins with TBS. We developed the slides with ImmPACT DAB Peroxidase (HRP) substrate (Vector Laboratories, Burlingame, CA) and then washed them 2X for 3 mins with TBS. We then stained the slides with Hematoxylin (Biocare Medical) and rinsed them for 5 mins in running water. We mounted the slides using cover slips and Cytoseal (Thermo Scientific) and imaged them using a light microscope. Images were

analyzed using ImageJ open source software, using the "IHC (more brown)" plug-in to obtain quantification using a gray scale [63]. The lower the gray value, the darker the tissue is stained.

Statistical analysis

For our flow cytometry data, we used a multiple-comparisons one-way ANOVA test using the Sidak's correction for multiple comparisons to compare the expression of TK1 on the surface of lung, breast, and colon cell lines vs isotype control. All samples were compared against isotype mouse IgG except for Commercial, which was compared against isotype rabbit IgG. We set a significant P-value at ≤0.05. Error bars represent the standard error of the mean. For our IHC analysis, we used Tukey's multiple comparison test to compare the means of each group to one another. One side P-value was set to ≤0.05. Error bars represent the standard deviation of the samples. We used Prism 7 (GraphPad, La Jolla, CA) to perform our statistical analysis and produce graphs for most analysis. We the R (v.3.2.2) statistical software and the ggplot2 software package (v.2.2.1) to generate graphs for TK1 gene expression bioinformatics analysis.

Results

TK1 expression is elevated on the surface of NCI-H460, A549, MCF7, MDA-MB-231, SW620, and HT-29 cells

Using flow cytometry, we observed an overall increase in fluorescence intensity in NCI-H460, A549, MCF7, MDA-MB-231, SW620, and HT-29 cells (Supplemental Figure 1). The data represents 8 independent staining procedures. Cells stained with A72 showed a significant increase in fluorescence in all cell lines but SW620 and A529 (*P≤0.05; **P≤0.005; ***P≤0.001). Cells stained with CB1 showed significant increase in fluorescence in all cells but MDA-MB-231 and A549 (Figure 3-1 A-D) (*P≤0.05; **P≤0.005; ***P≤0.001; ns=P>0.05).

Cells stained with ab91651 all showed to have an increase in fluorescence except SW620 cells (*P≤0.05; **P≤0.005; ***P≤0.001; ns=P>0.05). Overall, cells bound to CB1 had the lowest increase in fluorescent intensity. We used an anti-NFkB antibody as a non-specific control as well as an intracellular control. It allowed us to test whether the cells were intact, and the fluorescent intensity change was due to punctured/dead cells or intact cells.

Data revealed that the lung cell lines NCI-H460 and A549 had the highest TK1 surface expression out of all the other cell lines, followed by breast cell lines MDA-MB-231 and MCF7, and colorectal cell line HT-29 (Figure 3-1 B, 3-1 C). The SW620 cell line showed very little expression of TK1 on its surface, only and average of 10% of fluorescence total increase in cells bound to A72, A74, and CB1, and only 2.7% in cells bound to commercial antibody ab91651 (Figure 3-1 A). These results suggest that 5 of the 6 cell lines tested expressed TK1 on their cell surface.

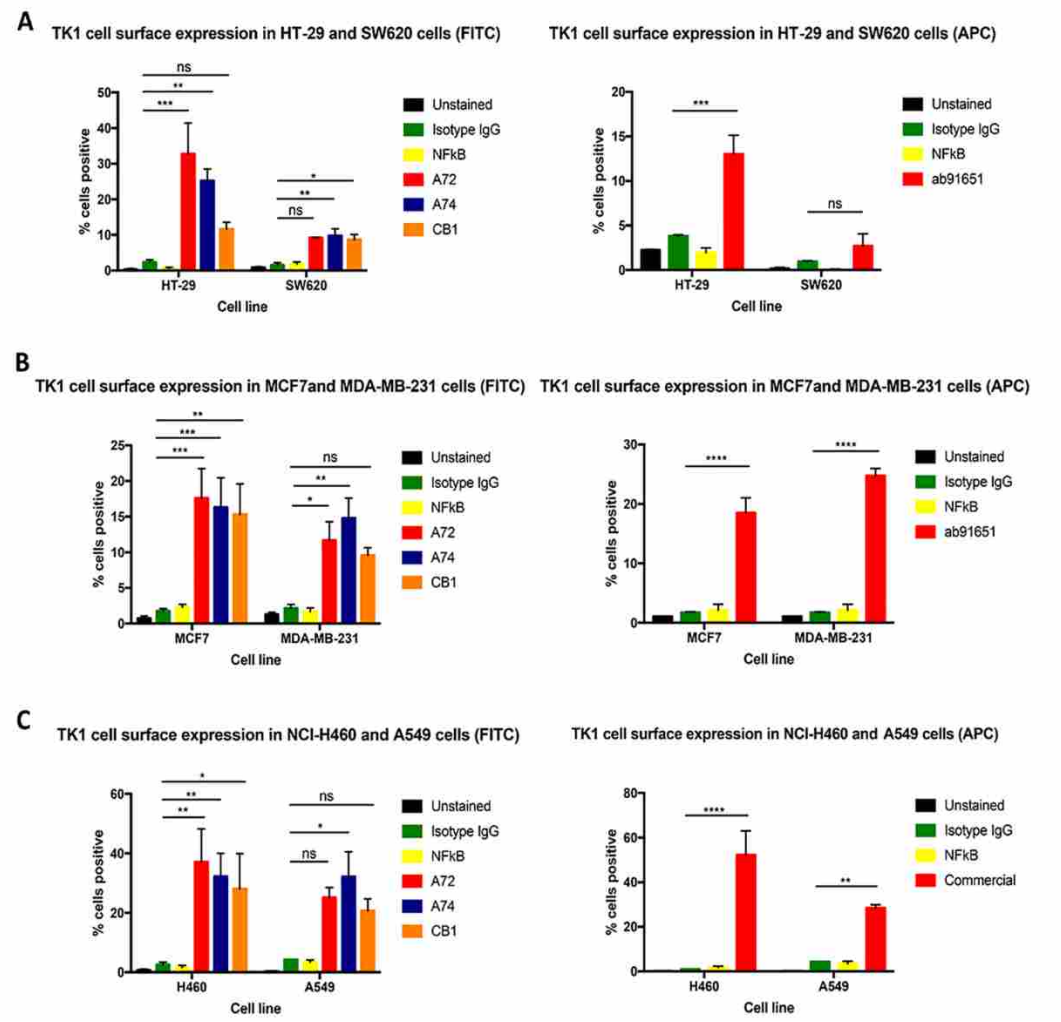

Figure 3- 1. Flow cytometry analysis of TK1 expression on the cell membrane of colon, breast, and lung cancer cell lines.

A) Flow cytometry histograms of cell lines treated with anti-TK1 antibodies. Cells treated with anti-TK1 antibodies (black line) showed a shift in fluorescence compared to isotype controls (gray area). B) Quantification of TK1 expression on the cell membrane of HT-29 and SW620 cell lines stained with FITC or APC-conjugated anti-TK1 antibodies. C) Quantification of TK1 expression on the cell membrane of MCF7 and MDA-MB-231 cell lines. The top bar graph shows MCF7 and MDA-MB-231 cell lines stained with FITC or APC-conjugated anti-TK1 antibodies. D) Quantification of TK1 expression on the cell membrane of NCI-H460 and A549 cell lines stained with FITC or APC-conjugated anti-TK1 antibodies. Statistical analysis was performed by comparing the mouse isotype control fluorescent levels to those of A72, A74, CB1, or ab91651. *P≤0.05; **P≤0.005; ***P≤0.001; ns=P>0.05

TK1 is strongly associated with the membrane of NCI-H460, MDA-MB-231, and HT-29 cells

To visualize TK1's localization and to ensure antibody binding was to the membrane only, we performed confocal microscopy in HT-29, MDA-MB-231, and NCI-H460 cells since these cell lines expressed high levels of TK1 on their membrane in flow cytometry. We stained the cells with isotype control, anti-NFkB, and anti-TK1 (A74) antibodies conjugated to FITC. We used intact cells to ensure FITC signals were not coming from intracellular TK1. We obtained single channel images, rhodamine for membrane, FITC for isotype IgG, A74 and NFKB antibodies, and overlaid them to observe associations between the signals. We observe minimal FITC signals for cells stained with isotype IgG and NFkB. However, we observe a much stronger signal from cells treated with anti-TK1 antibody (A74) (Figure 3-2). These images show a clear colocalization of TK1 antibody signal and membrane dye, confirming the presence of TK1 on the surface of HT-29, MDA-MB-231, and NCI-H460 cells.

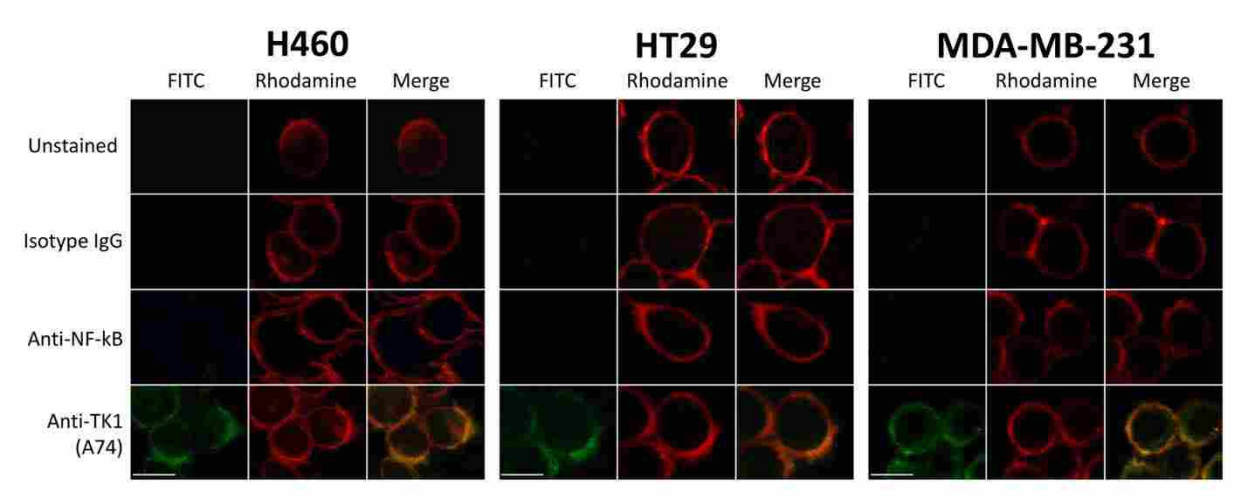

Figure 3- 2. TK1 co-localizes with the plasma membrane of lung, breast, and colon cancer cell lines. NCI-H460, HT-29, and MD-MBA-231 cells were stained with FITC-conjugated antibodies and a cell membrane specific dye (Rhodamine). Unstained cells, cells stained with isotype antibody, and cells stained with anti-NFkB antibody (FITC) were used as controls to determine the viability of cells and the non-internalization of the antibodies to prevent false positives. FITC images show staining on cells treated with anti-TK1 antibody A74. The FITC images were merged with the Rhodamine images, which show the plasma membrane. The images show a clear co-localization of TK1 with the plasma membrane of these cells

Additionally, plasma membrane proteins were isolated from the HT-29 cell line. The membrane proteins and cell extract were run on a 12% acrylamide SDS gel and then transferred to a nitro cellulose membrane and probed with anti-TK1 antibody (ab91651). We observe that TK1 is found in the membrane protein fraction of these cells further confirming the localization of TK1 on the membrane (Figure 3). Moreover, the plasma membrane and cytosolic protein fractions show oligomeric forms of TK1 (dimer and tetramer).

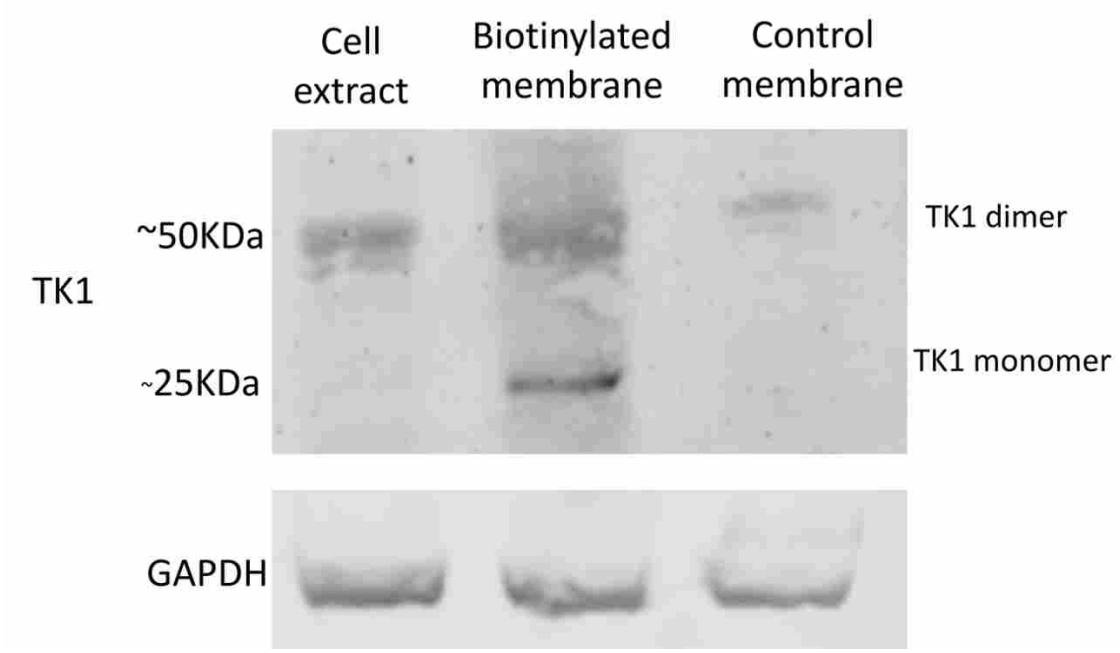

Figure 3- 3. Western blot of membrane proteins isolated from HT-29 cells probed with anti-TK1 antibody ab91651. Membrane proteins from HT-29 were biotinylated and isolated for Western blot analysis. Controls included membrane protein isolation from non-biotinylated cells and cell extracts. The results show TK1 is found in the membrane of HT-29 cells in monomeric (~25 kDa) and dimeric forms (~50 kDa).

Membrane TK1 expression is significantly lower in normal colon than malignant colon clinical samples

To maintain a healthy gastrointestinal health, the lining of the gastrointestinal track needs to undergo constant cell proliferation [64]. Since TK1's levels are proliferation-dependent, we wanted to test whether healthy normal colon cells expressed TK1 on their membrane to ascertain the clinical relevance of TK1 as biomarker target in colorectal cancer patients. We stained dissociated healthy and malignant colon tissue with anti-human CD45 antibody and PI to gate out resident lymphocytes and dead cells, and with anti-TK1 ab91651 and CD44 (positive control, adhesion protein) antibodies to test for surface expression of these two proteins. Flow cytometry revealed that the healthy normal colon tissue we tested (n=7) showed negligible expression of TK1 on the membrane when compared to isotype control (rabbit) (P=0.8004). Malignant colon tissue (n=7), however, showed significantly higher expression of TK1 on the membrane compared to normal colon tissue (P=0.0002) (Figure 3-4). CD44 expression levels were not significantly different between healthy normal and malignant colon tissues (P= 0.6634). These results are crucial in establishing clinical relevance of TK1's localization on the membrane as a unique event in cancer and not a proliferation-dependent event.

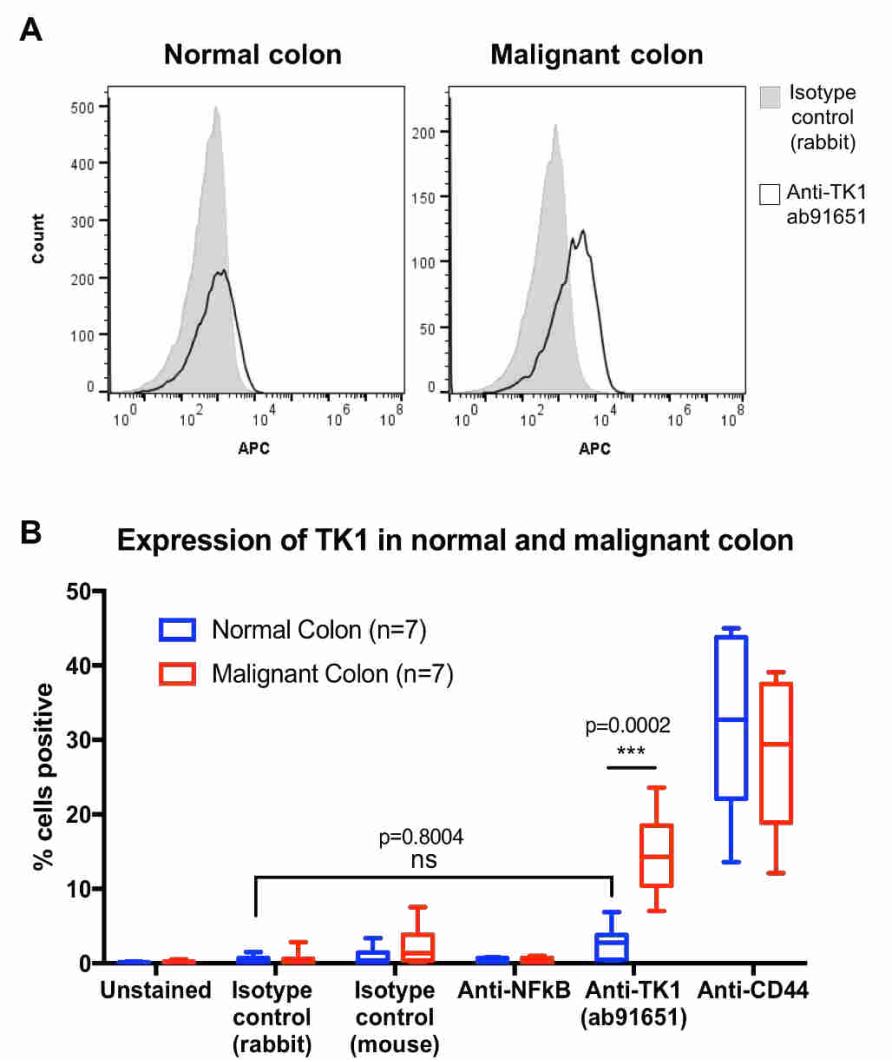

Figure 3- 4. Flow cytometry evaluation of TK1 expression on the surface of colorectal patient tissue.

Healthy normal and malignant colon tissue was dissociated into a single cell suspension solution and stained with anti-TK1 antibody 91651, isotype control, anti-CD44 (positive control), and anti-NFkB (negative control). Unstained cells were also used as a negative control. A) Flow cytometry histograms showing normal and malignant colon tissue stained with isotype control (gray area) and anti-TK1 antibody ab91651 (black line). There is a definitive shift in fluorescence in the malignant cells treated with ab91651, whereas there is no shift in fluorescence in the normal colon cells treated with the same antibody. B) Quantification and analysis of flow cytometry data on the expression of TK1 on the surface of normal and malignant colon. Malignant colon tissues show a significantly higher expression of TK1 on their membrane compared to normal colon tissues (P=0.002). Normal colon tissues show comparable results to those of the isotype control (P=0.8004), suggesting TK1 expression on the surface of normal colon tissues is negligible.

TK1 levels are significantly higher in malignant vs. normal healthy tissue

We stained lung, breast, and colon tissue arrays containing healthy normal, healthy normal adjacent, cancer adjacent, and malignant tissue with anti-TK1 antibodies to establish overall expression of TK1. We imaged all tissues with a light microscope at 20X. We conducted the analysis using a gray scale. The lower the gray value, the darker the staining. There was a significant increase in TK1 expression in malignant tissues compared to normal healthy tissues, where TK1 expression was negligible (Figures 3-5, 6, 7). However, there was also a portion of malignant tissues that stained negative for TK1 (Table 3-1).

TK1 staining in normal and malignant tissue

Tissue type	Negative	Positive
Lung adenocarcinoma	20	23
Lung squamous cell carcinoma	35	94
Normal lung	40	0
Cancer adjacent normal lung	10	0
Breast ductal carcinoma	6	19
Normal breast	24	0
Colon adenocarcinoma	9	26
Normal colon	10	0

Table 3- 1. TK1 staining in normal and malignant tissue.

Lung tissue array shows ~50% of the tissues stain positive for TK1 in both adenocarcinoma and squamous cell carcinoma (Figure 3-5 A, Table 3-1). We also observe that normal cancer adjacent tissue is negative for TK1 (Figure 3-5 A). We can observe a clear differential expression between malignant and normal healthy tissue in both lung adenocarcinoma and squamous cell carcinoma (Figures 3-5 B and 3-5 C). In breast tissue arrays, infiltrating ductal carcinoma positive for TK1 has a significantly lower average gray value than normal breast tissue stained for TK1 (Figure 3-6 A). TK1 staining localizes to the gland structures (Figure 3-6 A) in TK1+ tissue. Gland structures or stroma did not stain with TK1 antibody in TK1- tissue (Figure 3-6 B). These binary results are also observed in colorectal tissue arrays (Figure 3-7). However, metastatic adenocarcinoma stained negative for TK1 (n=9) (Figure 3-7 A). The darkest TK1 staining in colorectal adenocarcinoma can be found in groups of atypical glandular structures as seen in Figure 3-7 B. TK1- colorectal adenocarcinoma tissue shows no staining in the glandular structures (Figure 3-7 C).

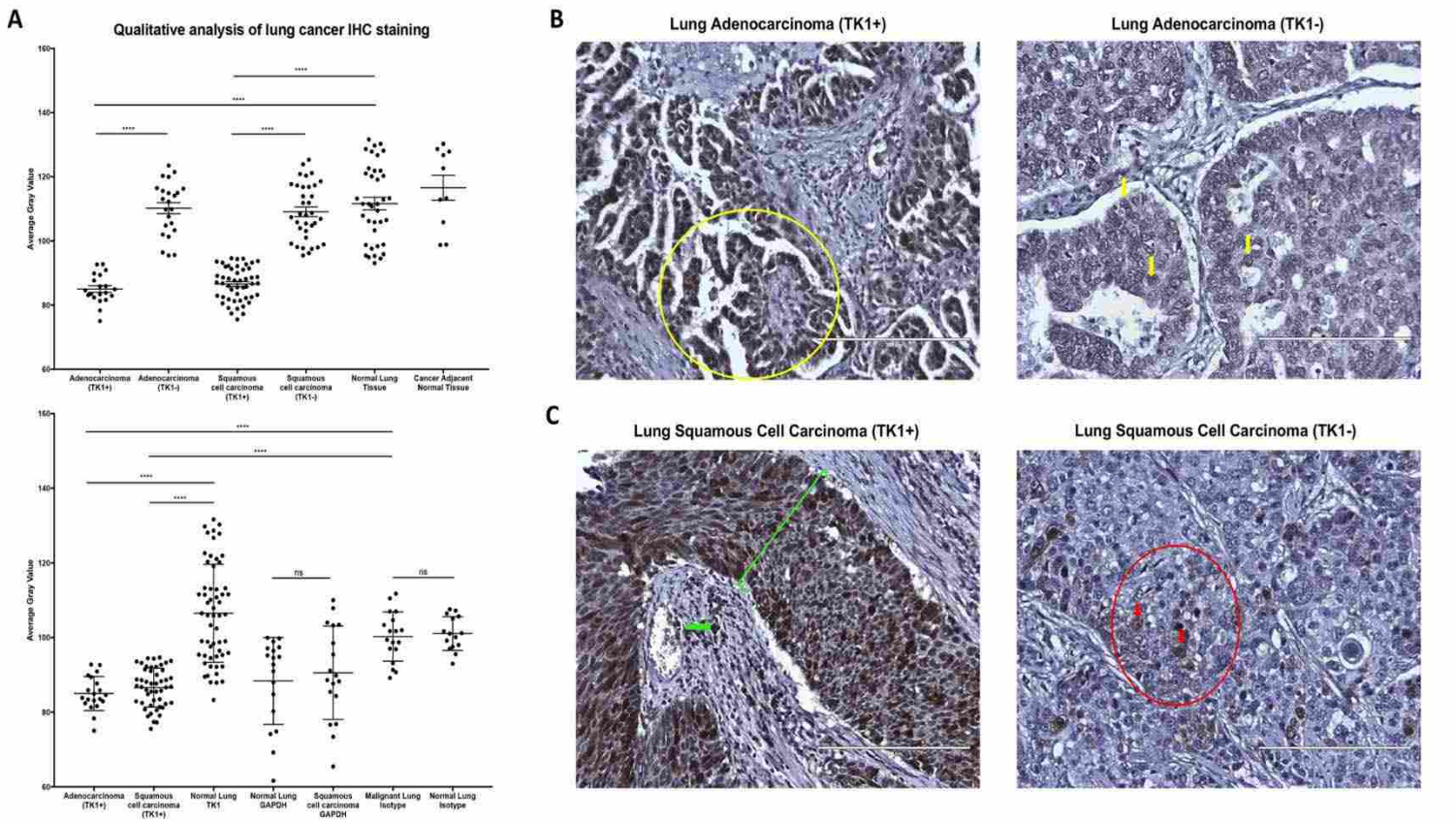

Figure 3- 5. Immunohistochemistry analysis of lung cancer tissue.
Lung cancer tissue arrays were stained with anti-TK1 antibody ab91651, GAPDH, or isotype antibody. GAPDH was used as a positive control to account for housekeeping gene expression. The isotype antibody was used to account for background noise and non-specific binding. Tissues were imaged in a light microscope at 20X. Analysis was conducted using a gray scale. The lower the gray value, the darker the staining. A) Quantitative analysis of lung cancer IHC staining. The top graph shows that there is a statistically significant expression of TK1 in ~53% of the lung adenocarcinoma tissues and in ~58% of the lung squamous cell carcinoma tissues. The bottom graph shows the TK1 expression next to GAPDH and isotype controls. Background levels show no statistical difference between malignant and normal healthy tissues. Malignant and normal healthy tissue showed non-statistical difference in GAPDH expression, whereas TK1 expression did show a statically significant difference between TK1+ and TK1- tissues. B) Images showing lung adenocarcinoma tissue positive and weakly positive for TK1, which we classified as TK1- with gray value quantification. The yellow circle in adenocarcinoma TK1+ image corresponds to lung papillary adenocarcinoma formed by abnormal proliferation of glanduliform structures of papillary disposition. The adenocarcinoma TK1- image shows pulmonary adenocarcinoma tissue with acinar pattern conformed by cells of convoluted nuclei, irregular membrane, and prominent central macronucleoli. The yellow arrows correspond to a diffuse weak positive nuclear staining for TK1. c Images showing lung squamous cell carcinoma tissue positive and weakly positive for TK1, which we classified as TK1- with gray value quantification. In the squamous cell carcinoma TK1+ image, the green line shows strong diffuse positive nuclear staining for TK1. The green arrow shows cytoplasmic background where there is evidence of infiltration in the underlying stroma shown by positive immunostaining against TK1. In the squamous cell carcinoma TK1- image, the red circle and arrows show weakly positive nuclear focal staining in poorly differentiated lung squamous carcinoma with solid pattern. ***P≤0.001; ns=P>0.05

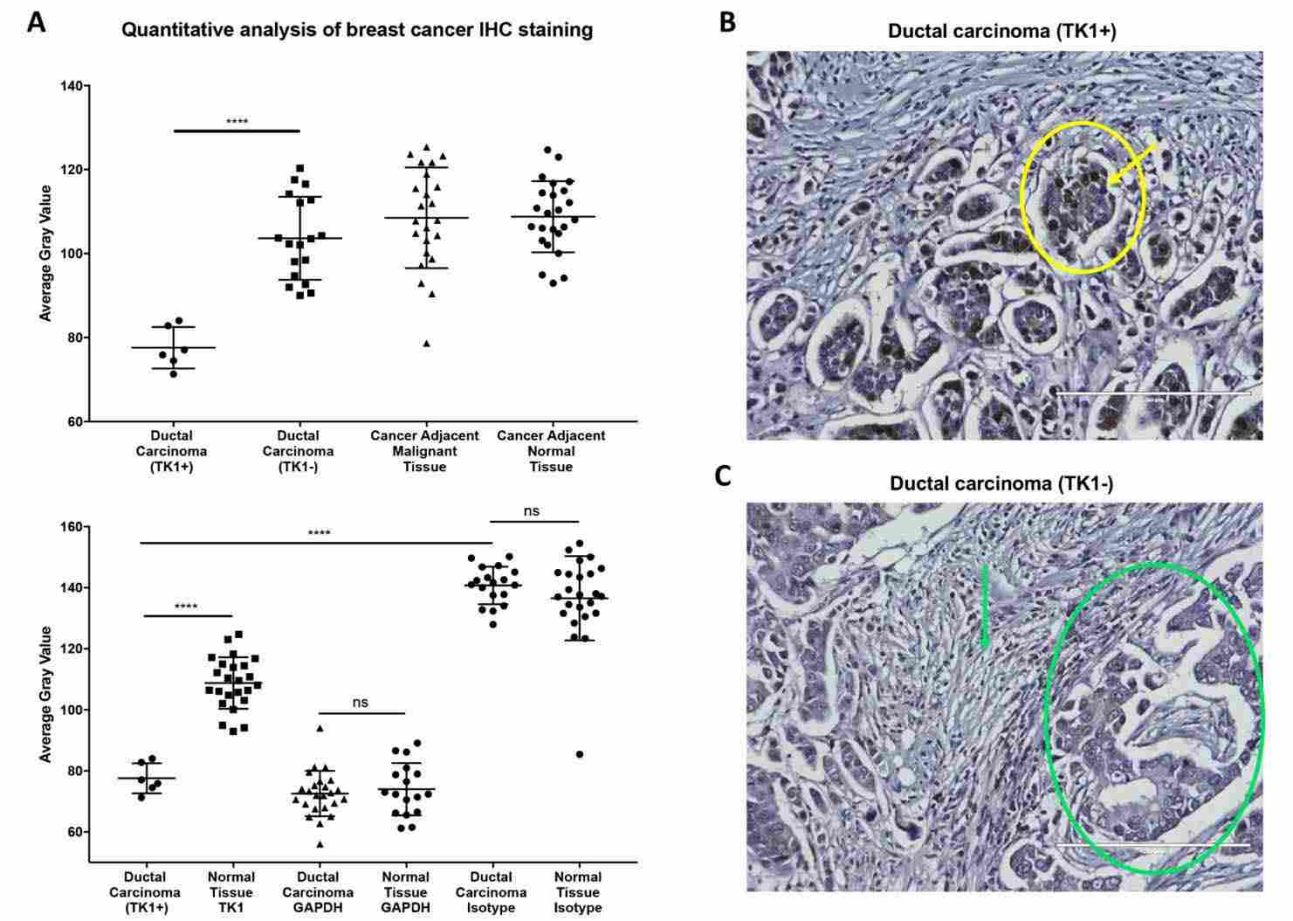

Figure 3- 6. Immunohistochemistry analysis of TK1 expression in breast cancer tissue.

Breast cancer tissue arrays were stained with anti-TK1 antibody ab91651, GAPDH, or isotype antibody. GAPDH was used as a positive control to account for housekeeping gene expression. The isotype antibody was used to account for background noise and non-specific binding. Tissues were imaged in a light microscope at 20X. Analysis was conducted using a gray scale. The lower the gray value, the darker the staining. A) Quantitative analysis of breast cancer IHC staining. The top graph shows that there is a statistically significant expression of TK1 in 20% of the ductal carcinoma tissues. The bottom graph shows the TK1 expression next to GAPDH and isotype controls. Background levels show no statistical difference between malignant and normal healthy tissues. Malignant and normal healthy tissue showed non-statistical difference in GAPDH expression, whereas TK1 expression did show a statically significant difference between TK1+ and TK1- tissues. B) Image showing breast ductal carcinoma positive for TK1. The yellow circle encloses a malignant gland structure corresponding to a moderately differentiated ductal carcinoma, and the arrow shows strong nuclear staining against TK1 in approximately 25% of the cells. C) Image showing breast ductal carcinoma negative for TK1. The green circle shows an atypical gland structure corresponding to moderately differentiated ductal carcinoma negative for staining against TK1. The green arrow shows the tumor stroma conformed by fibrotic tissue also negative for TK1. Overall, the tissues shown in figures 5b and 5c show what we observed in the tissue's average gray values represented in figure 5a, that some ductal carcinoma showed strong TK1 staining and some showed negative TK1 staining. ***P≤0.001; ns=P>0.05

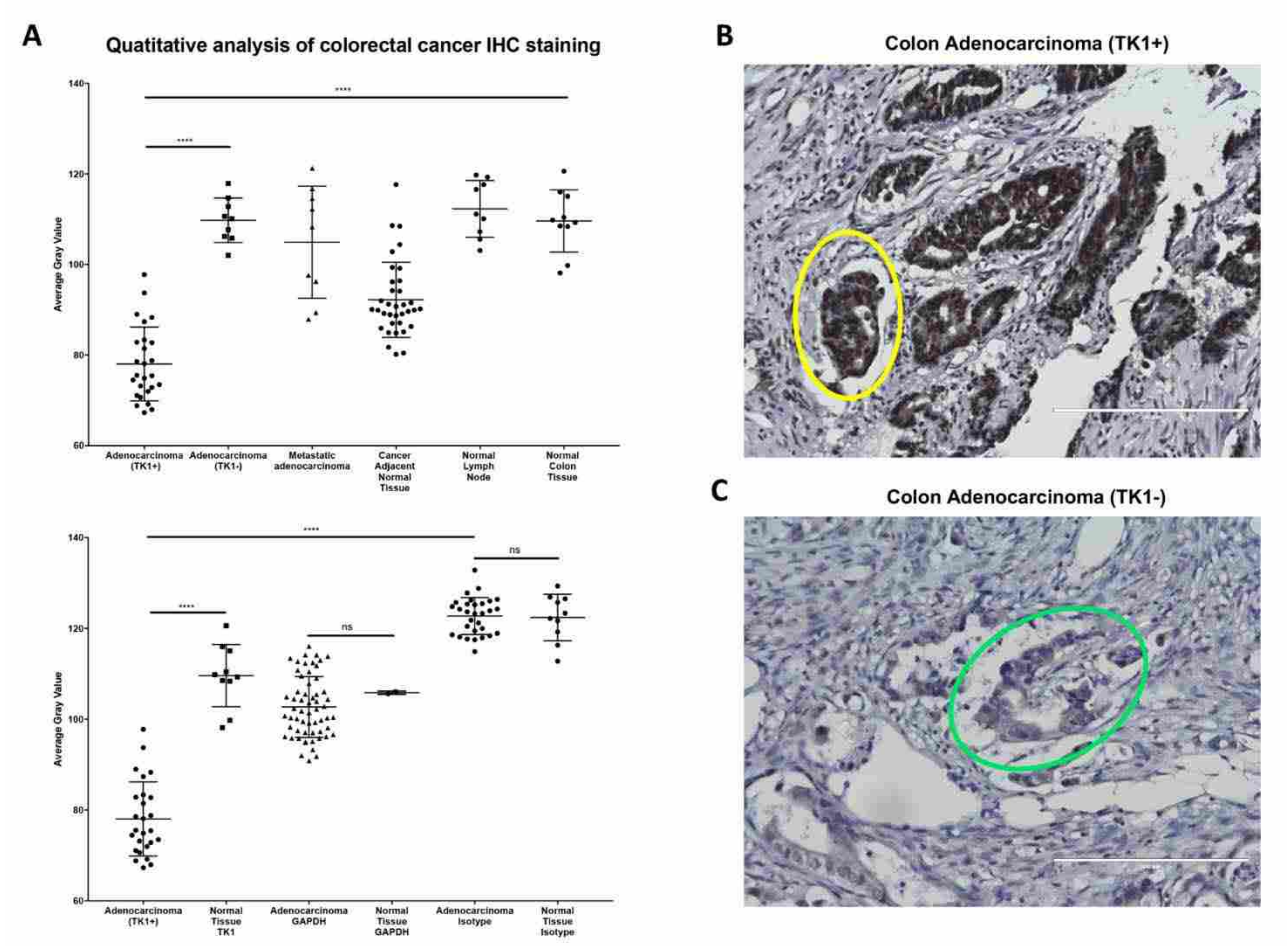

Figure 3- 7. Immunohistochemistry analysis of TK1 expression in colon cancer tissue.

Colon cancer tissue arrays were stained with anti-TK1 antibody ab91651, GAPDH, or isotype antibody. GAPDH was used as a positive control to account for housekeeping gene expression. The isotype antibody was used to account for background noise and non-specific binding. Tissues were imaged in a light microscope at 20X. Analysis was conducted using a gray scale. The lower the gray value, the darker the staining. A) Quantitative analysis of colorectal cancer IHC staining. The top graph shows that there is a statistically significant expression of TK1 in ~74% of the colon adenocarcinoma tissues. The bottom graph shows the TK1 expression next to GAPDH and isotype controls. Background levels show no statistical difference between malignant and normal healthy tissues. Malignant and normal healthy tissue showed non-statistical difference in GAPDH expression, whereas TK1 expression did show a statically significant difference between TK1+ and TK1- tissues. B) Image showing colorectal adenocarcinoma positive for TK1. The yellow circle encloses an atypical glandular structure positive for TK1 in over 90% of the cells. c Image showing colorectal adenocarcinoma negative for TK1. The circle an atypical glandular structure negative for TK1. Overall, the tissues shown in figures 3-7B and 3-7C show what we observed in the tissue's average gray values represented in figure 3-7A, that some colorectal adenocarcinoma tissues showed strong TK1 staining and some showed negative TK1 staining. ***P≤0.001; ns=P>0.05

TK1 gene expression levels are upregulated in malignant lung adenocarcinoma, lung squamous carcinoma, breast invasive carcinoma, and colorectal adenocarcinoma

We also evaluated TK1 expression using RNA-Sequencing data from The Cancer Genome Atlas. Our analysis reveals that TK1 levels are upregulated in both lung adenocarcinoma and lung squamous cell carcinoma, breast invasive carcinoma, and colorectal adenocarcinoma patients (Figure 3-8). Lung adenocarcinoma and lung squamous carcinoma seem to be the malignancies with the most differential expression of TK1 between normal and malignant patients, followed by breast invasive carcinoma, where we could also observe clear differential expression (Figures 3-8 A, 3-8 B, and 3-8 C). There was some overlap in TK1 expression in colorectal adenocarcinoma patients vs. normal patients, probably due to the highly proliferative nature of the colon, as TK1 levels rise during proliferation. However, TK1 levels in colorectal adenocarcinoma patients are still more upregulated than in healthy normal patients (Figure 3-8 D).

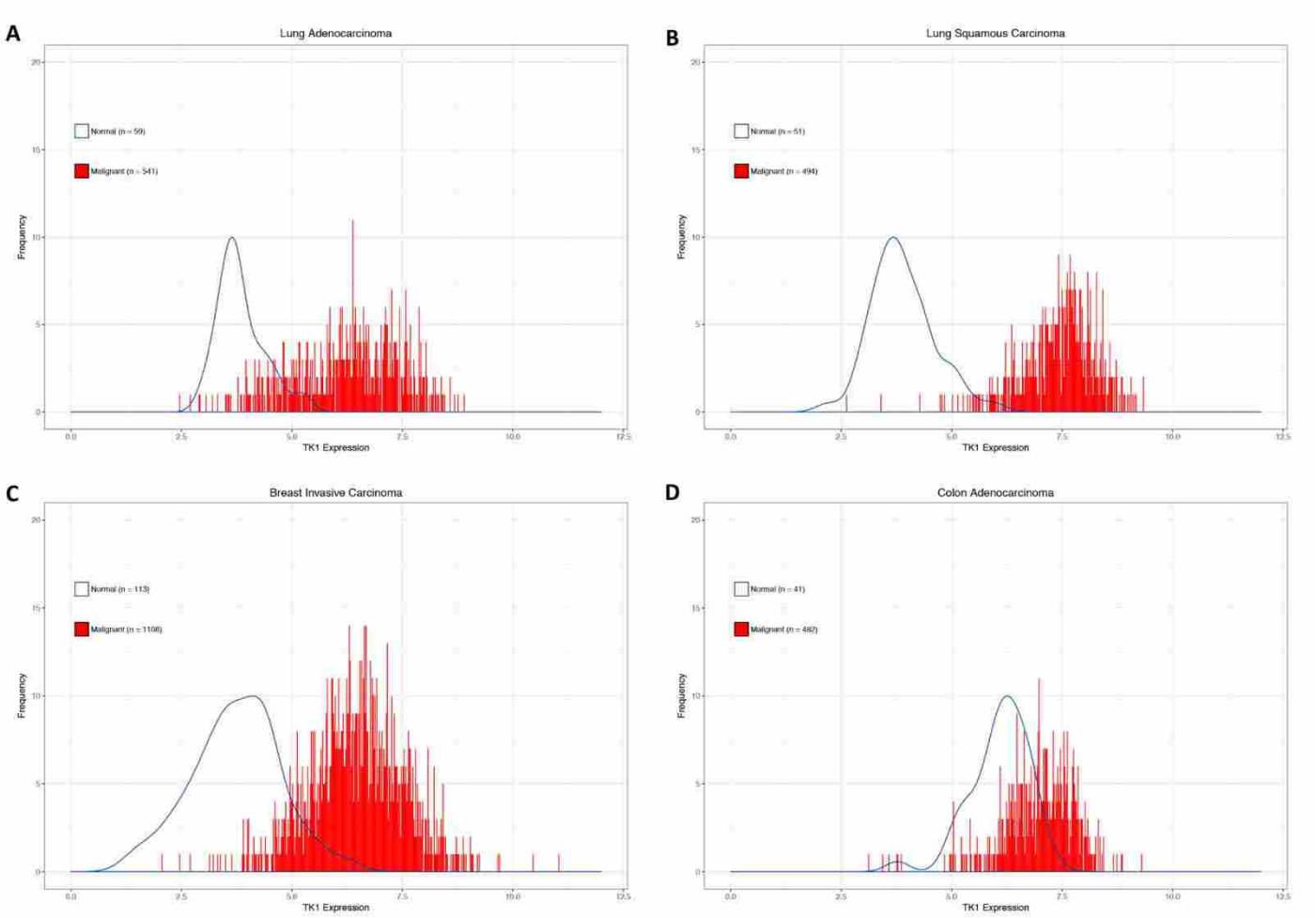

Figure 3- 8. Histograms of RNA-Sequencing data from The Cancer Genome Atlas showing increased TK1 gene expression in lung, breast, and colorectal cancer patients when compared to normal patients.

A) TK1 gene expression in lung adenocarcinoma vs. normal lung patients. B) TK1 gene expression in lung squamous cell carcinoma vs. normal lung patients. C) TK1 gene expression in breast invasive carcinoma vs. normal breast patients. D) TK1 gene expression in colon adenocarcinoma vs. normal colon patients

Triple negative breast cancer patients show higher levels of TK1 than HER2+ cancer patients

We evaluated TK1 gene expression using RNA-Sequencing data from TCGA in breast cancer patient available data for which hormone receptor status was available. Data was analyzed by tumors that were either HER2+ status or HER2- and ER-, and PR- status (triple negative breast cancer, TNBC). We found that TNBC tumor samples expressed higher levels of TK1 than HER2+ tumor samples (Figure 3-9). These data seem consistent with membrane expression of TK1 in MDA-MB-231 cells (TNBC), which express higher levels of TK1 on their surface than MCF7 cells (HER2+) when stained with ab91651 antibody (Figure 3-1C).

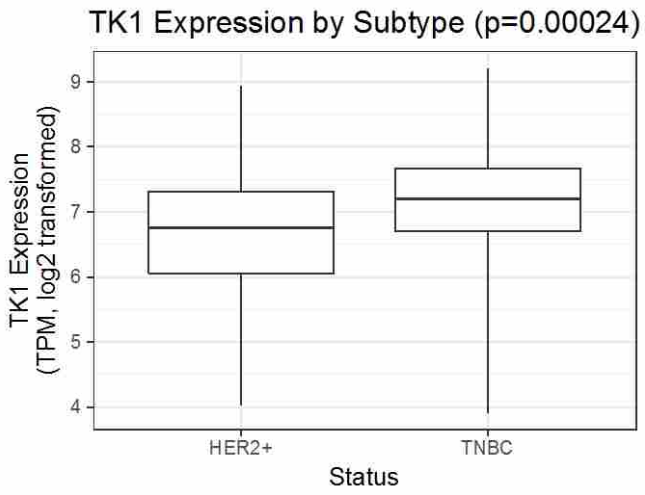

Figure 3-9. Boxplot of RNA-Sequencing data from The Cancer Genome Atlas showing TK1 gene expression in HER2+ breast tumors and triple negative breast cancer (TNBC) tumors.
The boxplot shows there is a significant upregulation in TK1 expression in TNBC tumors compared to HER2+ tumors.

TK1 expression levels in triple negative breast cancer show positive correlation with stem cell and EMT markers

RNA expression analysis was performed to evaluate the level of correlation between TK1 and six stemness and EMT genes (CD44, SNAI1, SNAI2, TWIST1, ZEB1, TGFB1). We found that in TNBC TK1 expression levels positively correlated with CD44 (rho=0.24) and SNAI1 (0.13), and negatively correlated with SNAI2 (rho=-0.14), TGFB1 (rho=-0.13), TWIST1 (rho=-0.02), and ZEB1 (rho=-0.35). On the other hand, we found that in HER2+ tumors, TK1 expression levels negatively correlated with all the markers (Figures 10 A-F). These results are interesting, as it reveals that TK1 levels may correlate with stemness and invasion potential in cancer cells.

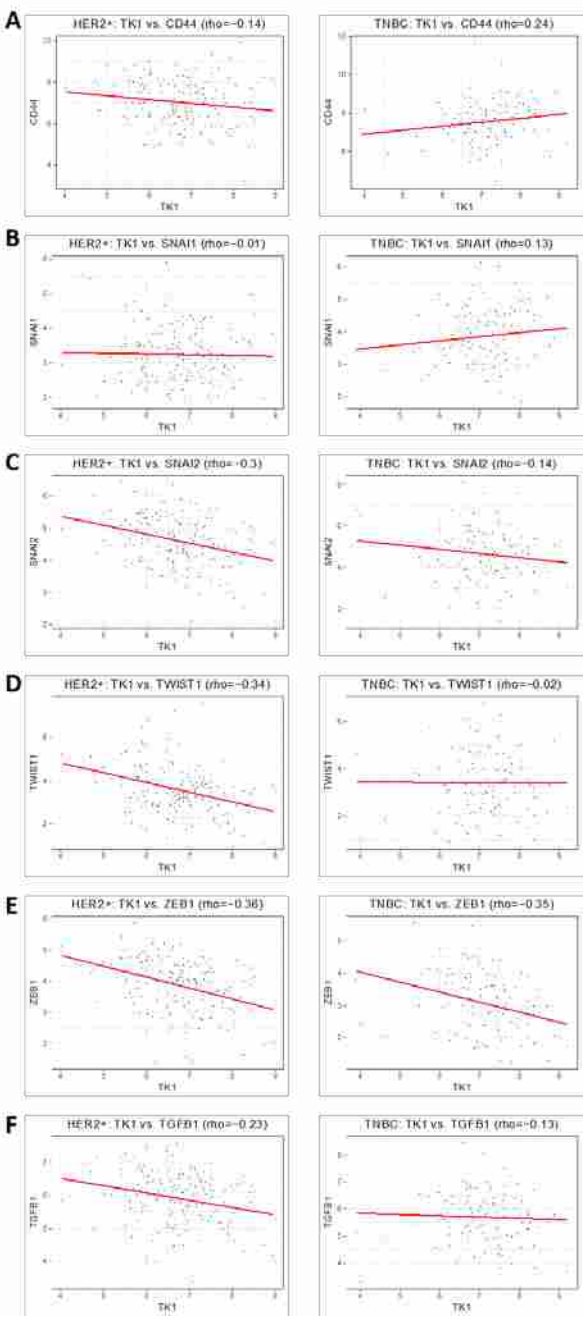

Figure 3-10. Scatterplots of RNA-Sequencing data from The Cancer Genome Atlas comparing TK1 expression to 6 stemness and EMT markers in HER2+ breast tumors and triple negative (TNBC) tumors.

A. Cell stemness marker CD44 is positively correlated to TK1 in TNBC tumors and negatively correlated to TK1 in HER2+ breast tumors. B. EMT marker SNAI1 is positively correlated to TK1 in TNBC tumors and negatively correlated to TK1 in HER2+ breast tumors. C. EMT marker SNAI2 is negatively correlated to TK1 in TNBC tumors and in HER2+ breast tumors. D. EMT marker TWIST1 is negatively correlated to TK1 in TNBC tumors and in HER2+ breast tumors. E. EMT marker ZEB1 is negatively correlated to TK1 in TNBC tumors and in HER2+ breast tumors. F. Stemness and EMT marker TGFB1 negatively correlated to TK1 in TNBC tumors and in HER2+ breast tumors.

Discussion

The salvage pathway enzyme TK1 plays a crucial role in pyrimidine deoxynucleotide synthesis during the cell cycle. Because of this critical association to proliferation and the cell cycle, TK1 has been established as a proliferation biomarker in many cancers, including lung, breast, and colorectal. Serum TK1 (sTK1) has been used in many applications for the early detection and diagnosis of cancer, as it is found upregulated in cancer patients. In this study, we present data supporting the expression and localization of TK1 on the cellular membrane of lung, breast, and colon cancer, suggesting TK1 as a surface marker for these malignancies and a different function for TK1 never reported before. The expression of TK1 on the surface of these solid malignancies seems to mirror that of other surface/stem cell markers such as NCAM in lung cancer, CD133 in lung and colon cancer, and CD298 in breast cancer [65–68]. Our results also correlated with some of our previous findings, which show that TK1 localizes on the surface of hematological malignancies such as Burkitt's lymphoma, acute lymphoblastic leukemia, promyelocytic leukemia, and T-cell lymphoma cells [69]. Interestingly, membrane TK1 seems to be found in monomeric and dimer form similar to membrane TK1 found in hematological malignancies, which suggest kinase enzymatic activity [69]. The actual function of membrane-expressed TK1 is still unknown, however.

Moreover, we show that in colon patient tissue, a highly proliferative tissue, TK1 is expressed on the membrane of only malignant cells and not healthy normal cells. This may mean that TK1's localization to the cell membrane is an event unique to malignancy. We have seen similar results in the expression of TK1 in hematological malignancies vs. normal proliferating lymphocytes, where TK1 only localized to the membrane of the cancer cells [69].

We also report clinical data from The Cancer Genome Atlas, where we explore TK1 gene expression levels, showing that TK1 levels are upregulated in lung, breast, and colorectal cancer patients compared to their healthy normal patients. The bioinformatics analysis reveals that the TK1 expression in some normal healthy tissues overlap with that of some malignant tissues. This is an important observation for clinical relevance, as the gene expression results correlate with our IHC results also shown in this study. IHC reveals that normal healthy tissue is negative for TK1, but some malignant tissue stains positive for TK1 and some malignant stains weakly positive or negative for TK1 in all lung, breast, and color tissue arrays. These results suggest that not all malignancies will have TK1 as a biomarker.

Clinically speaking, a good surface biomarker will be one that overexpresses on the membrane, shows stable expression levels in tumors, and is low or absent in normal cells/tissues [70]. For example, the Erb-B2 Receptor Tyrosine Kinase 2 (HER2) is overexpressed in subsets of breast, ovarian, gastric, colorectal, pancreatic and endometrial cancers [71]. In breast and colon cancer, HER2+ tumors are treated by targeting HER2 on the membrane[72,73]. Current treatments include Herceptin (trastuzumab), Perjeta (pertuzumab), Tykerb (lapatinib), and Kadcyla (T-DM1 or ado-trastuzumab emtansine). Comparing HER2 and TK1, both proteins are heterogeneously expressed in cancer tissues [20,74]. Moreover, surface expression levels of HER2+ cancer cell lines are comparable to surface expression of TK1. In fact, A549 and NCI-H460 cells lines show higher expression of TK1 on the surface to breast and colon cancer cell lines reported in the literature [75–77]. We also report that TK1 gene expression levels are significantly higher in TNBC vs. HER2+ breast tumors, suggesting TK1 as an alternative biomarker and potential target for TNBC. We also show that in TNBC tumors, TK1 levels positively correlate with 2 stemness and EMT markers, whereas in HER2+ tumors, TK1levels show the opposite correlation. This suggest

that increased levels of TK1 may aid or have a function in invasion and migration potential in cancer cells.

Further research is needed to help elucidate a mechanism by which TK1 reaches the cell membrane and to understand the function of TK1 on the membrane. This will help answer why some malignant tissues express TK1 and others do not. However, if the malignant tissue is indeed positive for TK1, TK1 could potentially be used as an immunotherapeutic target, either using antibodies against TK1, a drug-antibody conjugate, or a chimeric antigen receptor (CAR) T cell targeting TK1.

Declarations

Ethics approval and consent to participate

All procedures performed in studies involving human participants were in accordance with the ethical standards of the institutional and/or national research committee and with the 1964 Helsinki declaration and its later amendments or comparable ethical standards. Healthy and malignant colon tissues were obtained from Utah Valley Regional Medical Center in Provo, UT under informed consent and following a protocol established by Utah Valley Regional Medical Center.

Funding

This study was funded by the BYU Simmons Center for Cancer Research.

Acknowledgments

We would like to thank the Simmons Center for Cancer Research for the financial support, Dr. Juan Arroyo for his assistance in tissue staining and confocal microscopy, Dr. Himelda Chavez, for her pathology expertise and help in IHC analysis, and a team of surgeons at Utah Valley Regional Medical Center for providing normal and malignant colon tissue.

CHAPTER 4: TK1 Membrane Expression May Play a Role in the Invasion Potential of A549 Lung Cancer Cells

The following chapter is a manuscript submitted to the Journal of Cancer Therapy as a short report. All content and figures have been formatted for this dissertation but it is otherwise unchanged.

Abstract

Thymidine kinase 1 (TK1) is a well-studied cancer biomarker. It is commonly found upregulated in the serum of cancer patients, and its levels correlate with stage and grade, disease progression, and prognosis. It has recently been reported that TK1 localizes on the plasma cell membrane of hematological and solid malignancies, and not on the membrane of normal healthy cells, and while on the membrane, TK1 has enzymatic activity. However, the function of TK1 on the surface membrane is not well understood. Here, we hypothesize that it may have a role in tumor invasion and migration. It has been shown that TK1 expression levels positively correlate with epithelia to mesenchymal transition (EMT) markers in patients with breast cancer as they progress from HER2+ to triple negative breast cancer. In this study, we silenced TK1 expression by siRNA and show that TK1's membrane expression is significantly downregulated at 60 hours post transfection. Using a Matrigel-based quantitative invasion assay, we measured cell invasion potential in cells either expressing or lacking TK1 on their membrane and found that cells that lack TK1 on their membrane exhibit decreased invasion potential. These results suggest that TK1's presence on the membrane may play a role in invasion and cell migration in cancer.

Introduction

Thymidine kinase 1 (TK1) is a nucleotide salvage pathway enzyme primarily responsible for converting deoxythymidine to deoxythymidine monophosphate, and upon subsequent phosphorylation is incorporated into DNA [7]. During normal cell proliferation, TK1 is usually found in the cytoplasm where its expression is cell cycle-dependent, peaking during G1/S phase [78]. TK1 levels can also increase in response to DNA damage, especially after chemotherapy and radiotherapy. This increase is thought to provide cancer cells with a supply of nucleotides for DNA repair rather than for proliferation, and serves as a support mechanism to promote the survival of cancer cells [3]. Due to its tight regulation by the cell cycle, TK1 has been extensively studied in the context of cancer diagnostic biomarkers, where it has been shown to be upregulated in tissue and serum in both solid tumors and hematological malignances. TK1's prognostic and diagnostic potential has been demonstrated using the traditional TK activity radioassay for hematological malignancies and solid tumors including lung, breast, colon, bladder, cervical, and colorectal [18,21,22,29–31]. TK1 levels in serum have also been shown to have diagnostic potential in bladder cancer, cervical carcinoma, gastric cancer, non-small cell lung cancer, colorectal cancer, and renal cell carcinoma. In summary, high TK1 serum levels correlate with tumor aggressiveness and can be indicative of early events in carcinogenesis [15,28]. While TK1 has mostly been studied as a cancer biomarker in the serum, we have recently shown that TK1 localizes on the plasma membrane of cells and this is an event independent of proliferation and appears to be exclusive to malignant cells. For these reasons, TK1 may be a novel target for cancer immunotherapy. However, understanding TK1's function on the membrane is important as we approach the development of immunotherapy using TK1 as a target. Recently, it was reported that TK1 expression levels correlate with EMT markers in breast cancer in clinical samples as the disease progresses to triple negative breast cancer [79]. Additionally, due to serum

TK1 correlation with disease progression and aggressiveness, we hypothesized that membrane TK1 could have an immunoregulatory role and could aid in the invasion potential of cancer cells. In this study, we found that when membrane TK1 expression is silenced, cells lose invasion potential. These results suggest that TK1 may have a role in migration and immunoregulation, as well as in epithelial mesenchymal transitions (EMT).

Materials and methods

Cell line and cell culture

The non-small cell lung carcinoma A549 cell line was purchased from ATCC (Catalog # CCL-185™) and cultured in RPMI 1640 medium supplemented with 10% fetal bovine serum (FBS) and 2mM L-glutamine (both from Thermo Fisher Scientific, Waltham, MA). Cells were grown at 37 ºC and 5% CO_2 and fed 2-3 times per week by removing the medium, rinsing the cells with Dulbecco's Phosphate-Buffered Saline (DPBS, Gibco Thermo Fisher Scientific, Waltham, MA), incubating them with Accutase (Stem Cell Technology, Vancouver, Canada) for detachment and subculturing in a 1:4 ratio. For this experiment, cells were kept at a low passage to ensure best transfection efficiency.

siRNA library

Three validated siRNA against TK1 and control siRNA (GAPDH) were purchased from Thermo Fisher Scientific (catalog # 4390824, siRNA IDs s14158, s14159, and s14160 for TK1, and catalog # 4390849 for GAPDH). siRNA was resuspended in nuclease-free water at 50uM, aliquoted, and stored at -80 ºC. For working siRNA concentrations, siRNA was diluted to 10uM in nuclease-free water.

Transfection

Two hundred-thousand A549 cells were plated in 6 well-plates overnight to allow for attachment, after which, the medium was removed, and cells were washed with DPBS and 2mL

serum-free RPMI 1640 was added to each well. Lipid-nucleic acid complexes of RNAiMAX (Thermo Fisher Scientific, Waltham, MA, catalog # 13778030) and siRNA were prepared according to the manufacturer's instructions and added to the cells. 12 hours after transfection, medium and lipid-nucleic acid complexes were removed from cells and fresh complete RPMI 1640 medium was added to the cells. Cells were used at 60 hours post transfection, as recommended by manufacturer. (Cells treated with siRNA ID 14158 were named siRNA 58, those treated with siRNA ID 14159 were named siRNA 59, and those treated with siRNA ID 14160 were named siRNA 60

Flow cytometry

Transfected A549 cells were rinsed with DPBS, treated with Accutase at 37°C for 5-10 mins to allow for detachment, and then rinsed with complete medium. Cells were pelleted and resuspended at $1x10^6$ cells/mL in Cell Staining Buffer (BioLegend, San Diego, CA) and 200uL of cells were placed in individual microcentrifuge tubes and incubated with 5uL of Fc block (Human TruStain FcX™, BioLegend, San Diego, CA) for 10 minutes at room temperature, followed by incubation with 1 ug of anti-TK1 antibody (ab91651, Abcam, Cambridge, United Kingdom) for 15 minutes on ice. Cells were then washed with 1 mLCell Staining Buffer, incubated with anti-rabbit AlexaFluor647 antibody (Thermo Fisher, Waltham, MA, cat # A27040) and incubated on ice in the dark for 15 minutes. Cells were washed 2X with Cell Staining Buffer and resuspended in Fluorescence-activated cell sorting (FACS) buffer. FACS buffer was made with phosphate-buffered saline (PBS), 2% calf serum (Thermo Fisher, Waltham, MA), 1 mM EDTA (Thermo Fisher, Waltham, MA, CAS 6381-92-6), and 0.1% sodium azide (Sigma Aldrich, St. Louis, MO, CAS 26628-22-8). We collected $1x10^4$ events per

sample in a flow cytometer (Accuri C6 Plus, BD Biosicences, San Jose, CA) and data was analyzed using FlowJo software (FlowJo, Ashland, OR).

Invasion Assay

An xCELLigence RTCA DP instrument (Cat. 05469759001) was utilized to determine real time invasion and cell motility of A549 cells either expressing TK1 on their surface or after TK1 silencing. Invasion was assessed in 16 well CIM-Plates (Cat. 05665817001) (n=4) composed of an upper and lower chamber, each containing 16 wells. The top wells were coated with a 1:40 matrigel concentration and incubated for 4 hr. Cells were plated in the top chamber at a concentration of 50,000 cells/well in serum-free RPMI in a total volume of 100µL in the presence of the cells' corresponding media. The cells were allowed to migrate toward the bottom chamber wells which were filled with 160 µL of 10% FBS growth medium, as a source of chemoattractant (directional migration). The cells were then placed in the RTCA DP instrument and invasion readings were taken every 5 minutes for 24hr.

Statistical analysis

The flow cytometry data was analyzed with a one-way ANOVA test using the Sidak's correction for multiple comparisons to compare the expression of TK1 on the surface of the siRNA treated cells vs. isotype control. P-value significance was set at ≤ 0.05. Error bars represent the standard error of the mean. Statistical analyses were performed using Prism software.

Results

Flow cytometry

To asses TK1 silencing on the surface of A549 cells, a cell line known to express high levels of membrane TK1, we stained the control and siRNA treated cells with antibodies against

TK1. Flow cytometry revealed that A549 cells treated with siRNA targeting TK1 displayed decreased expression of TK1 on the surface. Cells treated with siRNA 58 and siRNA 59 showed significant reduction of TK1 on the surface, while siRNA 60 did not show a significant reduction (Figure 4-1). Cells treated with siRNA 58 had the most dramatic silencing in TK1 surface expression with a 93.82% reduction in surface expression compared to cells treated with control siRNA. Cells treated with siRNA 59 showed a 15.98% reduction at 60 hours post transfection.

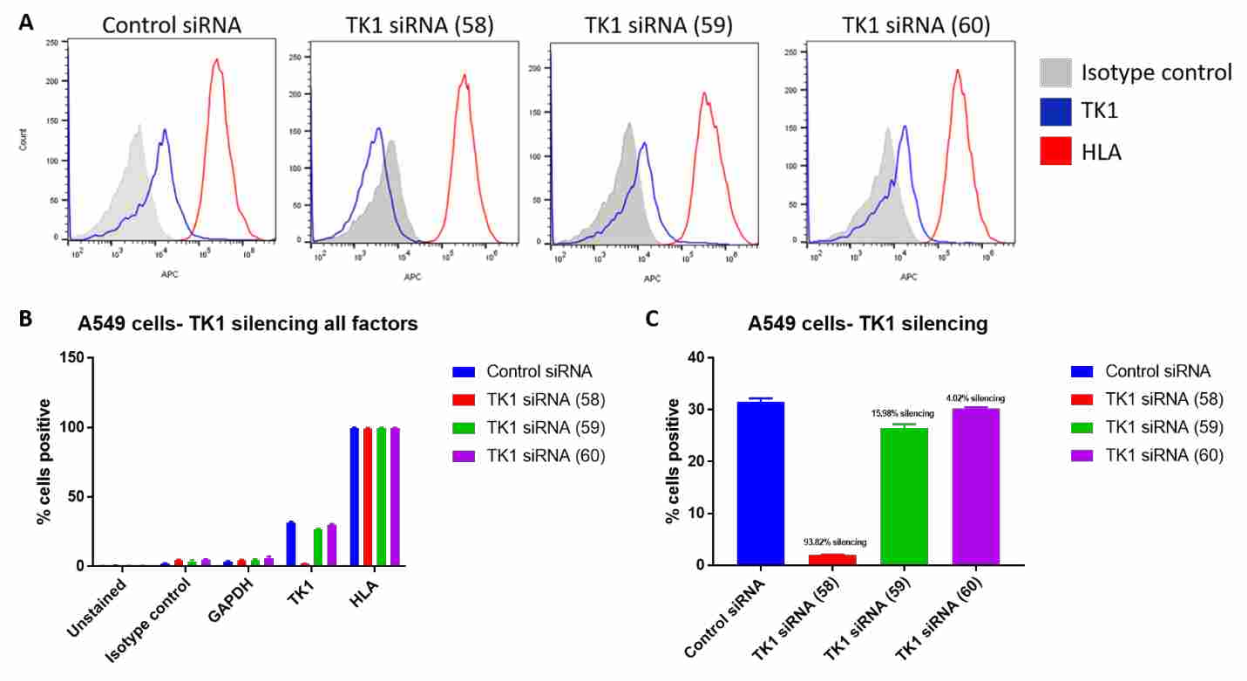

Figure 4- 1. Membrane expression of TK1 at 60 hours post siRNA transfection by flow cytometry.

A) Histograms showing membrane expression of TK1 compared to GAPDH and HLA. A549 cells transfected with siRNA 58 show a significant shift to the left when stained with TK1 antibody, suggesting decreased TK1 expression on the surface. B) Quantification of flow cytometry data showing the percentage of cells positive for APC stain. C) Quantification of flow cytometry data showing that transfection with siRNA 58 in A549 cells decreases TK1 expression by 93.82%.

Invasion study

To compare the invasion potential of A549 cells, with and without TK1 surface expression *in vitro*, we performed an invasion assay with A549 cells treated with control siRNA, siRNA 58, siRNA 59, and siRNA 60. In our study, the invasion potential of cells was measured by the cells crossing a layer of matrigel from serum-free medium towards complete medium, as they seek nutrients. In our results, we observed that when TK1 is highly silenced on the membrane, the invasion potential is reduced. In fact, only cells treated with siRNA 58, which had the most reduction of membrane TK1 expression, showed a significant reduction in invasion potential. Cells treated with siRNA 59 and siRNA 60 were statistically equally invasive to cells treated with control siRNA (Figure 4-2). We observed no change in cell viability before the invasion assay. Due to the short window of time post transfection, we did not evaluate growth rates. However, cell counts were similar between all transfected samples, so we assume there is no variability in cell growth rates.

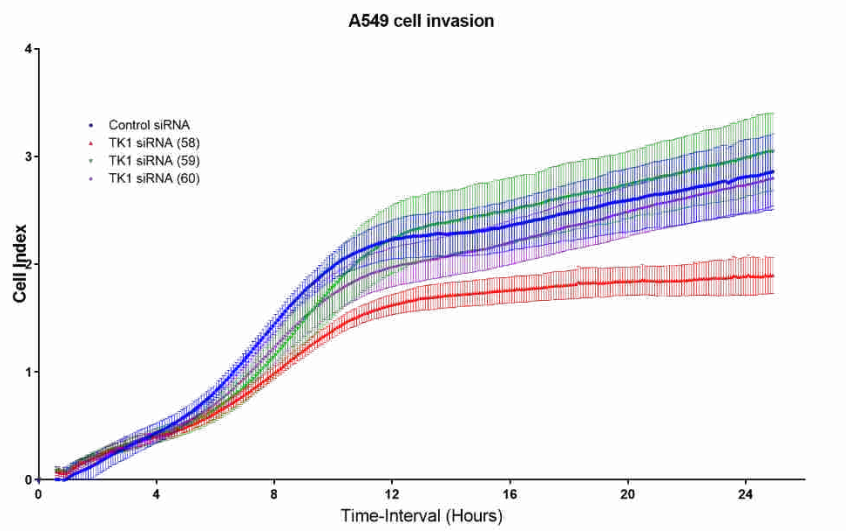

Figure 4- 2. Invasion assay with A549 cells transfected with TK1 siRNA.

Only A549 cells that had a drastic TK1 silencing show decreased invasion compared to control siRNA.

Discussion

TK1 has been studied as a serum biomarker since the late 80's. While its clinical application has been proven to be useful as a monitoring tool for disease progression and prognosis of most cancers, our group has found it to be a potential target in the clinic. TK1 was recently reported to be differentially expressed on the membrane of hematological and solid malignancies compared to normal cells. The localization of TK1 on the membrane appears to be an event unique in malignancy, as highly proliferative tissue like colon or normal lymphocytes induced to divide do not express TK1 on their surface. This posed the question as to why malignant cells upregulate TK1 on their surface and what the advantage in malignancy is. Recently, it was reported that stemness and EMT makers were more positively and strongly correlated to TK1 levels in triple negative breast cancer compared to HER2+ breast cancer, indicating that TK1 expression levels may also correlate with tumor invasion potential (summarized in Table 4-1) [79]. While not all genes show positive correlations, there is a positive trend in the Spearman' correlation coefficients between TK1 expression and these cell stemness and EMT markers between HER2+ and TNBC patients. Here we report that when we silence TK1 on the surface of A549 cells, their invasion potential decreases significantly. Further studies showing a connection of TK1 and migration or EMT markers could elucidate a potential immunoregulatory function.

Gene name	Function	HER2+: TK1 vs. gene (Spearman's correlation coefficient)	TNBC: TK vs. gene (Spearman's correlation coefficient)
CD44	Cell–cell interactions, cell adhesion and migration. Stemness marker.	0.14	0.24
SNAI1	Induction of epithelial to mesenchymal transition.	-0.01	0.13
SNAI2	Induction of epithelial to mesenchymal transition.	-0.3	-0.14
TWIST1	Induction of epithelial to mesenchymal transition.	-0.34	-0.02
ZEB1	Induction of epithelial to mesenchymal transition.	-0.36	-0.35
TGFB	Induction of cell migration and epithelial to mesenchymal transition.	-0.23	-0.13

Table 4- 1. Summary of Spearman's correlation coefficients between TK1 and cell stemness or EMT markers in HER2+ and TNBC patients.

CHAPTER 5: Macrophage Polarization and its Role in Cancer

The following chapter is taken from an article published in the Journal of Clinical & Cellular Immunology. All content and figures have been formatted for this dissertation but it is otherwise unchanged.

Abstract

The immune system plays an important role in the development and progression of cancer. Macrophages exhibit a variety of responses according to varying stimuli, and express different functions depending upon the microenvironment surrounding them. Macrophages can be pro-inflammatory (M1) or anti-inflammatory (M2). Research studies have shown that infiltration of macrophages can account for >50% of the tumor mass in some cancers, aid in metastasis by inducing angiogenesis, and signify a poor prognosis. Macrophages that migrate to the tumor site, remain there, and aid in angiogenesis and metastasis are termed tumor associated macrophages (TAMs) and are thought to express an M2 phenotype. This review will examine the polarization states of macrophages, their functions and role in cancer, their activation pathways and metabolism, and potential approaches to cancer immunotherapies using macrophages.

Introduction

Cancer is a group of diseases that involve unregulated cell growth and death, genome instability and mutations, tumor-promoting inflammation, induction of angiogenesis, evasion of the immune system, dysregulation of metabolic pathways, immortal cell replication, and activation of metastasis and invasion.[1] Cancer is the second leading cause of death in the United States after heart disease, and more than 1.6 million new cases are expected to be diagnosed each year. More than 580,000 Americans are expected to die yearly from cancer (about 1600 cancer

deaths per day), nearly 1 in 4 of all deaths overall.[80,81]⁸²⁸¹⁷²

The immune system plays an important role in the development and progression of cancer. In fact, immune cell infiltration to the tumor site can affect malignancy progression and metastasis.[83,84] Infiltration of macrophages to the tumor site has been shown to account for more than 50% of the tumor mass in certain breast cancer cases, suggesting macrophages have a significant role in tumor progression.[85–87]

Macrophages are cells derived from the myeloid lineage and belong to the innate immune system. They are derived from blood monocytes that migrate into tissue. One of their main functions is to phagocytose microbes and clear cellular debris. They also play an important role in both the initiation and resolution of inflammation.[88,89] Moreover, macrophages can exhibit different responses depending on the type of stimuli they receive from the surrounding microenvironment, varying from pro-inflammatory to anti-inflammatory.[90] In fact, two major macrophage phenotypes have been proposed: M1 and M2, which correspond to the extreme phenotypes of a spectrum of responses.

M1 macrophages are activated upon contact with certain molecules such as lipopolysaccharide (LPS), IFN-γ, IL-1β, TNF-α, and Toll-like receptor engagement, whereas M2 macrophages, also known as alternatively activated macrophages, exhibit immunomodulatory effects, tissue repair, and angiogenesis properties and can recruit regulatory T cells to inflammation sites. M2 macrophages are activated by anti-inflammatory cytokines such as IL-4, IL-13, and IL-10.[91,92]

The in vivo molecular mechanisms of macrophage polarization are poorly characterized because of the variety of signals macrophages experience in the cellular microenvironment.[88,93]

In recent years, progress has been made in identifying in vivo macrophage polarization under physiological conditions, especially during ontogenesis and pregnancy, and during pathological conditions such as allergies, chronic inflammation, and cancer. However, several macrophage populations are observed during specific pre-clinical and clinical conditions, as a result of the complex signaling between the tissue microenvironment and the immune system.[90] We do know, however, that in vitro macrophage polarization is plastic, and macrophages exposed to specific cytokines, can be polarized back and forth to either phenotype.[94,95] Interferon gamma (IFN-γ) and IL-4 are two cytokines that can polarize macrophages to M1 and M2 phenotypes, respectively.[94]

The presence of macrophages is crucial in tumor progression and growth, and has implications in determining prognosis.[96,97] Because macrophages can exhibit both pro-inflammatory and anti-inflammatory properties, it is important to understand their polarization and function in tumor progression and metastasis.

This review discusses the characteristics and functions of polarized macrophages, their role in cancer, their activation pathways and metabolic functions, and their use in potential cancer immunotherapy approaches.

M1 Phenotype

M1 macrophages, or classically activated macrophages, are aggressive and highly phagocytic, produce large amounts of reactive oxygen and nitrogen species, and promote a Th1 response.[90] M1 macrophages secrete high levels of IL-12 and IL-23, two important inflammatory cytokines. IL-12 induces the activation and clonal expansion of Th17 cells, which secrete high amounts of IL-17, and thus contribute to inflammation.[98] These characteristics allow M1 macrophages to control metastasis, suppress tumor growth, and control microbial infections.[99]

Moreover, the infiltration and recruitment of M1 macrophages to tumor sites correlates with a better prognosis and higher overall survival rates in patients with solid tumors.[96,97,100–103]

Inflammatory signals such as IFN-γ, TNF- α, IL-1ß and LPS can polarize macrophages to the M1 phenotype in vitro.[104,105] Transcription factors are also involved in the polarization of macrophages. Classically activated macrophages initiate the induction of the STAT1 transcription factor which targets CXCL9, CXCL10 (also known as IP-10), IFN regulatory factor-1 (IRF-1), and suppressor of cytokine signaling-1.[106] In the tumor microenvironment, Notch signaling plays an important role in the polarization of M1 macrophages, as it allows transcription factor RBP-J to regulate classical activation. Macrophages that are deficient in Notch signaling express an M2 phenotype regardless of other extrinsic inducers.[107] MicroRNA molecules (miRNAs) also regulate the polarization of macrophages. One crucial miRNA, miRNA-155, is upregulated when macrophages are transitioning from M2 to M1, and M1 macrophages overexpressing miRNA-155 are generally more aggressive and are associated with reduction of tumors.[108] Moreover, miRNA-342-5p has been found to foster a greater inflammatory response in macrophages by targeting Akt1 in mice. This miRNA molecule also promotes the upregulation of Nos2 and IL-6, both of which act as pro-inflammatory signals for macrophages.[109] Other miRNAs such as miRNA-125 and miRNA-378 have also been shown to be involved in the classical activation pathway of macrophages (M1).[110]

Classically activated macrophages are thought to play an important role in the recognition and destruction of cancer cells, and their presence usually indicates good prognosis. After recognition, malignant cells can be destroyed through several mechanisms, which include contact-dependent phagocytosis and cytotoxicity (i.e. cytokine release such as TNF-α).[99] Environmental signals such as the tumor microenvironment or tissue-resident cells, however, can

polarize M1 macrophages to M2 macrophages. In vivo studies of murine macrophages have shown that macrophages are plastic in their cytokine and surface marker expression and that re-polarizing macrophages to an M1 phenotype in the presence of cancer can help the immune system reject tumors.[111]

M2 Phenotype

M2 macrophages are anti-inflammatory and aid in the process of angiogenesis and tissue repair. They express scavenger receptors and produce large quantities of IL-10 and other anti-inflammatory cytokines.[108,112] Expression of IL-10 by M2 macrophages promotes a Th2 response, and Th2 cells, in turn, upregulate the production of IL-3 and IL-4. IL-4 is an important cytokine in the healing process because it contributes to the production of the extracellular matrix.[98] M2 macrophages exhibit functions that may help tumor progression by allowing new blood vessel growth, which feeds the malignant mass of cells, thus promoting their growth. The presence of macrophages (thought to be M2) in the majority of solid tumors negatively correlates with treatment success and longer survival rates.[83] Additionally, the presence of M2 macrophages has been linked to metastatic potential in breast cancer. Lin and colleagues (2006) found that early recruitment of macrophages to the breast tumor sites in mice increases angiogenesis and the incidence of malignancy.[113]

Single-marker identification of M2 macrophages reveals that they express CD163. However, further studies used a double-staining immunohistochemistry approach to identify M2 macrophages in their own microenvironment using CD163/CD68 and pSTAT1, RBP-J, or CMAF antibodies. These results showed that microenvironments from different model conditions known to stimulate a Th1 or Th2 response are all different, revealing the complexity of the microenvironment, thus making it hard to identify M2 macrophage populations in vivo.[114]

It is thought that the tumor microenvironment helps macrophages maintain an M2 phenotype.[98,115] Anti-inflammatory signals present in the tumor microenvironment such as adiponectin and IL-10, can enhance an M2 response.[116]

Macrophage polarization

The tumor microenvironment significantly affects macrophage polarization. The process of polarization can be diverse and complicated because of the complex environment of IL-10, glucocorticoid hormones, apoptotic cells, and immune complexes that can interfere with the function of innate immune cells.[90,111] The mechanisms of polarization are still unclear, but we know they involve transcriptional regulation. For example, macrophages exposed to LPS or IFN-γ will polarize towards an M1 phenotype, whereas macrophages exposed to IL-4 or IL-13 will polarize towards an M2 phenotype. LPS or IFN-γ can interact with Toll-like receptor 4 (TLR4) on the surface of macrophages inducing the Trif and MyD88 pathways, inducing the activation of transcription factors IRF3, AP-1, and NFκB and thus activating TNFs genes, interferon genes, CXCL10, NOS2, IL-12, etc. which are necessary in a pro-inflammatory response.[117] Similarly, IL-4 and IL-13 bind to IL-4R and activate the Jak/Stat6 pathway, which regulates the expression of CCL17, ARG1, IRF4, IL-10, SOCS3, etc., which are genes associated with an anti-inflammatory response (M2 phenotype).

Other transcription factors associated with macrophage polarization either towards an M1 or M2 response are IRF5, IRF4, Krüppel-like factor 4 (KLF4), CCAAT/enhancer-binding protein-β (C/EBPβ), PU.1, pSTAT1, RBP-J, and CMAF.[93,114,118–120]

Additional mechanisms of macrophage polarization include miRNA micromanagement. miRNAs are small non-coding RNAs of 22 nucleotides in length that regulate gene expression post-transcriptionally, as they affect the rate of mRNA degradation. Several miRNAs have been

shown to be highly expressed in polarized macrophages, especially miRNA-155, miRNA-125, miRNA-378 (M1 polarization), and miRNA let-7c, miRNA-9, miRNA-21, miRNA-146, miRNA147, miRNA-187 (M2 polarization).[110,120,121]

Macrophage polarization is a complex process. In the past years, there has been much controversy on the definition/description of macrophage activation and macrophage polarization. A recent paper published by Murray et al. describes a set of standards to be considered for the consensus definition/description of macrophage activation, polarization, activators, and markers. This publication was much needed to clarify the definition and characterization of activated/polarized macrophages [122].

Tumor Associated Macrophages (TAMs)

Cells exposed to a tumor microenvironment behave differently. For example, tumor associated macrophages found in the periphery of solid tumors are thought to help promote tumor growth and metastasis, and have a M2-like phenotype.[123]. Tumor associated macrophages can be either tissue resident macrophages or recruited macrophages derived from the bone marrow (macrophages that differentiate from monocytes to macrophages and migrate into tissue). A study by Cortez-Retamozo (2012) found that high numbers of TAM precursors in the spleen migrate to the tumor stroma, suggesting this organ as a TAM reservoir. TAM precursors found in the spleen were found to initiate migration through their CCR2 chemokine receptor.[124] Recent studies have found CSF-1 as the primary factor that attracts macrophages to the tumor periphery, and that CSF-1 production by cancer cells predicts lower survival rates and indicates an overall poor prognosis.[125–127] Other cytokines such as TNF-α and IL-6 have also been linked to the accumulation/recruitment of macrophages to the tumor periphery.[125]

It is thought that macrophages that are recruited around the tumor borders are regulated by an "angiogenic switch" that is activated in the tumor. The angiogenic switch is defined as the process by which the tumor develops a high-density network of blood vessels that potentially allow the tumor to become metastatic, and are necessary for malignant transition. In a breast cancer mouse model, it was observed that the presence of macrophages was required for a full angiogenic switch. When macrophage maturation, migration, and accumulation around the tumor was delayed, the angiogenic switch was delayed as well, suggesting that the angiogenic switch does not occur in the absence of macrophages, and that macrophage presence is necessary for malignancy progression.[128] Moreover, the tumor stromal cells produce chemokines such as CSF1, CCL2, CCL3, CCL5, and placental growth factor that will recruit macrophages to the tumor surroundings and provide an environment for macrophages to activate the angiogenic switch, during which macrophages will produce high levels of IL-10, TGF-β, ARG-1 and low levels of IL-12, TNF-α, and IL-6. The level of expression of these cytokines suggests macrophages modulate immune evasion. It is important to point out that in solid tumors, macrophages will be attracted by hypoxic environments and will respond by producing hypoxia-inducible factor-1α (HIF-1α) and HIF-2α, which regulate the transcription of genes associated with angiogenesis. During the angiogenic switch, macrophages can also secrete VEGF (stimulated by the NF-κB pathway), which will promote blood vessel maturation and vascular permeability.[129]

Tumor associated macrophages are thought to be able to maintain their M2-like phenotype by receiving polarization signals from malignant cells such as IL-1R and MyD88, which are mediated through the IκB kinase β and NF-κB signaling cascades. In fact, inhibition of NF-κB in TAMs promotes classical activation.[130] Moreover, another study suggested p50 NF-κB

as the factor involved in suppression of M1 macrophages, and that the inflammation reduction helped in tumor growth. When they created a p50 NF-κB knock-out mouse, they found out that M1 aggressiveness was restored and that tumor survival was reduced.[131]

Because the tumor mass contains a great number of M2-like macrophages, TAMs can be used as a target for cancer treatment. Reducing the number of TAMs or polarizing them towards an M1 phenotype can help destroy cancer cells or impair tumor growth.[132–134] Luo and colleagues in a study published in 2006, used a vaccine against legumain, a cysteine protease and stress protein upregulated in TAMs, as a potential tumor target. When the vaccine against legumain was administered to mice, the results showed that the angiogenesis genes were down-regulated and tumor growth was halted.[133]

Metabolism and activation pathways

Metabolic alterations present in tumor cells are controlled by the same mutations that produce cancer.[135,136] As a result of these metabolic alterations, cancer cells are able to produce signals that can modify the polarization of macrophages and promote tumor growth.[137,138]
M1 and M2 macrophages demonstrate distinct metabolic patterns that reflect their dissimilar behaviors.[139] The M1 phenotype is characterized by increased glycolysis and glucose metabolism which is skewed towards the oxidative pentose phosphate pathway, decreased oxygen consumption, and the production of large amounts of radical oxygen and nitrogen species, as well as inflammatory cytokines such as TNF-α, IL-12, and IL-6.[139,140] The M2 phenotype is marked by increased fatty acid intake and fatty acid oxidation, decreased flux towards the pentose phosphate pathway, increased overall cell redox potential, and upregulated scavenger receptors and immunomodulatory cytokines such as IL-10 and TGF-β.[139]

Multiple metabolic pathways play important roles in macrophage polarization. Protein kinases, such as Akt1 and Akt2, alter macrophage polarization by allowing cancer cells to survive, proliferate, and use an intermediary metabolism [141]. Other protein kinases can direct macrophage polarization through glucose metabolism by increasing glycolysis and decreasing oxygen consumption.[140,142] Shu and colleagues were the first to visualize macrophage metabolism and immune responses in vivo, using a PET scan and a glucose analog.[143]

L-arginine metabolism also exhibits discrete shifts important to cytokine expression in macrophages and is exemplary of distinct metabolic pathways altering TAM-tumor cell interactions.[144] Classically activated (M1) macrophages favor inducible nitric oxide synthase (iNOS). The iNOS pathway produces cytotoxic nitric oxide (NO), and cells consequently exhibits anti-tumor behavior. Alternatively activated (M2) macrophages have been shown to favor the arginase pathway, and produce ureum and l-ornithine, which contribute to progressive tumor cell growth.[144,145]

Direct manipulation of metabolic pathways can alter macrophage polarization. The carbohydrate kinase-like (CARKL) protein, which plays a role in glucose metabolism, has been used to alter macrophage cytokine signatures.[139,140] When CARKL is knocked down by RNAi, macrophages tend to adopt an M1-like metabolic pathway (metabolism skewed towards glycolysis and decreased oxygen consumption), whereas when CARKL is overexpressed, macrophages adopt an M2-like metabolism (decreased glycolytic flux and more oxygen consumption) [139]. When macrophages adopt an M1-like metabolic state through LPS/TLR4 engagement, CARKL levels decrease and the macrophages activate genes controlled by the NF-κB pathway such as TNF-α, IL-12, and IL-6, while also increasing cell redox potential by increasing concentrations of NADH:NAD+ and GSH:GSSSG complexes. During an M2-like

metabolic state, macrophages upregulate CARKL and genes regulated by STAT6/IL-4 (IL-10 and TGF-β).

Obesity can also affect macrophage polarization. Obesity is associated with a state of chronic inflammation, an environment that drives the IL4/STAT6 pathway to activate NKT cells, which further activate macrophages towards an M2 response. During late-stage diet-induced obesity, macrophages migrate to adipose tissue, where immune cells alter levels of TH1 or TH2 cytokine expression in the adipose tissue, causing an M2 phenotype bias and possibly increased insulin sensitivity.[146]

Switching the environment to a M1 phenotype bias by targeting metabolic pathways in TAMS may offer an alternative means of reducing tumor growth and metastasis.

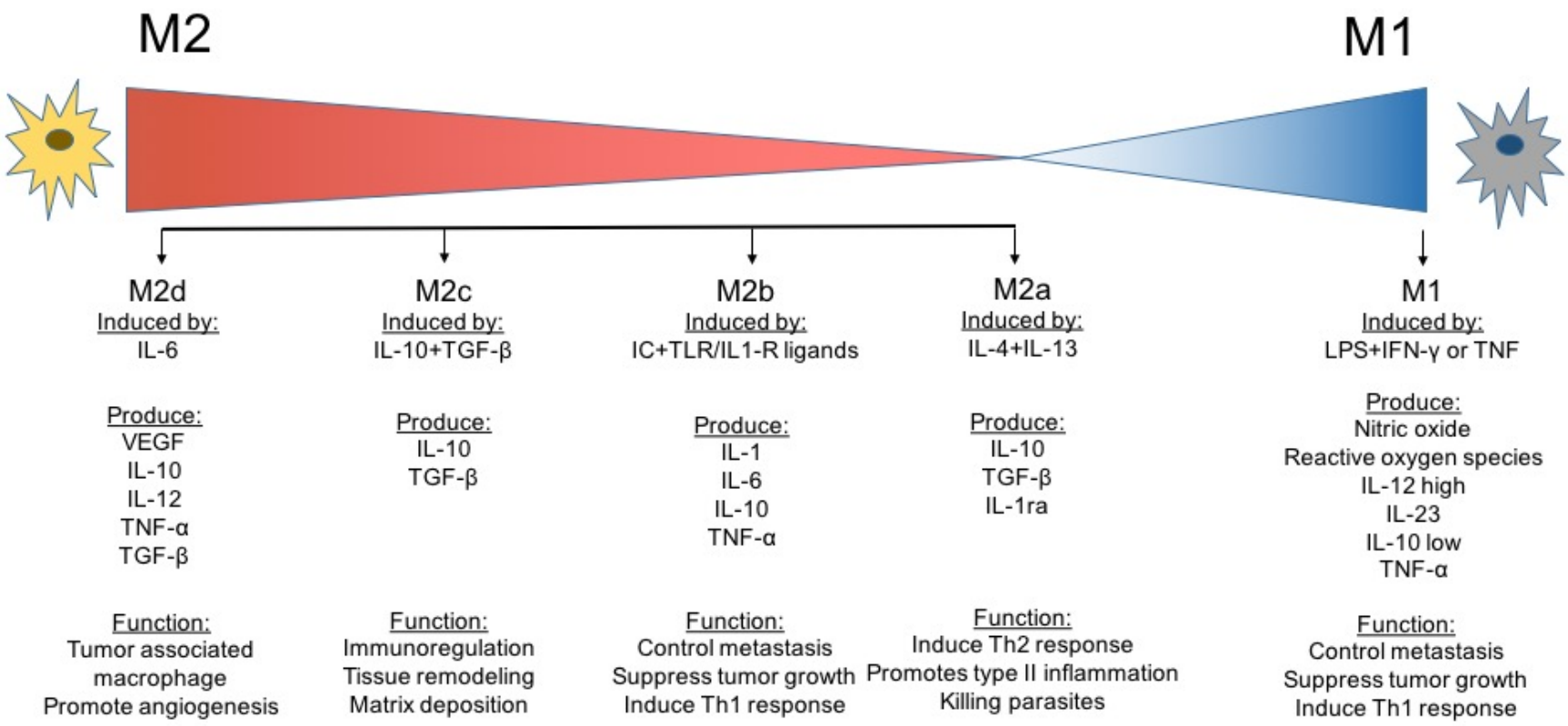

Figure 5- 3. Macrophage polarization is a spectrum.

Macrophage immunotherapy approaches against cancer

Cancer immunotherapy involves stimulation of the immune system to recognize, reject, and destroy cancer cells. Cancer immunotherapy with macrophages has the goal to polarize macrophages towards a pro-inflammatory response (M1), thus allowing the macrophages and other immune cells to destroy the tumor. Many cytokines and bacterial compounds can achieve this in vitro, although the side effects are usually too severe when replicated in vivo. The key is to find a compound that will have minimal or easily managed side effects in the patient. Immunotherapy using macrophages has been used in the past decades and new approaches are being developed every year.[147,148] Early immunotherapy established a good foundation for better cancer therapies and increased patient survival rates.[149]

Some approaches to cancer immunotherapy are the use of cytokines or chemokines to recruit activated macrophages and other immune cells to the tumor site and allow the tumor cells to be recognized as foreign and destroyed.[150,151] IFN- α and IFN-β have been shown to inhibit tumor progression by inducing differentiation and apoptosis.[152] Also, IFN treatments are anti-proliferative and can increase S phase time in the cell cycle.[153,154] Zhang (2002) performed a study in nude mice in which they used IFN-β gene therapy to target human prostate cancer cells. Their results show that adenovirus-delivered IFN-β gene therapy involves macrophages and helps suppress growth and metastasis.[155]

Another cytokine that can be used in cancer immunotherapy is macrophage inhibitory factor (MIF). MIF is usually found in solid tumors and its presence usually means poor prognosis. MIF, as its name describes, inhibits aggressive macrophage function, and therefore causes macrophages to express an M2 response. An M2 response can aid tumor growth and progression. Simpson, Templeton & Cross (2012) found that MIF induces differentiation of

myeloid cells, macrophage precursors, into a suppressive population of myeloid cells that express an M2 response. By targeting MIF, they were able to deplete this suppressive population of macrophages and inhibit their growth and thus control tumor growth and metastasis.[156]

The chemokine receptor type 2, CCR2, is crucial to the recruitment of monocytes to inflammatory sites and it has been shown as a target to prevent the recruitment of macrophages to the tumor site, thus preventing angiogenesis and metastasis. Sanford and colleagues (2013) studied a novel CCR2 inhibitor (PF-04136309) in a pancreatic cancer mouse model, showing that the CCR2 inhibitor depleted monocyte/macrophage recruitment to the tumor site and decreased tumor growth, metastasis, and increased antitumor immunity.[157] Another recent study showed that macrophages co-cultured with 10 different human lung cancers upregulated CCR2 expression. Moreover, they showed that using a CCR2 antagonist in a lung cancer mouse model reduced tumor growth and metastasis.[158]

Other studies have used liposomes to deliver drugs to deplete M2 macrophages from tumors and to stop angiogenesis. Cancer cells that express high levels of IL-1β grow faster and induce more angiogenesis in vivo. Kimura and colleagues (2007) found that macrophages exposed to tumor cells expressing IL-1β produced higher levels of angiogenic factors and chemokines such as vascular endothelial growth factor A (VEG-A), IL-8, monocyte chemoattractant protein 1, etc. When they used clodronate liposomes to deplete macrophages, they found fewer IL-1β-producing tumor cells. They also found that by inhibiting NF-κB and AP-1 transcription factors in the cancer cells, tumor growth and angiogenesis were reduced, which may suggest that macrophages that are found near the tumor site may be involved in the stimuli that allow macrophages to promote tumor growth and angiogenesis.[159]

Compounds such as methionine enkephalin (MENK) have anti-tumor properties in vivo and in vitro. MENK has the ability to polarize M2 macrophages to M1 macrophages by down-regulating CD206 and arginase-1 (M2 markers) while upregulating CD64, MHC-II, and the production of nitric oxide (M1 markers). MENK can also upregulate TNF-α and down-regulate IL-10.[160]

Recent studies have focused on bisphosphonates as a potential inhibitor of M2 macrophages. Bisphosphonates are commonly used to treat metastatic breast cancer patients to prevent skeletal complications such as bone resorption.[161] While bisphosphonates stay in the body for only short periods of time, they can target osteoclasts, cells in the same family as macrophages, due to high affinity for hydroxyapatite. Once bisphosphonates bind to the bones, the bone matrix internalizes the bisphosphonates by endocytosis and once in the cytoplasm, bisphosphonates can inhibit protein prenylation, an event that prevents integrin signaling and endosomal trafficking, forcing the cell to go apoptotic. Until recently, it was unknown whether bisphosphonates could target tumor associated macrophages, but a recent study by Junankar et al. has shown that macrophages uptake nitrogen-containing bisphosphonate compounds by pinocytosis and phagocytosis, events that do not occur in epithelial cells surrounding the tumor.[162] Forcing TAMs to go apoptotic may reduce angiogenesis and metastasis.

Additional approaches to cancer immunotherapy include the use of biomaterials that may elicit an immune response. Cationic polymers are used in immunotherapy because once dissolved in water they can react with nucleic acids, adjuvants, etc. Chen et al. (2010) used cationic polymers including PEI, polylysine, cationic dextran and cationic gelatin to produce a strong Th1 immune response. They were also able to induce proliferation of CD4+ cells and to induce secretion of IL-12 in macrophages, a cytokine produced by M1 macrophages.[160] Huang

and colleagues (2013) also used biomaterials to modulate TAMs to an anti-tumor response by targeting TLR4. This study found that TAMs were able to polarize to an M1 phenotype and express IL-12. They found that these cationic molecules have direct tumoricidal activity. They were also able to show tumor reduction in mice.[163]

Cancer immunotherapy approaches using macrophages		
Type	Name	Result
Cytokine/ chemokine	IFN- α and IFN-β	Inhibit tumor progression
		Induce apoptosis in cancer cells
		Induce differentiation of monocytes to macrophages
	CCR2	Prevents recruitment of monocytes/macrophages to the tumor site
	Anti-MIF shRNA	Depletes M2 macrophage population from tumor site
Inorganic molecules	MENK	Polarizes macrophages from M2 to M1
		Downregulates CD2016, arginase 1, and IL-10
		Upregulates CD64, MHC-II, TNF-α, and nitric oxide
	Bisphosphonates	Induce apoptosis in TAMs
		Reduce the number of infiltrating TAMs to the tumor site
		Impairs angiogenesis
	Cationic polymers (PEI, polylysine, cationic dextran and cationic gelatin)	Induce a Th1 response
		Induce proliferation of CD4+ cells
		Induce upregulation of IL-12 in macrophages
Vesicles	Liposomes	Deplete IL-1β producing cancer cells
		Inhibit production of angiogenic factors (VEGF-A, IL-8, monocyte chemoattractant protein 1)

Table 5- 1. Cancer immunotherapy approaches using macrophages

Conclusion

Macrophages play an important role in tumor progression and metastasis because of the plasticity they express during activation, especially in vivo. Depending on the signals present in the tumor microenvironment, macrophages can express pro-inflammatory (M1 phenotype) or anti-inflammatory (M2 phenotype) responses. The tumor microenvironment can polarize macrophages towards an M2 response, an anti-inflammatory response, which can lead to tumor progression, angiogenesis, and metastasis. M2 macrophages resemble tumor associated macrophages (TAMs) which help recruit blood vessels at the tumor site and allow the tumor cells to invade other tissues.

It is obvious that macrophages play a significant role in cancer progression, and immunotherapies involving macrophages should be considered in the treatment of this disease. The polarization of macrophages towards an M1 response with minimal side effects may prove to be a powerful therapy against solid tumors. Inflammatory signals such as LPS or TNF-α can easily polarize macrophages towards an M1 phenotype in vitro. However, use of substances such an LPS and TNF-α in vivo exacerbate a whole-body inflammatory response involving cells of both the innate and adaptive immune systems. They can cause fever and inflammation in several tissues including the mucosal surfaces and the lungs. These inflammatory signals are highly cytotoxic as well.[164–166] This can be detrimental to cancer patients and compromise their health.

Current approaches to cancer immunotherapy using macrophages involve the use of macrophage-granulocyte colony-stimulation factor (GM-CSF), cytokines and chemokines such as MIF and interferons (IFN-α and IFN-β), and vaccines and biomaterials that can elicit immune responses. These approaches have been shown to reduce tumor size and angiogenesis, recruit immune cells to the tumor site, and prevent the polarization of macrophages to an M2 phenotype.

Because immunotherapy requires the activation of the immune system, it is difficult to find a cytokine, chemokine, compound, or biomaterial that will not produce some side effects. However, because macrophages belong to the innate immune system and exhibit pro-inflammatory and anti-inflammatory properties, they are ideal immunotherapy candidates.

Further work is needed to identify substances and protocols that can adeptly re-educate the immune system to attack cancer cells, prevent angiogenesis and metastasis, and to protect the host from developing a damaging inflammatory response.

APPENDIX 1: How Does the Tumor Microenvironment Affect Macrophage Aggressiveness?

The following appendix contains data that accompanies a published abstract in Cancer Research. These data were presented at the American Association for Cancer Research Annual Meeting in 2014. I have modified the abstract to reflect recent changes in macrophage nomenclature.

Abstract

The immune system plays an important role in the development and progression of cancer. In fact, immune cell infiltration can affect malignancy progression and metastasis. Infiltration of macrophages to the tumor site has been shown to account for more than 50% of the tumor mass in some breast cancers suggesting macrophages have a significant role in tumor progression. Macrophages are cells derived from the myeloid lineage and belong to the innate immune system. They differentiate from blood monocytes in tissue and one of their main functions is to phagocytose microbes and clear cellular debris. Macrophages also play an important role in inflammation and the resolution of inflammation. They exhibit a variety of responses depending on the type of stimuli they receive, varying from pro-inflammatory to anti-inflammatory. Two major macrophage phenotypes have been proposed: M1 and M2. M1 macrophages, or classically activated macrophages, show a pro-inflammatory profile that is characterized by aggressive phagocytosis and anti-microbial properties. M2 macrophages, also known as alternatively activated macrophages, exhibit immunomodulatory, repair, and angiogenic properties. This project explored macrophage function by studying the aggressiveness of macrophages exposed to different cancer cell lines (Raji, H460, MCF7, MDA-MB-231, HT-29, SW620, and PC3) and their spent media. We used U937-derived macropahges

and as phagocytes. Macrophage aggressiveness was measured through flow cytometry by quantification of macrophage engulfment rates of fluorescent spherical beads. We found that cancer cell lines with higher aggressiveness had a more radical suppression of macrophage engulfment (81% engulfment reduction compared to control) than less aggressive cell lines (1% engulfment reduction compared to control). We also found that spent media had a lower effect on macrophage engulfment overall, indicating cell to cell contact is important to suppress macrophage engulfment. Spent media from aggressive cell lines had a similar effect to the cells themselves, suggesting cytokine and vesicle communication. We also studied how these cell lines affected macrophage polarization by qPCR, finding that lower engulfment rates correlate with an M2 cytokine profile (high IL-10, low IL-12) and higher engulfment rates correlate with an M1 cytokine profile (low IL-10, high IL-12). Further studies will help us understand more of the signals that cancer cells give to their environment to prevent macrophage engulfment and to help maintain an M2 phenotype.

Materials and Methods

Cell lines and culture

U937, Raji, H460, HT-29, MCF7, MDA-MB-231, SW620, and PC3 cell lines were purchased from ATCC. All cell lines were authenticated by STR analysis. We cultured U937, Raji, and H460, HT-29, and PC3 cell lines in RPMI 1640 supplemented with 10% FBS and 2mM L-glutamine and grown at 37°C with 5% CO_2. MCF7, MDA-MB-231, and SW620, cell lines were cultured in DMEM supplemented with 10% FBS and 4mM L-glutamine grown at 37°C with 5% CO_2. To obtain spent media, we cultured Raji, H460, MCF7, MDA-MB-231, HT-29, SW620, and PC3 in their respective complete medium for 48 hours. We collected the spent media and centrifuged it at 300 x g for 15 minutes to pellet cells and cellular debris. The

supernatant was used in the experiments. Normal mononuclear lymphocytes were separated from whole blood using lymphocyte separation medium, then washed and resuspended in RPMI 1640 medium (supplemented with 20% human serum from the blood donor). Spent media was collected by collecting the media after 48 hours of culture and centrifuging it at 300 x g for 15 minutes to pellet cells and cellular debris. The cellular pellet was used as cells in the experiments.

Preparation of Macrophages

We stimulated U937 cells, a monocytic cell line, with phorbol 20nM 12-myristate 13-acetate (PMA) for 24 hours to allow for differentiation. After 24 hours, we changed media and cultured the attached cells for an additional 24 hours. We detached the cells by scrapping and resuspended them at $1x10^6$ cells/mL and dyed them with eFluor670 proliferation dye (eBioscience) following manufacturer's instructions.

Engulfment Assay

We incubated differentiated U937 cells with either Raji, H460, MCF7, MDA-MB-231, HT-29, SW620, or PC3 cancer cells or their spent media for 48 hours. For the co-culture with cancer cell lines, we used 12- well plates, placing a 0.4uM trans-permeable well inserts and adding $5x10^5$ differentiated dyed U937s at the bottom of the well and the $5x10^5$ cancer cells on top of the trans-permeable well. For the spent media treatment, we placed $5x10^5$ differentiated dyed U937s at the bottom of the wells of a 12-well plate and added 500uL of spent media from either Raji, H460, MCF7, MDA-MB-231, HT-29, SW620, PC3, or normal lymphocytes. After 48 hours of incubation, we removed the trans-permeable wells and added 75 uL of FBS-coated PE-conjugated microspheres (beads) and incubated for 1 hour. To coat the beads in FBS, we resuspended 1 drop of beads into 4mL of FBS and incubated for 30 minutes. After incubating the

U937 cells with beads for 1 hour, we detached the U937s from the wells using cell scrapers. Cells were washed 3X to remove medium and beads that were not phagocytosed.

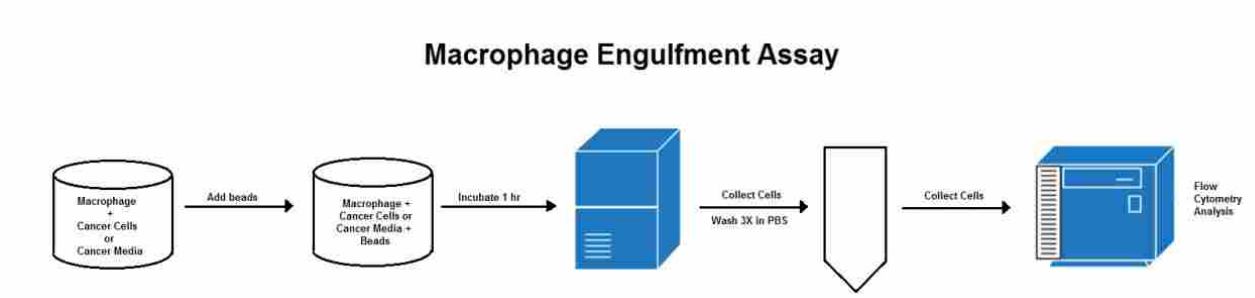

Figure A1- 1. Diagram of the macrophage engulfment assay.

Flow Cytometry Analysis

U937s were analyzed for bead engulfment using BD FACSCanto flow cytometer. $1x10^4$ events were collected per sample. We first gated on APC^+ cells, which represented U937 cells, and then gated on PE^+ cells. APC^+PE^+ cells represent U937 cells that engulfed at least one bead. The population of APC^+PE^+ cells can be further gated into 1 bead, 2 beads, and 3+ beads, depending on their fluorescence. The more beads the macrophage engulfs, the more aggressive or inflammatory it is.

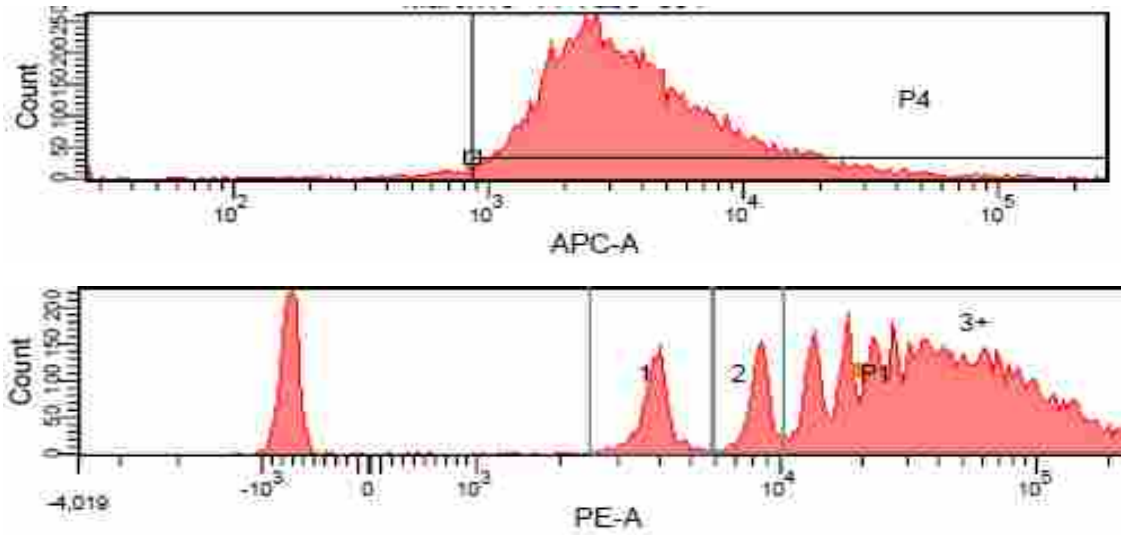

Figure A1- 2. Flow cytometry analysis of the engulfment assay.
The top histogram (gate P4) represents cells that are APC+. The bottom histogram is derived from gate P4 and represents cells APC+PE+. The peaks represent cells with either 1, 2, or 3+ beads engulfed.

Gene expression analysis

RNA was extracted from the U937 cells using the RNAAqueous Total RNA Isolation Kit following manufacturer's instructions. RNA was stored at -80℃ until use. For qPCR, we used the qScript XLT 1-Step RT-qPCR ToughMix (Quantabio) and IL-1B, IL-10, and IL-12 generic Taqman primers (ThermoFisher). We used Actin as our primer control. We performed the qPCR reaction in a StepOne Real Time PCR System (ThermoFisher) using the comparative qPCR setting. We analyzed the raw data using the double delta Ct analysis comparing actin gene expression to IL-1B, IL-10, and IL-12.

Results

U937-derived macrophage engulfment is decreased when they are exposed to cancer cell spent media and cancer cells

Total macrophage engulfment was reduced when we exposed U937-derived macrophages to HT-29 spent media and cells, to MCF7 and MDA-MB-231 spent media and cells, Raji spent media and cells, PC3 cells, and normal lymphocyte spent media (Figure A1-3).

3+ Bead engulfment population decreases when U937-derived are exposed to cancer cell spent media and cancer cells

When we looked at the individual bead populations within the macrophages that engulfed at least one bead, we notice that there is a significant decrease of bead engulfment in the 3+ Bead population. As the 3+ Bead population decreases, the 1 Bead population either decreases as well or increases. We believe this is because the macrophages are becoming less aggressive and polarizing towards and anti-inflammatory profile, such as M2. We observed the most change in colon cancer cell lines HT-29 and SW620, breast cancer cell lines MFC7 and MDA—MB-231, prostate cancer cell line PC3, and Burkitt's lymphoma cell line Raji. We observed an increase in the 3+ Bead population in the normal lymphocyte cell treatment. This was expected as normal cells wouldn't induce immunosuppression in macrophages (Figure A1-4).

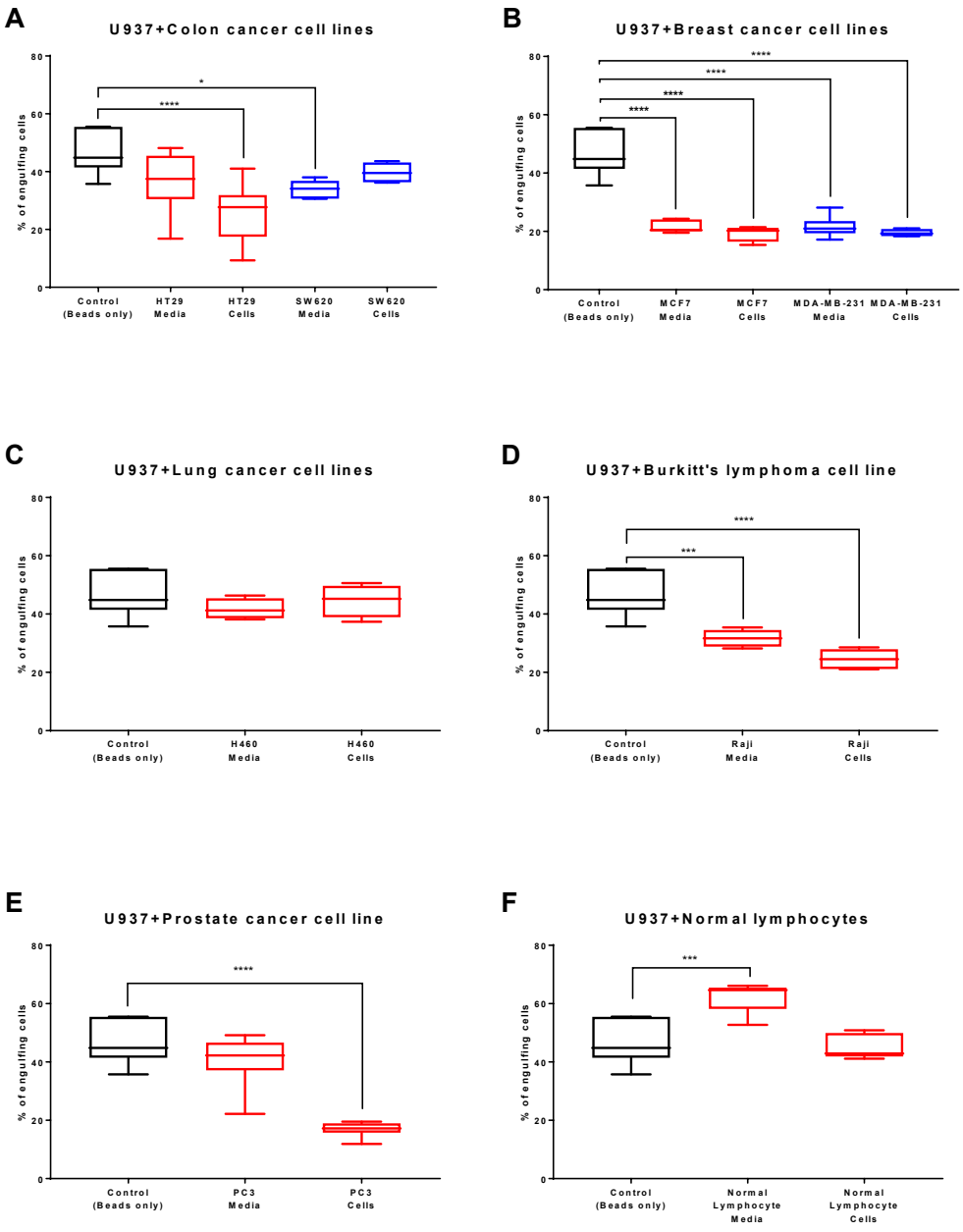

Figure A1- 3. Quantification of U937-derived macrophage engulfment after treatment with conditioned media or cells.

A) Treatment was HT-29 or SW620 conditioned media and cells. B) Treatment was MCF7 or MDA-MB-231 conditioned media or cells. C) Treatment was H460 conditioned media or cells. D. Treatment was Raji conditioned media or cells. E) Treatment was PC3 conditioned media or cells. F) Treatment was normal lymphocyte conditioned media or cells. P-value ≤0.05= *, P-value ≤0.01= **, P-value ≤0.001= ***, P-value ≤0.0001.

A U937+Colon cancer cell lines

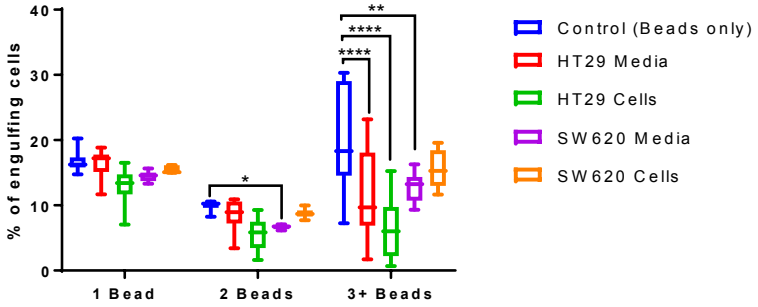

B U937+Breast cancer cell lines

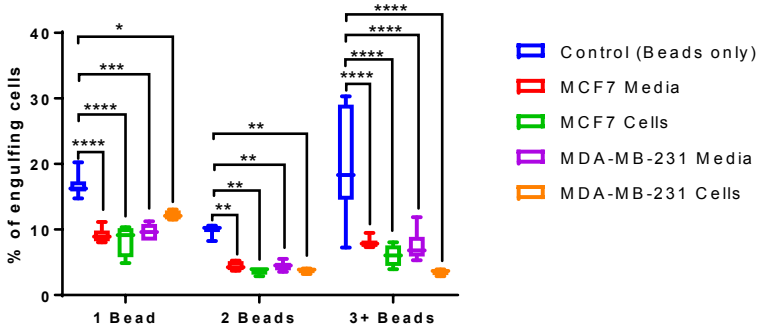

C U937+Lung cancer cell line

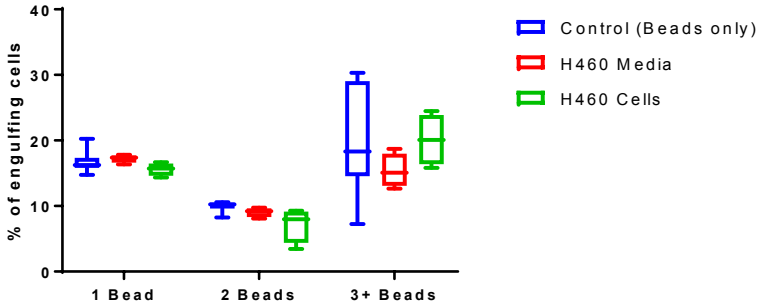

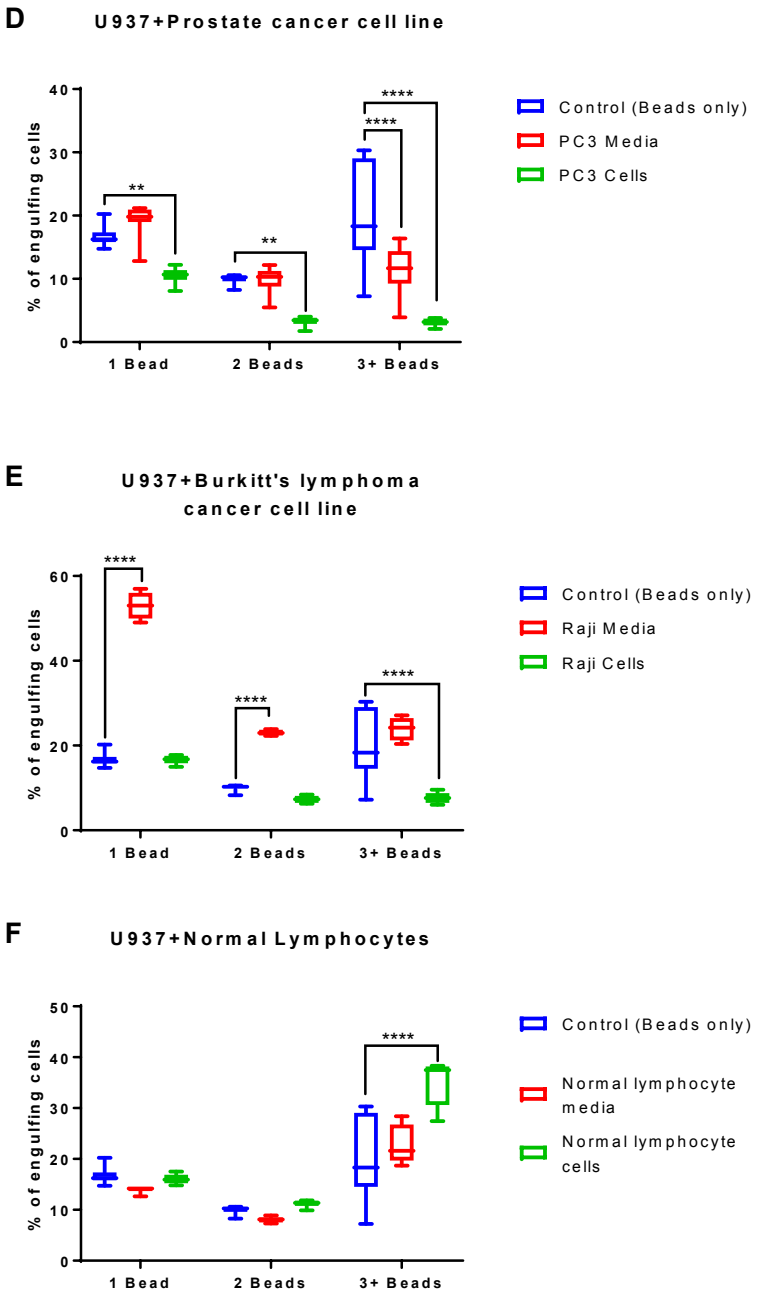

Figure A1- 4. Quantification of bead population engulfment among treatments.

A) Treatment was HT-29 or SW620 conditioned media and cells. B) Treatment was MCF7 or MDA-MB-231 conditioned media or cells. C) Treatment was H460 conditioned media or cells. D. Treatment was Raji conditioned media or cells. E) Treatment was PC3 conditioned media or cells. F) Treatment was normal lymphocyte conditioned media or cells. P-value ≤0.05= *, P-value ≤0.01= **, P-value ≤0.001= ***, P-value ≤0.0001.

U937-derived macrophages gene expression profile mimics M2 macrophages

Gene expression analysis by qPCR revealed that U937-derived macrophages show an upregulation of IL-10 and downregulation of IL-1B and IL-12, consistent with an M2 phenotype gene expression profile (Figure A1-5).

Conclusion

Macrophages have been shown to have a significant role in tumor progression. Research has shown that the tumor microenvironment can affect macrophage behavior. In this study, we demonstrated that cancer cells and cancer cell spent media decreased macrophage engulfment, especially in the 3+ bead population. We also found that the more aggressive the cancer cells, the lower the engulfment rates. These findings open new prospective research on what components from the media or the cancer cell metabolic products that mediate this lower engulfment rates. In our experiments, cells that engulfed 3+ beads were characterized as M1. Further research using qPCR may more clearly demonstrate and confirm the phenotypic changes in macrophages caused by interactions with cancer cells. This may be used to better understand the influence of the tumor microenvironment on macrophage phenotype

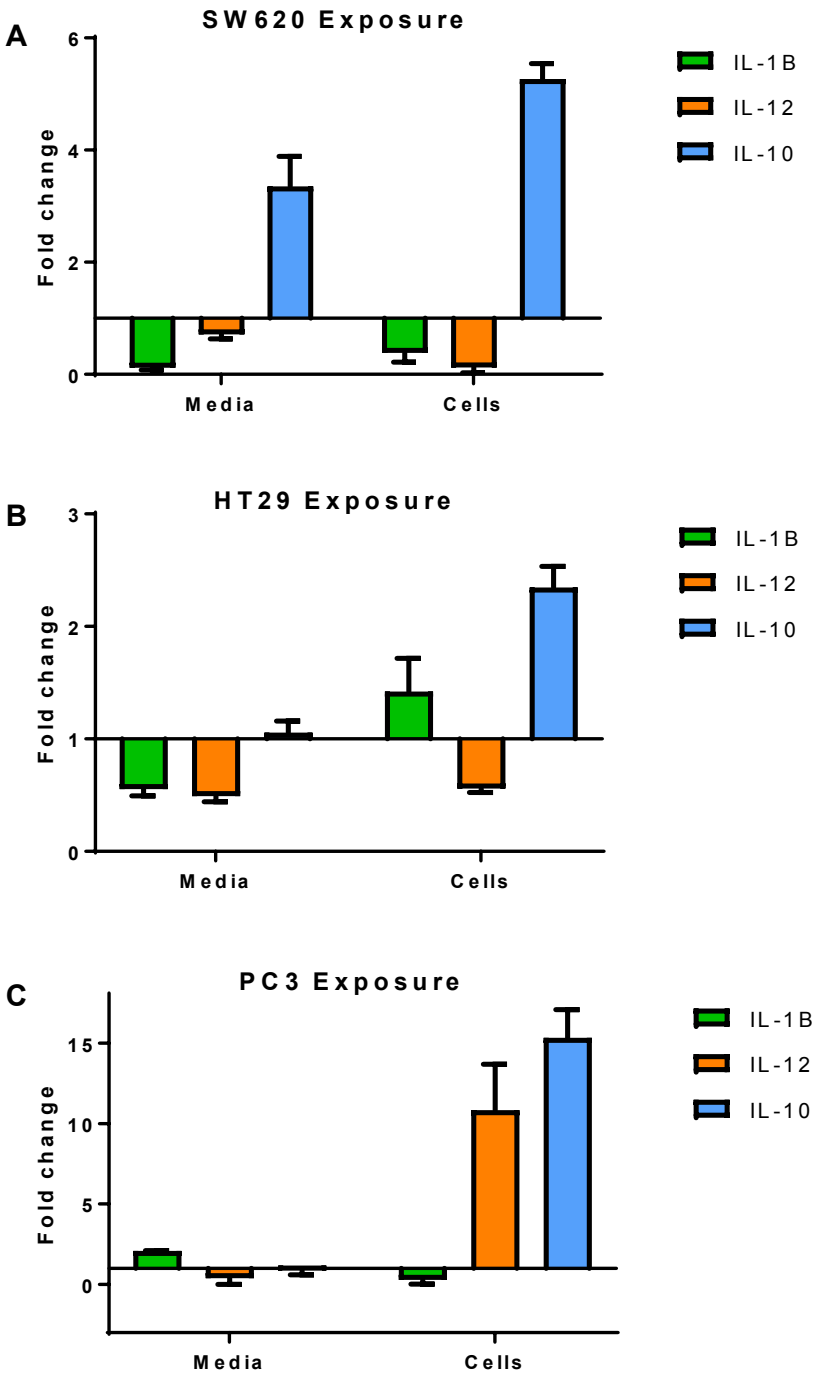

Figure A1- 5. Gene expression profile of U937-derived macrophages after exposure conditioned media or cell treatment.

A) Treatment was SW620 conditioned media or cells. B) Treatment was HT29 conditioned media or cells. C) Treatment was PC3 conditioned media or cells.

APPENDIX 2: Prostate Cancer Microenvironment Modulates Macrophage Phagocytosis

The following appendix contains data that accompanies a published abstract in Cancer Research. These data were presented at the American Association for Cancer Research Annual Meeting in 2015.

Abstract

Macrophages play an important role in the body's immune system. There are two main phenotypes of macrophages, M1 and M2. M1 polarized macrophages participate in tumorcidal activity and pro-inflammatory responses. M2 macrophages perform anti-inflammatory responses and promote tissue repair, angiogenesis, and tumor growth. Macrophages within the vicinity of cancer cells may be influenced by the microenvironment and change their gene expression accordingly. Macrophages can express different cytokine profiles depending on their polarization state (M1 or M2). We investigated whether macrophages exposed to cancer cells demonstrate a M2 or M1 phenotype. We stimulated U937 cells with phorbol 12-myristate 13-acetate (PMA) for 24 hours to allow for adhesion and differentiation. We co-cultured PMA-stimulated U937 macrophages with PC3 and DU145 prostate cancer cell lines in a 1:1 ratio with a transpermeable membrane to allow for cell to cell contact and communication, and with PC3 and DU145 conditioned media for 48 hours. We isolated the RNA from the treated macrophages and performed qPCR to assess gene expression levels of the following cytokines: IL-10, a cytokine demonstrating a M2 phenotype was upregulated by 10 and 15-fold for PC3 and DU145 cells respectively and by 3 fold in both cell lines exposed to conditioned media. We also found a trend of downregulation with the cytokines IL-1, IL-12, and TNF - alpha, which also depict a M2 phenotype. We also assessed macrophage function by measuring engulfment by flow cytometry.

Treated macrophages were allowed to phagocytose fluorescent microbeads for 1 hour. Flow cytometry analysis revealed that total bead engulfment decreased by up to 80% in macrophages treated with PC3 cells. Moreover, the population of macrophages that engulfed 3+ beads decreased significantly from both the cells and media treatments. Macrophages treated with DU145 cells and spent media also showed a similar trend to macrophages exposed to PC3 cells. The results show that macrophages exposed to PC3 and DU145 cancer cell lines polarized towards an M2 phenotype and could be important in the success of cancer within the microenvironment. Further research will reveal whether this process of a M2 polarization of macrophages is mediated by cytokines and cell vesicles or other factors.

Materials and Methods

We stimulated U937 cells with phorbol 12-myristate 13-acetate (PMA) for 24 hours to allow cell differentiation. After differentiation, U937s were stained with an APC cell proliferation dye for flow cytometry purposes. We seeded PC3 and DU145 cells at $1x10^6$ cells/mL with exosome-free RPMI 1640 for 96 hours, after which we collected the spent media and spun it down, filtered it with a 0.2uM filter, and mixed it with ExoQuick TC (System Biosciences). This mixture was incubated at 4°C overnight and then spun down at 1500 x g for 30 minutes. The supernatant was removed and the pellet was spun down again at 1500 x g for 15 additional minutes. All supernatant was then carefully removed and the pellet was resuspended in 500uL of PBS and used immediately. PMA-stimulated U937 cells were incubated with 20uL of exosome suspension solution for 1, 2, 3, 4, 5, 6, 12, and 24 hours at 37°C. After incubation time, PE-fluorescent latex beads were added to the U937 cells for 1 hour and allowed the U937 cells to phagocytose the beads. After 1 hour, the U937 cells were washed twice with PBS to detach removed any free beads. Then, the U937 cells were analyzed in a flow cytometer to

account for bead engulfment. Also, we isolated RNA from the U937 cells and prepared it for 1-step qPCR to analyze gene expression of IL-10 and IL-12.

Results

Flow cytometry analysis of the engulfment assay

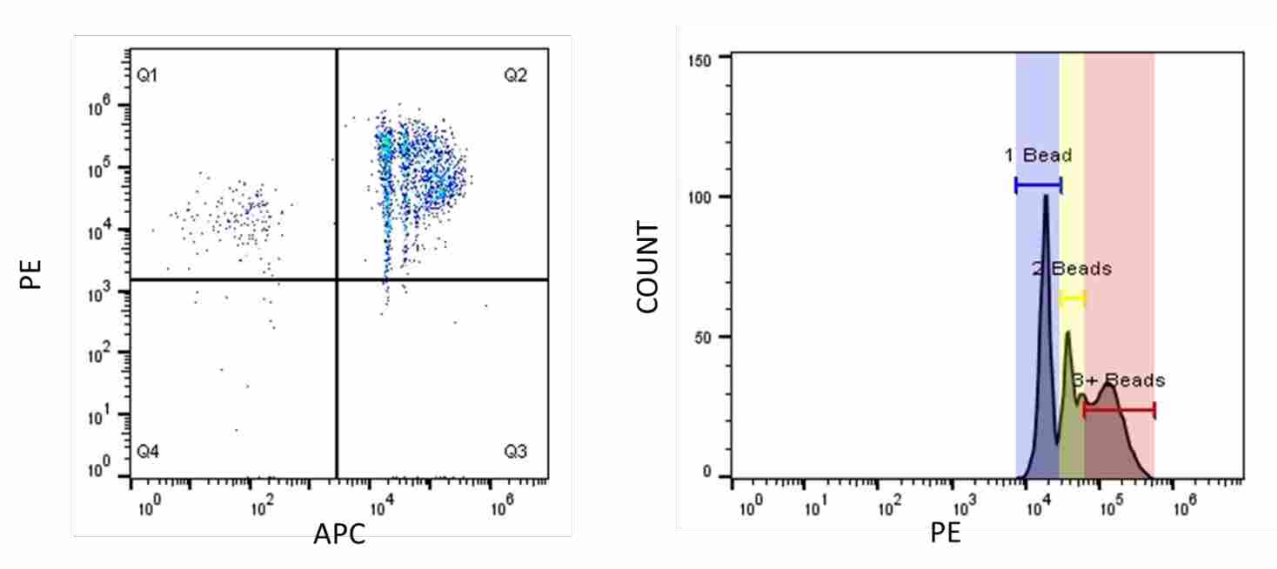

Figure A2- 1. Flow cytometry analysis of the engulfment assay.

Cells that are APC+PE+ are selected and a histogram plotted to show the different PE peaks observed. The difference in PE florescence account for macrophages engulfing either 1, 2, or 3+ beads.

Macrophage engulfment decreases when exposed to either DU145 or PC3 cells but not when exposed to spent media

We observed that macrophage engulfment did not change when exposed to PC3 or DU145 spent media, but it significantly decreased when the prostate cancer cell lines were in direct contact with the macrophages. This may indicate that something on the membrane of the prostate cancer cell lines, rather than a secreted protein, is signaling for macrophages to decrease phagocytosis (Figure A2-2).

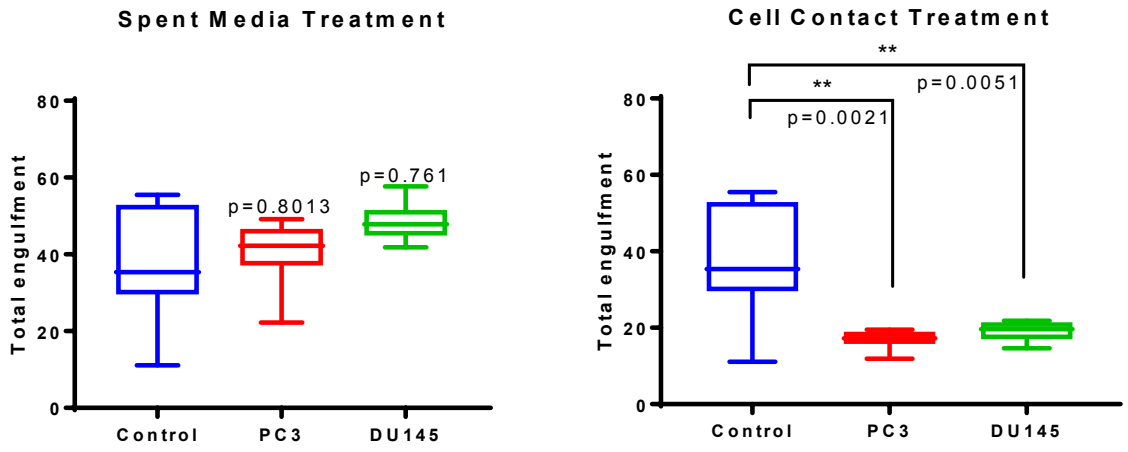

Figure A2- 2. Engulfment quantification of macrophages exposed to either PC3 or DU145 spent media or cells.

Macrophage engulfment decreases after 5 hours of treatment with prostate cancer-derived exosomes

We observed that when we exposed macrophages to exosomes, total phagocytosis decreased around 5 hours with both the PC3 and DU145-derived exosomes. After that time frame, macrophages regain normal phagocytic capabilities. This suggests that exosomes be suppressing macrophage function in 5 hours after treatment, after which macrophages recover (Figure A2-3).

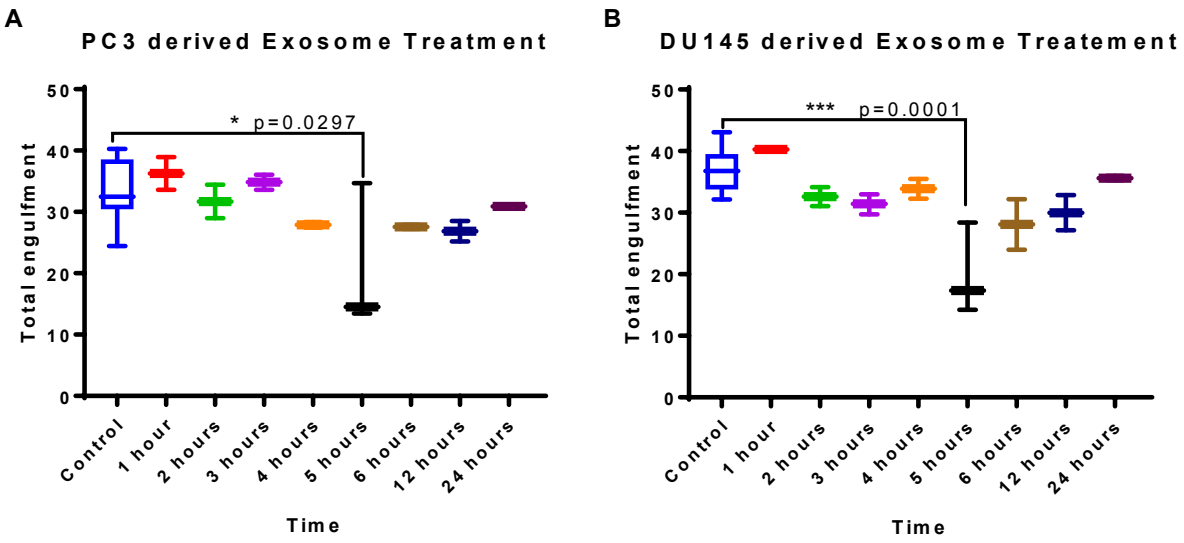

Figure A2- 3. Macrophages exposed to PC3 or DU145-derived exosomes over a period of time.

We observe that at 5 hours after treatment there is a decrease in macrophage engulfment.

Aggressive engulfment (3+Bead population) significantly decreases after 4-6 hour treatment with prostate cancer-derived exosomes

The population of macrophages that engulfed 3+ Beads significantly decreased after 4-6 hours of treatment with exosomes derived from PC3 and DU145 cell lines. After that time frame, macrophages regain their normal phagocytic capacity (Figure A2-4).

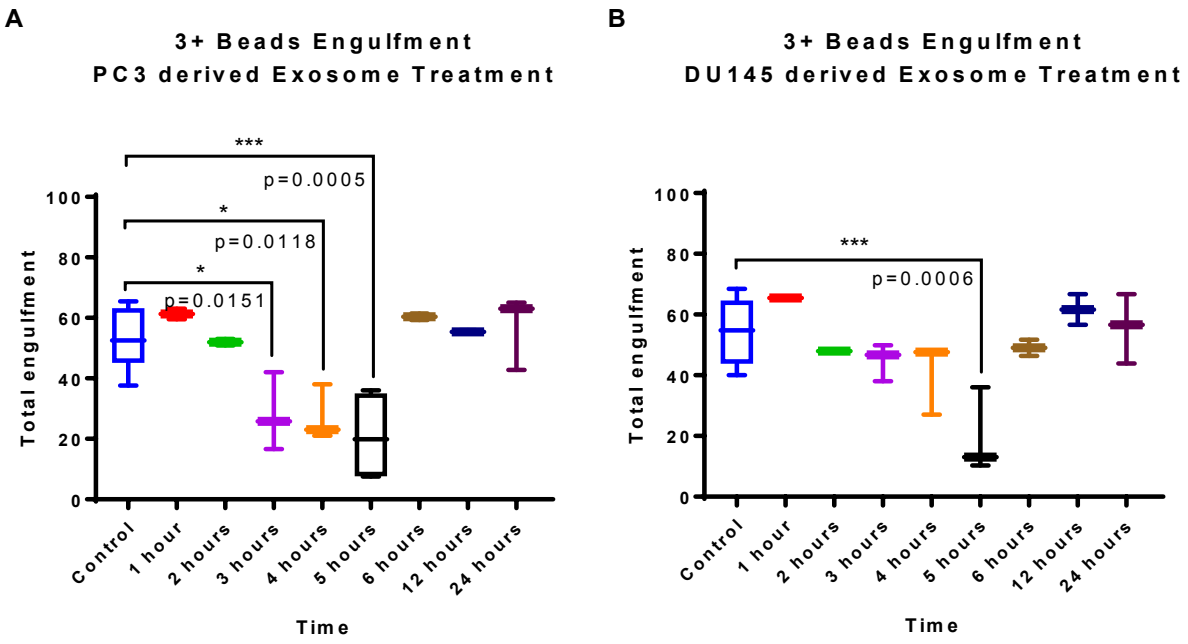

Figure A2- 4. The population of aggressive macrophages (3+Beads) exposed to PC3 or DU145-derived exosomes over time.

We observe that macrophage engulfment decreases between 3-5 hours after adding PC3-derive exosomes and at 5 hours after adding DU145-derived exosomes.

Gene expression shows an upregulation of IL-10 and a decrease of IL-12 in macrophages exposed to DU145-derived exosomes

Consistent with the engulfment data shown above, we observed that macrophages exposed to DU145-derived exosomes show an upregulation of IL-10 and downregulation of and IL-12 at 4 hours, mimicking an M2 phenotype gene expression profile. (Figure A2-5).

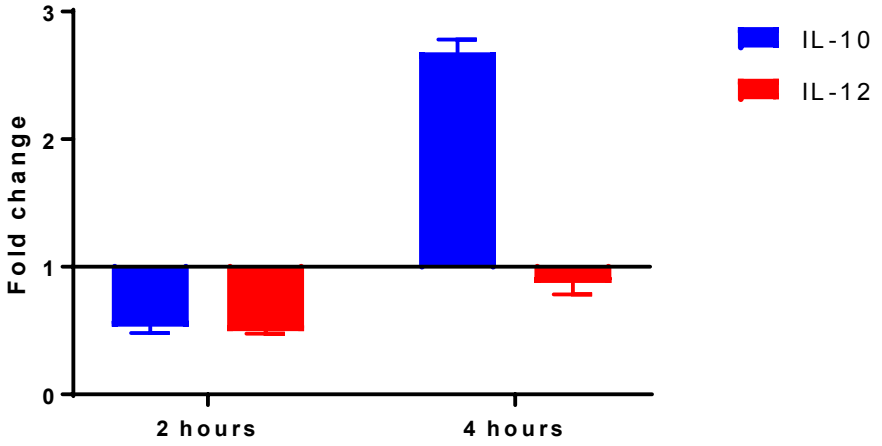

Figure A2- 5. qPCR gene expression analysis of macrophages exposed to DU145-derived exosomes at 2 and 4 hours showing an increase of IL-10 and IL-12 at 4 hours.

Conclusions

Macrophages are immune cells that have the ability to destroy tumors given the right signals (M1 phenotype). In the tumor microenvironment, however, macrophages "polarize" into a tumor promoting M2 phenotype. These tumor-associated macrophages (TAM's) play a significant role in tumor progression by facilitating metastasis and angiogenesis. Exosomes are small vesicles secreted by cells that contain parts of the genome, some protein, and large amounts of RNA, including miRNA. Exosomes secreted by one cell are able to distribute their contents into another cell, and thus mediate cellular communication. Of special interest is the exchange of miRNA. miRNA is able to silence genes involved in immune response, and may thereby play a role in the silencing of M1-phenotypic genes in macrophages U937 cells that were exposed to prostate cancer exosomes have a reduction in their phagocytic capacity between 3-6 hours of exosome treatment. Phagocytosis resumes to normal levels 6-24 hours after exposure. Gene expression analysis suggests that these macrophages may be changing their phenotype towards an M2 profile. These are preliminary results are interesting and further investigation will

elucidate the phenotypic changes these macrophages may be going through in the presence of exosomes.

APPENDIX 3: Oxidants and Antioxidants: A Question of Balance

The following appendix contains unpublished data from a study done on the role of antioxidants in cell response against oxidative stress and reactive oxidative species (ROS). This data was also presented at the American Association for Cancer Research annual meeting in 2013 as "Differences in cellular antioxidant activity in Burkitt's lymphoma and normal human lymphocytes."

Abstract

Cancer is a disease characterized by the uncontrolled growth of cells and invasion of these cells to other tissues. Less than 10% of all cancer mutations are caused by genetic factors while most mutations arise because of environmental factors. Environmental factors such as smoking, poor diet and obesity, alcohol, etc are known to trigger oxidative stress. Oxidative stress occurs when the concentration of reactive oxygen species (ROS) exceeds cellular antioxidant capacity. This in turn leads to oxidative damage and DNA mutations. Cells, however, have an antioxidant defense system that alleviates the effects of oxidative stress by preventing ROS from being formed or by stopping their damaging effects. A major part of this defense system is called the Antioxidant Response Element (ARE) which is located upstream of the promoter region of antioxidative and cytoprotective genes. The ARE is activated when oxidative stress occurs. Cells can also uptake antioxidants from their environment through passive and active transport when needed. The role of antioxidants is not to remove oxidants entirely, but to reduce them to sub-lethal levels within the cell. Diet plays an important role as a preventive measure against diseases caused by ROS. In this study, we established a method to investigate

the relationship between cell damage and nutrient uptake after exposing normal and cancer cells to a simulated oxidant environment (that induced ROS) and then to an antioxidant rich environment. We incubated Raji cells (Burkitt 's lymphoma) and normal human lymphocytes with 20mM AAPH (2 2′-azobis(2-amidinopropane) dihydrochloride) and then exposed them to different known antioxidants namely, L-ascorbic acid, α-tocopherol, α-lipoic acid, glutathione, and resveratrol for 10, 20, 45, and 60 minutes. We analyzed the cell lysates or antioxidant activity after incubation with antioxidants using the oxygen radical absorbance capacity assay (ORAC) and measured for antioxidant activity. Results show that Raji cells have significantly higher antioxidant activity after exposed to an oxidant environment than when exposed to only an antioxidant environment (p-values > 0.05). On the other hand, normal human lymphocytes maintain relatively similar antioxidant activity when exposed to an oxidant followed by exposure an antioxidant environment, even when stimulated to undergo cell division (p-values <0.05). These results suggest that normal human lymphocytes are able to quench ROS quickly and are able to protect their DNA from damage and subsequent mutations, whereas Raji cells lack this mechanism and need to absorb more antioxidants from the environment, presumably because they are unable to produce enough antioxidants themselves. These results may help explain why cancer cells, which are usually depleted of antioxidants, are found to use antioxidants to protect themselves from chemotherapy drugs.

Introduction

As recently as 2011, cancer was still the second highest killer in the United States, after cardiovascular disease [167]. However, strong correlations have been observed between lifestyle and cancer incidences. According to the American Cancer Society, tobacco use is responsible for at least 30% of all cancer deaths and about 87% of lung cancer deaths, while alcohol

consumption increases the risk of liver, breast and colorectal cancers [82]. Diet and exercise also affect cancer risk where an estimate of 1 out of 3 occurrences of cancer in the United States are linked to obesity, poor nutrition or lack of physical activity [82]. Obesity plays the biggest role out of these three, contributing to 14% to 20% of all cancer-related deaths [82]. These figures suggest that in most cases cancer is a preventable disease and that everyday lifestyle choices can aid in the reduction of cancer incidences.

The process of carcinogenesis starts when normal cells accumulate mutations that cause cells to: grow uncontrollably, reject cellular signals that could stop their growth, resist apoptosis, induce angiogenesis, and produce abnormalities in their DNA and chromosomes, etc. [1,168–170]. Less than 10% of all mutations that lead to cancer are caused by inherited genetic factors. Most mutations arise as a result of environmental factors [171].

Environmental factors such as smoking, poor diet and obesity, alcohol, radiation, carcinogens, etc can trigger oxidative stress. Oxidative stress takes place when the concentration of reactive oxygen species (ROS) exceeds cellular antioxidant capacity [172]. This in turn leads to oxidative damage and DNA mutations [173].

ROS are partially reduced forms of oxygen that are often produced naturally in the cell as a by-product of metabolic processes involving oxygen. These processes include the electron transport chain during cellular respiration. ROS participate in cell signaling and are needed for activation of transcription factors and for the control of expression of tumor suppressor genes such as p53 and Rb [173,174]. In order to maintain cellular equilibrium, ROS must be produced and consumed at approximately equal rates [173].

Normal cellular processes are estimated to produce about 2×10^{10} superoxide and hydrogen peroxide compounds per cell per day [175]. However, ROS can also be induced as a

result of exposure to ultraviolet light, radiation, and smoke [176]. The increase of ROS possesses the potential to cause oxidative injury to macromolecules such as nucleic acids, proteins and lipids. Cellular damage caused by ROS can lead to necrosis and ATP depletion, which can prevent apoptosis, one of the "symptoms" of cancer [177]. Oxidative stress has also been linked to other diseases such as atherosclerosis, Parkinson's disease, diabetes and Alzheimer's disease [178]. Exercise can also dramatically elevate the level of ROS in the body [179]. During exercise, mitochondria in skeletal muscle produce nitric oxide synthase (NOS), an enzyme that produces an intermediate of nitric oxide (NO^-), a highly reactive molecule. NO^- and O_2 (in radical form) can react to produce peroxinitrite, $ONOO^-$, which is a powerful oxidant that can break the ROS cellular equilibrium and can lead to DNA injury. Physical activity can also activate leukocyte infiltration, which may lead to inflammation due to ROS release. Leukocytes, especially phagocytes, are large producers of ROS that kill bacteria and foreign antigens but can also cause tissue damage. Research has shown that there is an increase of neutrophil infiltration into skeletal muscle after strenuous physical activity, which elevates normal levels of ROS in the cell [180]. Research also confirms higher ROS levels in humans after downhill running [179,181,182].

Cells, however, have an antioxidant defense system that alleviates the effects of oxidative stress by preventing ROS from being formed or by removing them or neutralizing them from the cell [183]. This defense system is called the Antioxidant Response Element (ARE) which is a transcription factor binding site located upstream of the promoter region of antioxidative and cytoprotective genes. A family of transcription factors called NFE2 activates the ARE. NFE2 is usually bound to Keap 1, a cytoplasmic protein. Under normal conditions, Keap1 induces the ubiquitination of NFE2, which has a half-life of 20 minutes. Under oxidative stress, cysteine residues in Keap1 are disrupted and NFE2 is released. NFE2 migrates to the nucleus, where it

binds to the ARE and induces the transcription of several antioxidant-producing enzymes [184]. Cells can also uptake antioxidants from their environment through passive and active transport when needed [185].

Substances such as L-ascorbic acid (vitamin C), α-Tocopherol (vitamin E), resveratrol, glutathione, and lipoic acid serve as antioxidant sources against oxidative stress and therefore are thought to have chemopreventive properties.

L-ascorbic acid (vitamin C) has proven to be one of the most successful chemopreventive compounds for non-hormone-dependent cancers. Vitamin C is a water-soluble compound that is absorbed by cells through passive and active transport (active transport accounts for the greater portion of vitamin C accumulation in cells) [186]. In humans, vitamin C must be acquired from diet due to lack of gulonolactone oxidase, an enzyme that synthesizes L-ascorbic acid [187]. Studies show that higher ingestion of vitamin C has a high correlation with lower risk for pancreatic, cervical, and colorectal cancer [188]. Also, higher intake of vitamin C during pregnancy decreases risk of brain tumors during childhood. Vitamin C also aids in the regeneration of vitamin E and other antioxidants [188].

Vitamin E, a lipophilic antioxidant referred to a group of tocopherols and tocotrienols, has also shown chemopreventive properties. Mostly absorbed through active transport using lipoprotein channels, vitamin E protects cell membranes from lipid peroxidation and quenches ROS when fat is oxidized [189,190]. The most abundant form of vitamin E in cells is α -tocopherol and although has the highest antioxidant activity of all vitamin Es, δ-tocopherol and λ-tocopherol are more effective at free radical quenching and therefore are considered the types of vitamin E that account for cancer preventive properties [191].

Glutathione is the major soluble endogenous antioxidant found in cells. It is a simple compound made of glutamate, cysteine, and glycine. Its role is to scavenger free radicals and peroxides. Glutathione or its precursors are absorbed by active transport, using gamma-glutamyltransferase, and passive transport, which is dependent on sodium ions [192,193]. Glutathione is usually found in its reduced form and is rapidly consumed when oxidants are produced, maintaining cellular equilibrium [194]. Glutathione has several other functions including the regeneration of vitamin C and vitamin E, DNA synthesis and repair, and it is often involved in cell proliferation and death [193]. Under oxidative stress, normal cells respond by upregulating the production of glutathione. In cancer cells, glutathione production is unregulated where some cancer cell lines exhibit glutathione depletion and other cancer cell lines such as bone marrow, breast, lung, larynx, and colon have shown increased levels of glutathione which protects them from the harmful effects of chemotherapy drugs [193,194]

Lipoic acid, called the "universal antioxidant", is a small amphipathic molecule with two thiol groups that can be oxidized or reduced [195]. The reduced form of lipoic acid or dihydrolipoic acid (DHLA) is the major form of lipoic acid that reacts with ROS, however, the oxidized form can also inactivate free radicals. Both forms of lipoic acid are able to regenerate vitamin C and vitamin E. Lipoic acid is mostly obtained from diet but cells can synthesize it in small amounts if needed. Because of its amphipathic properties, lipoic acid can easily cross biological membranes and protect the cell from oxidants in every cell compartment [195]. Lipoic acid has been shown to protect cells from gamma radiation in mice [196], and to induce apoptosis in murine melanoma cells, ovarian epithelial cancer cells, and breast cancer cells without inducing apoptosis in normal non-transforming cells [197–200].

Resveratrol is an antioxidant found in the skin of grapes, berries, and other fruits. It is a phytochemical produced by plants in response to a fungal infection [201]. Resveratrol has been found to be a preventive compound for several pathologies such as cardiovascular disease, viral infections, Alzheimer's disease, and cancer. Resveratrol has been shown to stop tumor initiation, promotion, and progression [201,202]. Resveratrol has the ability to quench ROS such as superoxide and hydroxyl radicals. It especially protects the mitochondria, an organelle that produces high concentrations of ROS [203]. Resveratrol can be absorbed by cells through passive transport. It can also be absorbed by carrier-mediated transport as resveratrol associates with several serum proteins to enter the cells. This allows resveratrol to be readily absorbed by cells [202].

The role of antioxidants is not to remove oxidants entirely, but to maintain them at optimum levels within the cell. The importance of natural dietary substances is promoted as an effective precursor in preventative measures regarding illness and health deficient symptoms due to ROS presence within the body. Finding the right balance between oxidants and antioxidants in the cell is important to maintain proper cellular health.

This study establishes a method to investigate the relationship between cell damage and antioxidant uptake after exposing normal and cancer cells to a simulated oxidant stress environment. We hypothesize that cells previously exposed to an oxidant agent and then to an antioxidant environment will exhibit higher antioxidant activity than cells exposed to an antioxidant environment only, suggesting that diet and exercise combined provide the best way to protect our cells from the damaging effects of oxidative stress.

Materials and Methods

Chemicals

RPMI 1640 medium, Fetal Bovine Serum, and Hank's Balanced Solution were purchased from Thermo Scientific (Logan, UT). 2,2′-azobis (2-aminidopropane) dihydrochloride (AAPH) was purchased from Wako Chemicals USA, Inc. (Richmond, VA). Fluorescein-sodium salt and phosphate buffered saline (PBS), 200 Proof Ethanol, L-Ascobic acid, Resveratrol, α-Tocopherol, glutathione, and α-lipoic acid were purchased from Sigma-Aldrich, Inc. (Milwaukee, WI). Trolox (6-hydroxy-2,5,7,8-tetramethyl-2-carboxylic acid) was purchased from Enzo Life Sciences, Inc. (Plymouth, PA). Dimethyl sulfoxide (DMSO) was purchase from purchased from EMD Chemicals (Billerica, MA).

Materials

Costar 96-well black clear bottom plates were purchased from Corning Inc. (Corning, NY). Raji cells (Burkitt's lymphoma cell line) were obtained from the American Type Culture Collection (ATCC) (Manassas, VA).

Equipment

Readings were taken in a BMG FLUOstar Optima microplate reader (BMG Laboratories, serial #413-0225). Data was analyzed using Microsoft Excel and IBM SPSS Statistics.

Burkitt's lymphoma cell culture

Raji cells (Burkitt's lymphoma) were cultured in RPMI 1640 supplemented with 10% Fetal Bovine Serum and kept in an incubator with 5% carbon dioxide at 37 ˚C.

Lymphocyte separation

Normal human lymphocytes were separated from whole blood using Lymphocyte Separation Medium (LSM). Whole blood was obtained under IRB approval from young volunteers (18-24 years-old). Heparinized whole blood was diluted in a 1:1 ratio with 1X Hank's Buffered Saline Solution (HBSS). Diluted blood was layered on top of LSM in conical

vial and centrifuged at 800g for 20 minutes. The leukocyte-rich layer was removed and washed with PBS. Leukocytes were re-suspended in RPMI 1640 medium supplemented with 20% human serum and 3% LPS; and cultured for 24 hours to allow for monocyte differentiation and attachment to the culture flask. Lymphocytes in suspension were removed from the flask, washed with PBS, re-suspended in RPMI 1640 medium supplemented with 10% FBS, and used immediately.

Sample preparation

L-Ascorbic Acid: 10mM. 0.0176g of L-Ascorbic acid was diluted in 10 ml PBS.

Resveratrol: 10mM. 0.0228g of resveratrol was diluted in 10ml of DMSO.

α-Tocopherol: 10mM. 0.0431g of α-Tocopherol was diluted in 10ml of 15% ethanol.

Glutathione: 10mM. 0.0307g of glutathione was diluted in 10ml of PBS.

α-Lipoic Acid: 10mM. 0.0206g of α-lipoic acid was diluted in 10ml of 15% ethanol.

Incubations

Lymphocytes and Raji cells at 1.0 x 10^6 cells/mL were incubated with the various samples (ascorbic acid, tocopherol, resveratrol, glutathione, and lipoic acid) for 10, 20, 45, and 60 minutes. The cells were washed with PBS and lysed open by freeze-thawing. The lysate was centrifuged at 15,300 g for 30 minutes. The supernatant was stored at -20°C until analysis using the ORAC assay.

Simulation of Oxidative Stress assay

Lymphocytes and Raji cells at 1.0 x 10^6cells/mL were incubated with 19.9 mM AAPH for 10 minutes to simulate oxidative stress. The cells were washed with PBS and re-suspended in RPMI 1640 at 1.0 x 10^6cells/mL. The cells were incubated with the various samples (ascorbic acid, tocopherol, resveratrol, glutathione, and lipoic acid) for 10, 20, 45, and 60 minutes and

washed with PBS and lysed open. The lysate was centrifuged at 15,300 g for 30 minutes. The supernatant was stored at -20°C. Note that lipoic acid was used in its oxidative form to account for antioxidant capacity of cells when continuously exposed to an oxidizer that can be recycled.

ORAC assay

The Oxygen Radical Absorbance Capacity Assay was used to analyze all of our samples. For this experiment, we used a modified ORAC based on published methods [204–206]. The ORAC assay measures the decay of fluorescence after exposed to a free radical initiator (AAPH). All readings were taken using Costar 96-well black with clear bottom plates, with 20µ sample or PBS, 200µL fluorescein, and 20µL AAPH in each well.

Readings were taken every 2 minutes for 90 minutes using a 485nm excitation filter and a 590 nm emission filter with a BMG FLUOstar Optima microplate reader.

Standard curve data

Trolox, a water-soluble analogue of vitamin E, was used as a control standard. To obtain standard curves for each trial, Trolox was run at concentrations of 50µM, 25µM, 12.5µM. Data from each standard curve was used to convert raw net area under the sample curve (net AUC) values to Trolox Equivalents per liter (TE/L). Subsequent calculations converted TE/L to TE/L per 1.0 x 10^6 cells.

Cytotoxicity

Cells at 1.0 x 10^6cells/mL and at 90% or higher viability were exposed to different dilutions of 320mM AAPH (1:1, 1:2, 1:4, 1:8, 1:16, and 1:32) and incubated for 24 hours. After 24 hours of incubation, cell counts and cell viability counts were performed. The dilution 1:16 was found to maintain 90% cell viability and increase cell counts. We performed this incubation

with dilutions of AAPH to eliminate the possibility of cells showing higher antioxidant uptake because of cell membrane damage.

Results

All the following data are reported in Trolox Equivalents per litter per 1.0 x 10^6 cells (TE/L/1.0 x 10^6 cells). Data from each sample was repeated four times, with 12 replicates for each sample, giving a total of 48 results per sample.

We measured the antioxidant activity in Raji and normal lymphocytes after incubation with L-ascorbic acid (vitamin C), α-tocopherol (vitamin E), glutathione, lipoic acid, resveratrol, or PBS (control) and after oxidative treatment and followed by incubation with the mentioned antioxidants (Table A1-1 and 2). Mean values are reported in Trolox Equivalents per liter per 1x10^6 cells (TE/L per 1x10^6 cells).

Table A3-1					
ANTIOXIDANT AND TREATMENT		**TIME IN MINUTES**			
		10	**20**	**45**	**60**
L-Ascorbic Acid	Incubation	1706.31	1812.53	1775.38	2080.73
	Oxidative treatment	1964.62	3156.77	2783.21	2456.49
α-Tocopherol	Incubation	2054.26	2238.43	1788.79	1512.96
	Oxidative treatment	1816.45	1940.89	2827.29	2690.45
Glutathione	Incubation	1222.04	972.20	962.70	1042.55
	Oxidative treatment	1891.67	2156.48	2600.05	2335.08
Resveratrol	Incubation	4387.78	3639.42	4156.90	4820.41
	Oxidative Treatment	2026.91	3995.61	4118.37	4425.34
Lipoic Acid	Incubation	1487.16	1166.82	1266.43	1326.65
	Oxidative treatment	1151.06	1124.58	1406.15	1802.59
Control (PBS)	Incubation	2016.38	2420.02	1753.53	2688.23
	Oxidative treatment	1302.95	1751.83	1865.28	2208.59

Table A3- 1. Antioxidant activity in normal lymphocytes after incubation with L-ascorbic acid (vitamin C), α-tocopherol (vitamin E), glutathione, lipoic acid, resveratrol, or PBS and after oxidative treatment and followed by incubation with the mentioned antioxidants

Table A3-2					
ANTIOXIDANT AND TREATMENT		TIME IN MINUTES			
		10	20	45	60
L-Ascorbic Acid	Incubation	1805.86	1629.22	1703.50	1803.69
	Oxidative treatment	1603.81	3056.42	2608.09	3087.14
α-Tocopherol	Incubation	1339.87	1292.38	1482.90	1475.00
	Oxidative treatment	1767.28	2190.20	2329.61	2625.68
Glutathione	Incubation	2006.79	1614.80	1625.69	1743.60
	Oxidative treatment	1884.03	2589.20	2209.45	2582.08
Resveratrol	Incubation	2489.82	2608.60	2092.61	2587.45
	Oxidative Treatment	3069.06	6227.59	5080.96	6284.72
Lipoic Acid	Incubation	931.87	895.75	934.44	885.63
	Oxidative treatment	1467.11	1617.89	1599.85	1504.90
Control (PBS)	Incubation	2439.40	2159.70	2142.62	1889.55
	Oxidative treatment	2079.44	2718.65	3011.89	3872.41

Table A3- 2. Antioxidant activity measured in Raji cells after incubation with L-ascorbic acid (vitamin C), α-tocopherol (vitamin E), glutathione, lipoic acid, resveratrol, or PBS. Values are shown in Trolox Equivalents per liter per $1x10^6$ cells (TE/L per $1x10^6$ cells).

Figures A3-1 and A3-2 show side by side the differences in cellular antioxidant activity of lymphocytes and Raji cells after being exposed to an antioxidant environment, and after being exposed to oxidative stress and to an antioxidant environment. Trends are similar with lymphocytes and Raji cells, where antioxidant activity increases after the cells have been exposed to oxidative stress (AAPH) compared to cells that have been exposed to antioxidant environment only. Resveratrol registers the highest antioxidant activity. Lipoic acid was used in its oxidized form to account for constant oxidative stress.

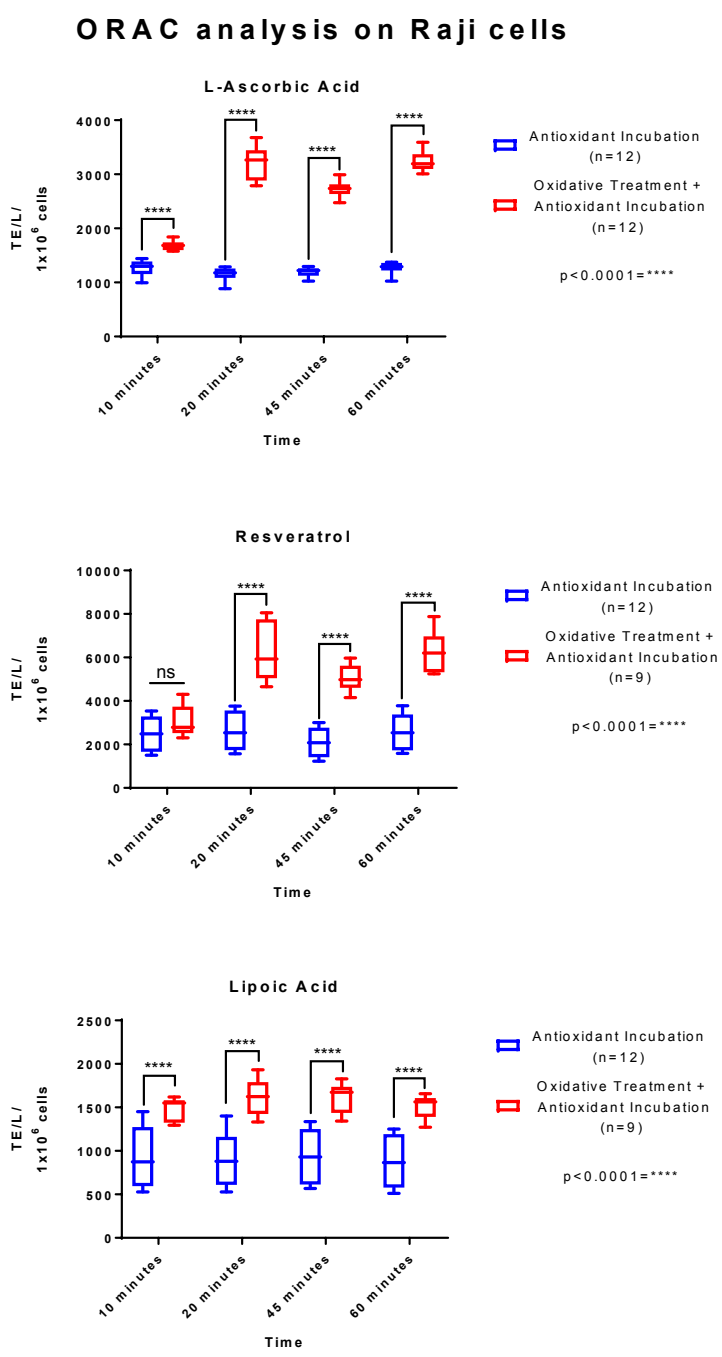

Figure A3- 1. Differences in cellular antioxidant activity in Raji cells followed antioxidant incubation and oxidative treatment + antioxidant incubation.

Continues in next page.

ORAC analysis on Raji cells

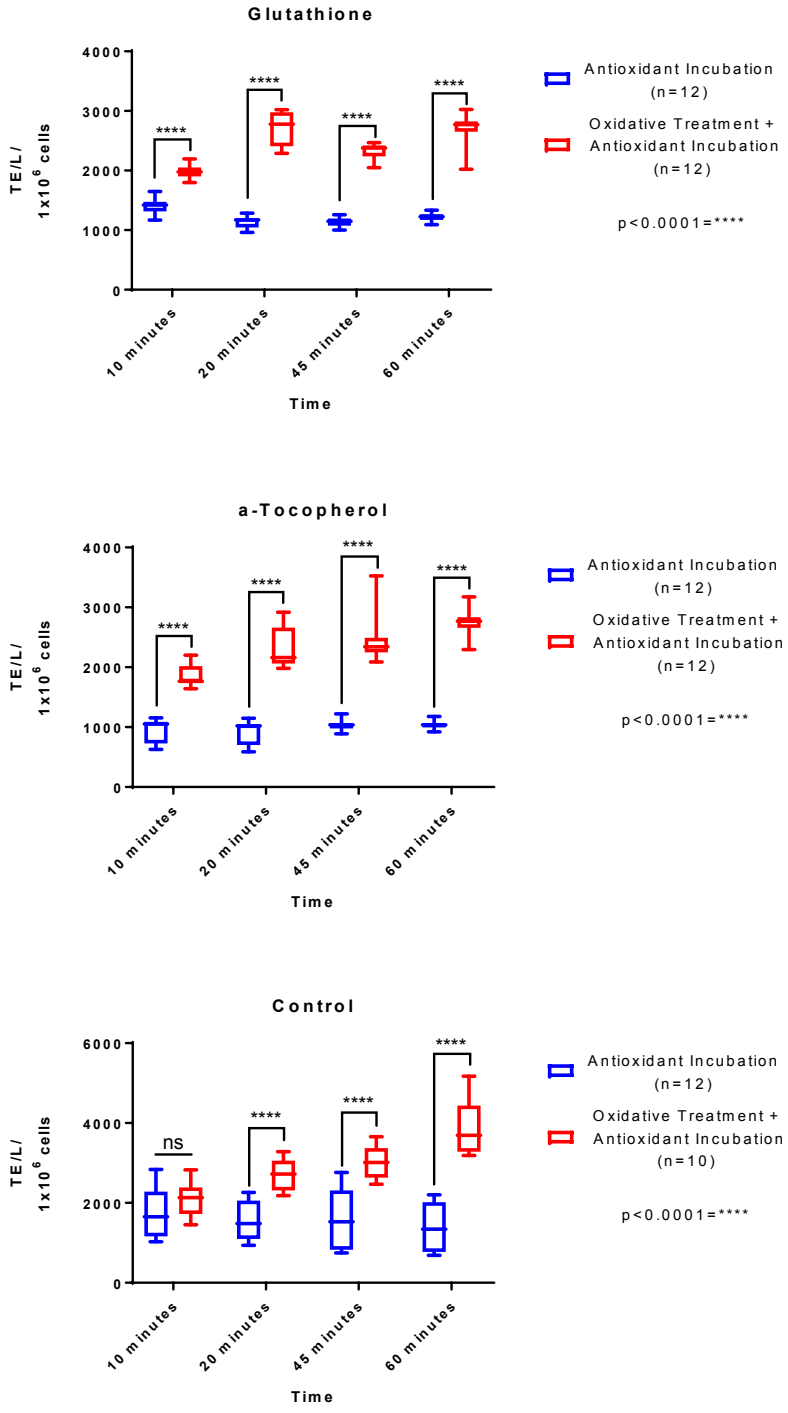

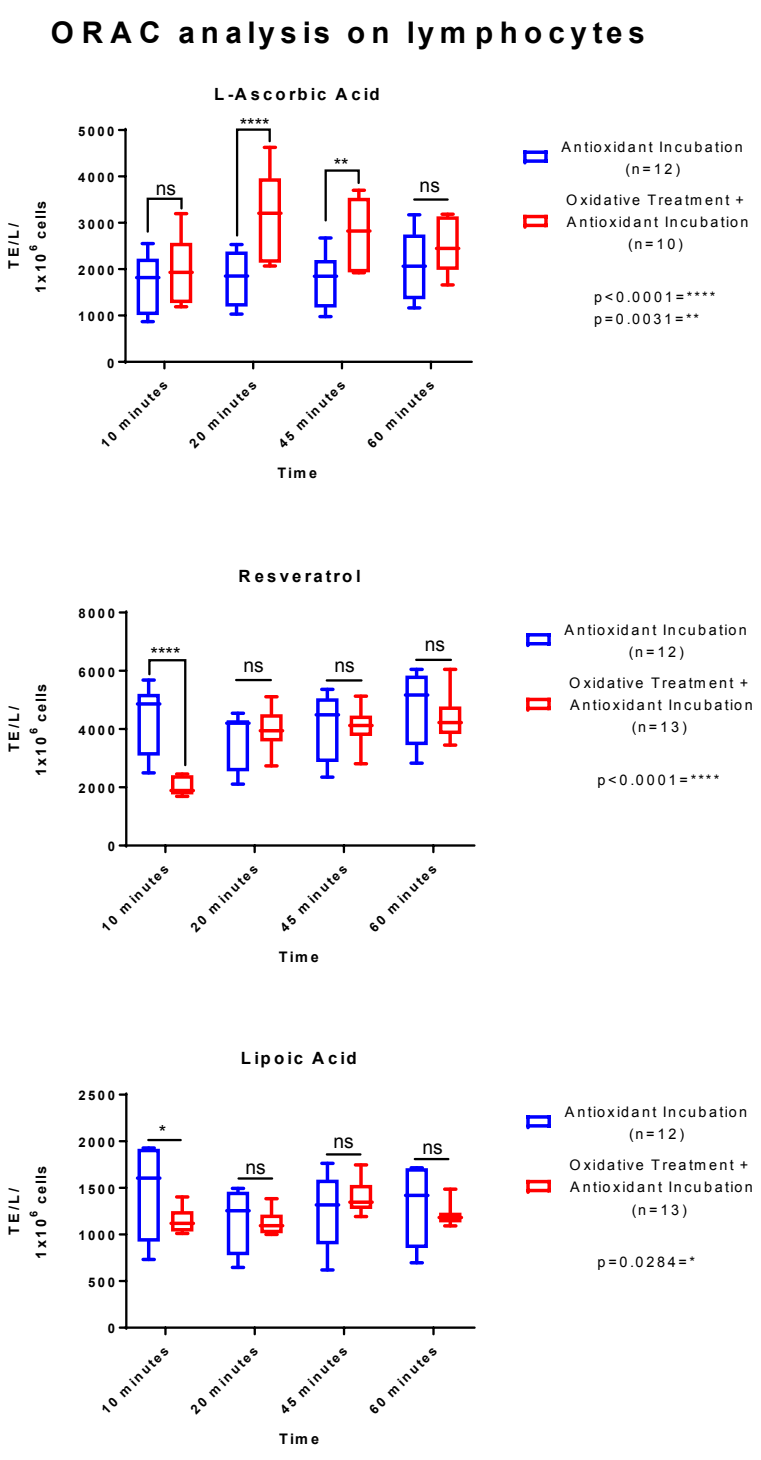

Figure A3- 2. Differences in cellular antioxidant activity in Raji cells followed antioxidant incubation and oxidative treatment + antioxidant incubation.

Continues in next page.

ORAC analysis on lymphocytes

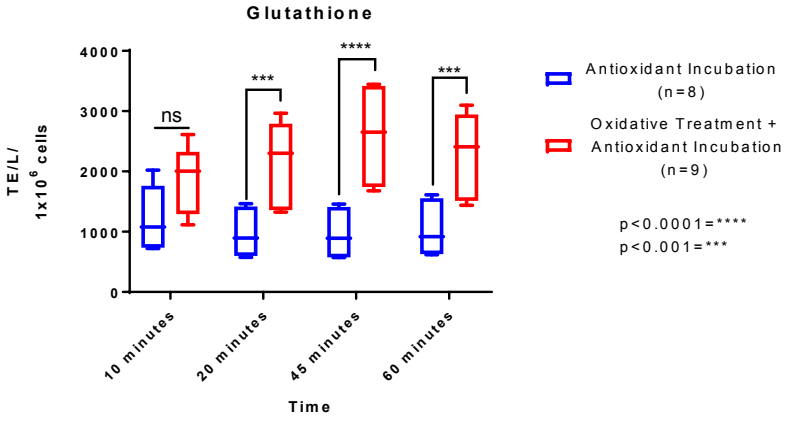

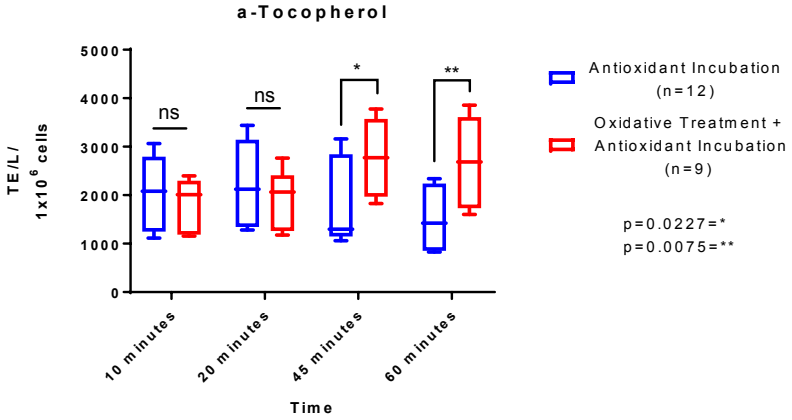

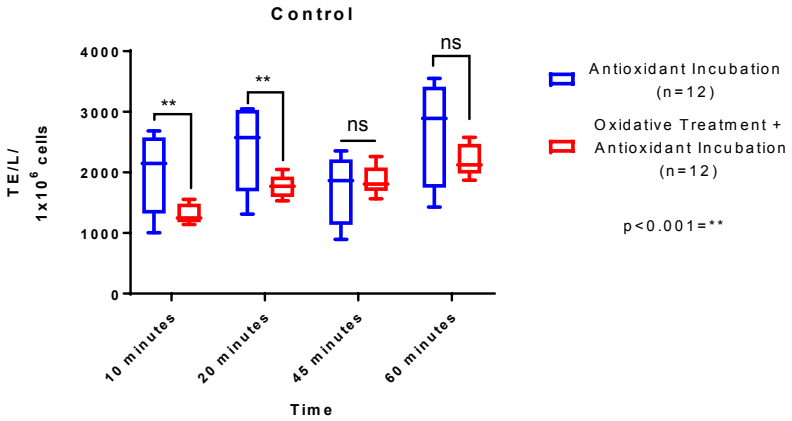

Conclusion

This paper investigates the relationship between oxidative stress and antioxidant uptake in Burkitt's lymphoma compared to normal lymphocytes. We used L-ascorbic acid (vitamin C), α-Tocopherol (vitamin E), glutathione, lipoic acid, and resveratrol as antioxidant sources for the cells in concentrations that allowed for minimal cytotoxicity and were physiologically relevant (data not shown).

When we used normal lymphocytes and measured the amount of antioxidant activity present in our control sample, we observed that when cells are incubated with PBS they do not change their antioxidant activity, which averages 2219.54 TE/L per 1.0 x 10^6 cells in one hour (Table 1). When we exposed normal lymphocytes to the oxidative treatment (19.9mM AAPH for 10 minutes), we observed a statistically significant decrease in antioxidant activity at 10 and 20 minutes (2-sided p-value=0.003, and 2-sided p-value=0.007 respectively) due to the oxidative treatment. At 45 and 60 minutes, we observed no difference in antioxidant capacity in the cells pre-treated with AAPH and the cells that were incubated with saline solution (2-sided p-value=0.52, and 2-sided p-value=0.07 respectively), suggesting that the normal lymphocytes can deal with oxidative stress between 20 and 45 minutes after being exposed to it, and that they are able to obtain an oxidant-antioxidant balance.

Raji cells showed an average of 2157.82 TE/L per 1.0 x 10^6 cells in one hour. After oxidative treatment, however, Raji cells demonstrated a continuous increase in antioxidant capacity with time from 20 minutes on (2-sided p-value <0.001 at times 20, 45, and 60 minutes). These results show that Raji cells have higher antioxidant activity with time than normal lymphocytes after being previously exposed to oxidative stress, suggesting that Raji cells cannot deal with oxidative stress as well as normal lymphocytes and cannot maintain a proper oxidant-

antioxidant balance. It is important to understand that the balance between ROS and antioxidants is critical in protecting the cell from oxidative stress; high antioxidant activity in the cell may not always be beneficial, as it may mean that the cell has a deficiency in the recycling antioxidant mechanism, which is involved in immune system regulation using the NF-κB transcription factor [207].

Normal lymphocytes incubated with L-ascorbic acid show an average of 1843.74 TE/L per 1.0 x 10^6 cells in one hour; whereas Raji cells show an average of 1735.57 TE/L per 1.0 x 10^6 cells in one hour. After oxidative stress, normal lymphocytes show a decrease in antioxidant capacity at 10 minutes but then it significantly increases at 20 and 45 minutes (2-sided p-value=0.003 and 0.004 respectively) to finally restore balance at 60 minutes compared to incubation with L-ascorbic acid only. Raji cells, after oxidative treatment, show an increase in antioxidant activity at times 20, 45, and 60 minutes (all 2-sided p-values <0.001), showing its highest antioxidant activity at 60 minutes with 3087.14 TE/L per 1.0 x 10^6 cells. The antioxidant capacity of the cell lysates seems to remain elevated from 20 minutes on, which again suggests the uptake of L-ascorbic acid into the cells but the lack of a mechanism to control oxidative stress.

Lymphocytes exposed to oxidative treatment and incubated with α-tocopherol (vitamin E) had statistically significant increases in antioxidant activity at minutes 45 and 60 (2-sided p-values 0.02 and 0.005 respectively) compared with lymphocytes incubated with α-tocopherol only. Raji cells show a pattern similar to the one shown in our control sample (Figure 12) where antioxidant activity increases with time.

Lymphocytes incubated with glutathione significantly increase their antioxidant capacity when cells are exposed to oxidative treatment first. Raji cells incubated with glutathione show

higher antioxidant activity than lymphocytes with the same treatment and show a similar trend to lymphocytes when exposed to oxidative treatment before incubation with glutathione.

Resveratrol is the only compound we used that is not made by animal cells; therefore, most of the antioxidant capacity shown in our readings comes from resveratrol that has been absorbed by cells. Incubation of lymphocytes with resveratrol gives an average of 4251.13 TE/L per 1.0 x 10^6 cells in one hour and incubation of lymphocytes with resveratrol after oxidative stress gives an average of 3641.56 TE/L per 1.0 x 10^6cells in one hour, a difference that is not statistically significant (2-sided p-value= 0.31). In figure 5 we observe that at 10 minutes antioxidant activity is higher in incubation than in samples with oxidative treatment (2-sided p-value <.0001) due to the nature of the oxidative treatment. Antioxidant capacity increases in the samples with oxidative stress, however, at 20 minutes, and restores oxidant-antioxidant balance with the incubation samples thereon. Raji cells show a different trend compared to normal lymphocytes. Incubation with resveratrol averages 2444.62 TE/L per 1.0 x 10^6 cells in one hour whereas incubation with resveratrol after oxidative stress averages 5165.58 TE/L per 1.0 x 10^6 cells in one hour. Significant increases in antioxidant capacity are seen at 20, 45, and 60 minutes (2-sided p-values <0.001). In comparison with lymphocytes, Raji cells do not absorb as much resveratrol as normal lymphocytes do (Table 1 and Table 2), however, after oxidative stress Raji cells absorb much more resveratrol. Resveratrol is largely absorbed by the cell through passive and carrier-mediated transport, which is what we observe when we use the ORAC assay to read cytoplasmic antioxidant activity [202].

To test how cells would react to oxidative stress when constantly exposed to an oxidant, we used an oxidized form of lipoic acid. Normal lymphocytes exposed to oxidized lipoic acid show an average of 1311.76 TE/L per 1.0 x 10^6 cells in one hour. When we pre-exposed normal

lymphocytes to AAPH and then to oxidized lipoic acid, we observe an average of 1371.09 TE/L per 1.0 x 10^6 cells in one hour. The only significant difference is observed at 10 minutes, where the cells exposed to AAPH and then to oxidized lipoic acid show lower antioxidant capacity than cells just incubated with oxidized lipoic acid (2-sided p-value=0.04), which is expected. Raji cells, however, showed a different trend. When Raji cells were incubated with oxidized lipoic acid, the antioxidant capacity averaged 911.92 TE/L per 1.0 x 10^6 cells in one hour whereas the when the Raji cells were treated with AAPH and then with lipoic acid the antioxidant capacity averaged 1547.44 TE/L per 1.0 x 10^6 cells in one hour. We observed significant difference at every time point (2-sided p-values= 0.002, <0.001, <0.001, and <0.001 for 10, 20, 45, and 60 minutes respectively).

Overall, our study shows that cancer cells cannot maintain balance after oxidative stress, as we see that they increase and keep increasing antioxidant capacity over time. Normal cells stop increasing their antioxidant capacity when they sense that the oxidative stress has been reduced. Our study also shows that the differences we see between Raji cells and normal lymphocytes with this oxidative treatment may suggest that cancer cells can increase their antioxidant capacity when they are exposed to oxidative stress, a mechanism that may be employed to protect themselves from the damaging effects of chemotherapy drugs.

APPENDIX 4: Yeast Two-Hybrid Reveals Novel Proteins Interacting with TK1

The following appendix contains unpublished data from a yeast two-hybrid analysis that we performed trying to find novel proteins interacting with TK1. We originally wanted to gain preliminary data that would allow us to continue with our hypothesis that TK1 was found on the membrane and wanted to see whether it could localize there through a protein-protein interaction.

Yeast two-hybrid assay

We used the Matchmaker Gold Yeast Two-Hybrid system. In this two-hybrid system, the libraries of prey proteins are expressed as fusions to the Gal4 activation domain (AD) and the bait proteins are expressed as fusions to the Gal4 DNA binding domain (DNA-BD). When the bait and prey proteins interact, the DNA-BD and the AD are brought into proximity and activate the transcription of four independent reporter genes (AUR1-C, ADE2, HIS3, and MEL1). The translation of these genes allow yeast to grow in SD –leu-trp-his-ade agar plates.

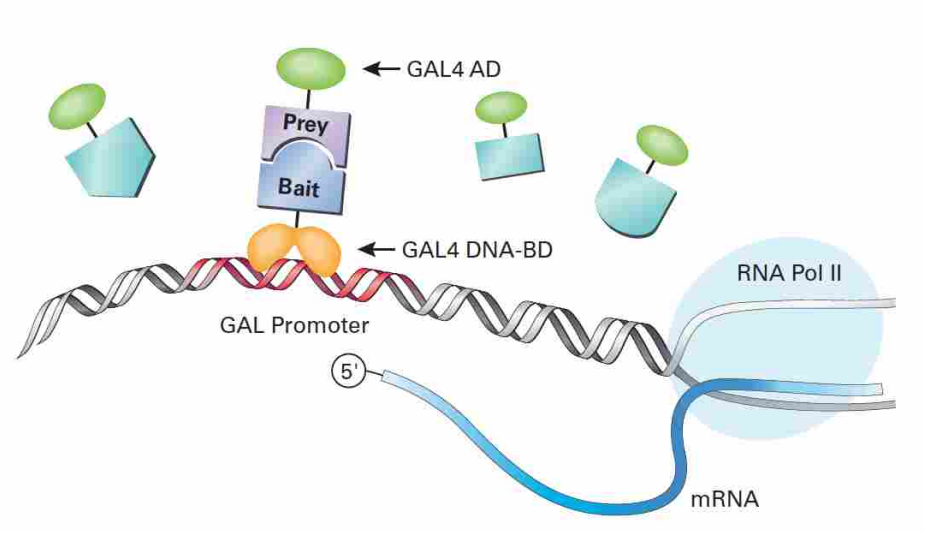

Figure A4- 1. Diagram of the Matchmaker Gold Yeast Two-Hybrid system.

Vectors

For the library of prey proteins, we selected the Normalized Yeast Two-Hybrid cDNA Library from Clonetech (catalog # 630481). The cDNA library was constructed using the pGADT7-RecAB vector.

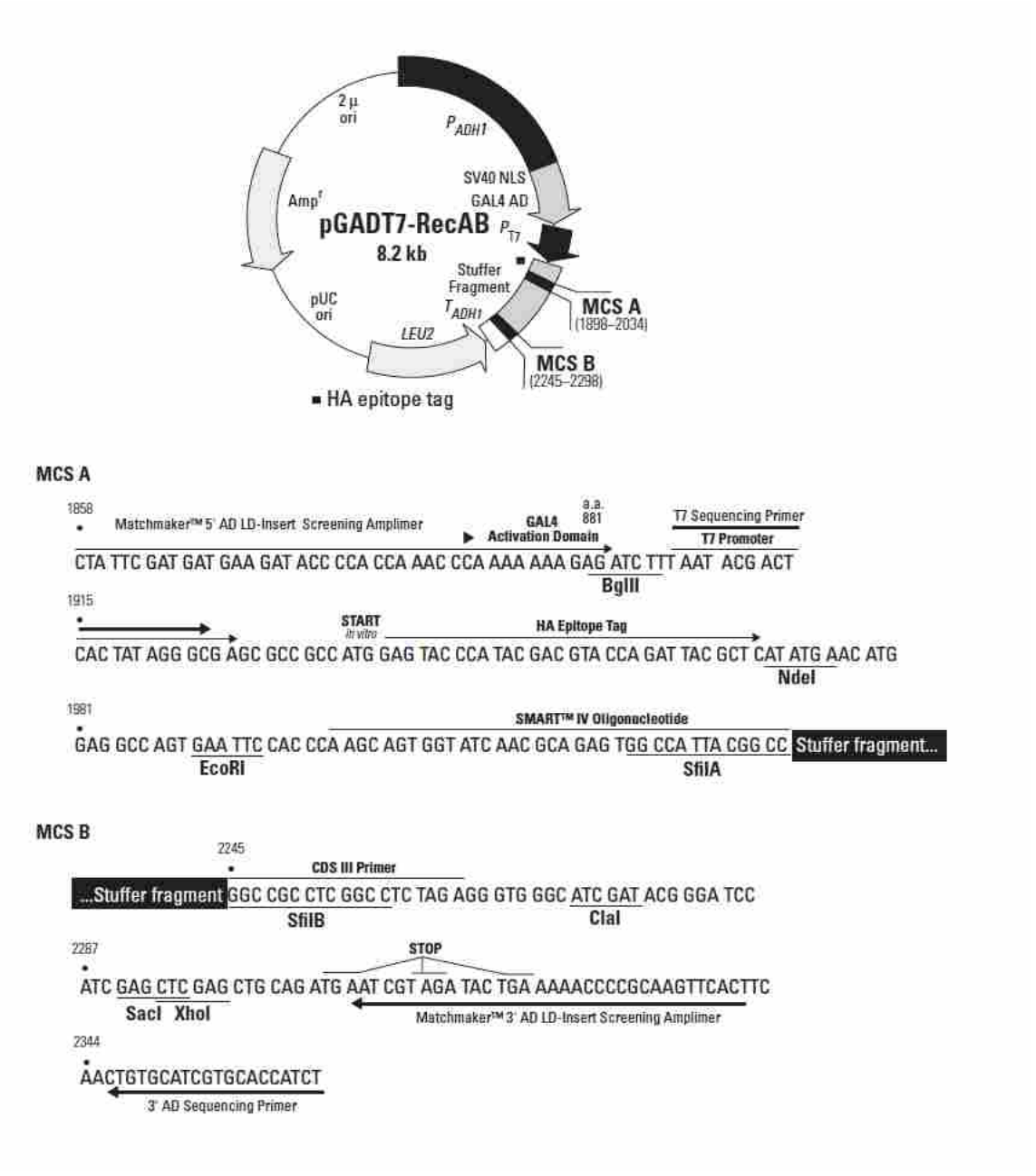

Figure A4- 2. Vector information from the Normalized Yeast Two-Hybrid cDNA Library from Clonetech.

For the bait protein, we cloned a yeast codon optimized human TK1 sequence into a pGBKT7 bait vector.

TK1 Sequence

The yeast codon optimized sequence for TK1 used is the following:

ATGTCCTGCATCAACTTACCTACCGTATTGCCTGGTTCTCCTTCAAAGACTAGAGGTC
AAATTCAAGTTATATTGGGTCCTATGTTCTCTGGTAAATCTACTGAATTGATGAGAA
GAGTTAGAAGATTCCAAATTGCTCAATACAAGTGTTTAGTTATTAAATACGCAAAGG
ATACAAGATACTCTTCATCTTTTTGTACTCATGATAGAAACACAATGGAAGCATTGC
CAGCTTGTTTGTTAAGAGATGTTGCACAAGAAGCATTGGGTGTTGCTGTTATTGGTA
TTGATGAAGGTCAATTTTTCCCAGATATCGTTGAATTTTGTGAAGCTATGGCAAATG
CTGGTAAAACTGTTATTGTTGCTGCATTGGATGGTACATTCCAAAGAAAGCCATTCG
GTGCAATCTTGAATTTGGTTCCATTGGCTGAATCAGTTGTTAAATTGACTGCAGTTTG
TATGGAATGTTTTAGAGAAGCTGCATACACTAAAAGATTGGGTACAGAAAAAGAAG
TTGAAGTTATTGGTGGTGCTGATAAGTACCATTCAGTTTGTAGATTATGTTACTTTAA
AAAGGCTTCTGGTCAACCAGCTGGTCCAGATAATAAGGAAAATTGTCCAGTTCCAG
GTAAACCAGGTGAAGCCGTAGCCGCAAGAAAGTTATTCGCCCCACAACAAATTTTA
CAATGTTCACCTGCCAAT

We transformed the pGBKT7-TK1 plasmid into the 1031 yeast strain and grew it in SD-trp selective medium. We then mated the pGBKT7-TK1 yeast with the cDNA library. We plated the mated yeast in SD-leu-trp-his-ade agar plates and incubated at 30°C incubator for up to 1 week. The colonies that grew were then grown in SD-leu selective medium to be able to select for the library plasmid only. The library plasmid was then extracted and transformed into E. Coli

(DH5α strain) and grown in LB amp selective medium. The plasmids were isolated again and sent for sequencing.

Primers

The primers used for sequencing were the following:

Forward: CTATTCGATGATGAAGATACCCCACC

Reverse: CAGAGGTTACATGGCCAAGATTG

Results and analysis

The results from sequencing were match to the human genomic and transcript database using Basic Local Alignment Search Tool (BLAST). We checked that the sequencing matched the coding region presented on the BLAST hits. We then used the ExPasy Translate tool to translate the protein sequence in-frame using the pGDAT7-RecAB vector information provided by Clonetech. The in-frame start codon can be found after this nucleotide sequence: AGCGCCGCC.

In-frame amino acid matches were then aligned with the wild type protein sequence from the BLAST hits. This allowed us to determine whether the library plasmids contained a true protein hit.

We performed the yeast two-hybrid experiment three times and obtained a total of 106 yeast colonies. After analysis, we obtained 17 true hits, 4 of which are novel.

Dependency assays

We then performed dependency assays to determine whether authenticity of the hits. To do this, we transformed the following into 1031 yeast:

- Empty pGBKT7 vector with empty pGDAT7-RecAB

- pGBKT7-TK1 with empty pGDAT7-RecAB
- Empty pGBKT7 vector with library plasmid match
- pGBKT7 vector with library plasmid match

We selected for yeast containing both plasmids by plating the transformed yeast on SD-leu-trp agar plates. We then plated the yeast into SD-leu-trp-his-ade agar plates to select for true interactors.

Novel proteins interacting with TK1

This is a list of the novel proteins that interact with TK1:

1. Ring finger protein 2 (RNF2)
2. G elongation factor, mitochondrial 2 (GFM2)
3. COP9 signalosome subunit 5 (COPS5)
4. DMRT like family A1 (DMRTA1)

REFERENCES

1. Hanahan D, Weinberg R a. Hallmarks of cancer: the next generation. *Cell*. 2011;144(5):646-674. doi:10.1016/j.cell.2011.02.013

2. Torre LA, Siegel RL, Ward EM, Jemal A. Global Cancer Incidence and Mortality Rates and Trends--An Update. *Cancer Epidemiol Biomarkers Prev*. 2016;25(1):16-27. doi:10.1158/1055-9965.EPI-15-0578

3. Alegre MM, Robison RA, O'Neill KL. The Clinical Significance and Biology of Thymidine Kinase 1. In: *Oncology Theory & Practice*. 1st ed. iConcept Press; 2014.

4. Bi M-H, Han W, Liu J-J, Wang H-Y, Gao Z-Y, Tian W-L. Clinical significance of serum thymidine kinase 1 (TK1) expression in patients with non-small cell lung cancer. *Int J Clin Exp Med*. 2016;9(5):8536-8542. www.ijcem.com. Accessed September 22, 2016.

5. Austin WR, Armijo AL, Campbell DO, et al. Nucleoside salvage pathway kinases regulate hematopoiesis by linking nucleotide metabolism with replication stress. *J Exp Med*. 2012;209(12):2215-2228. doi:10.1084/jem.20121061

6. Welin M, Kosinska U, Mikkelsen N-E, et al. Structures of thymidine kinase 1 of human and mycoplasmic origin. *Proc Natl Acad Sci U S A*. 2004;101(52):17970-17975. doi:10.1073/pnas.0406332102

7. Chen Y-L, Eriksson S, Chang Z-F. Regulation and functional contribution of thymidine kinase 1 in repair of DNA damage. *J Biol Chem*. 2010;285(35):27327-27335. doi:10.1074/jbc.M110.137042

8. Sherley JL, Kelly TJ. Regulation of human thymidine kinase during the cell cycle. *J Biol Chem*. 1988;263(17):8350-8358.

9. Ke P-Y, Hu C-M, Chang Y-C, Chang Z-F. Hiding human thymidine kinase 1 from APC/C-mediated destruction by thymidine binding. *FASEB J*. 2007;21(4):1276-1284. doi:10.1096/fj.06-7272com

10. Bohman C, Eriksson S. Deoxycytidine Kinase from Human Leukemic Spleen: Preparation and Characterization of the Homogeneous Enzyme. *Biochem J Biol Chem J Biochem {Tokyo) J Biol Chem Biochem Biophys Res Commun Biochem Nat {London) J Biol Chem*. 1988;27(321):4258-4265. http://pubs.acs.org/doi/pdf/10.1021/bi00412a009. Accessed October 16, 2017.

11. Radivoyevitch T, Saunthararajah Y, Pink J, et al. dNTP Supply Gene Expression Patterns after P53 Loss. *Cancers (Basel)*. 2012;4(4):1212-1224. doi:10.3390/cancers4041212

12. Schwartz JL, Tamura Y, Jordan R, Grierson JR, Krohn KA. Effect of p53 activation on cell growth, thymidine kinase-1 activity, and 3′-deoxy-3′fluorothymidine uptake. *Nucl Med Biol*. 2004;31(4):419-423. doi:10.1016/j.nucmedbio.2004.01.002

13. Haveman J, Sigmond J, van Bree C, Franken N, Koedooder C, Peters G. Time course of enhanced activity of deoxycytidine kinase and thymidine kinase 1 and 2 in cultured human squamous lung carcinoma cells, SW-1573, induced by γ-irradiation. *Oncol Rep*. October 2006. doi:10.3892/or.16.4.901

14. McKenna PG, O'Neill KL, Abram WP, Hannigan BM. Thymidine kinase activities in mononuclear leukocytes and serum from breast cancer patients. *Br J Cancer*. 1988;57(6):619-622. http://www.pubmedcentral.nih.gov/articlerender.fcgi?artid=2246471&tool=pmcentrez&rendertype=abstract. Accessed July 1, 2015.

15. Gronowitz JS, Hagberg H, Källander CF, Simonsson B. The use of serum deoxythymidine kinase as a prognostic marker, and in the monitoring of patients with non-Hodgkin's lymphoma. *Br J Cancer*. 1983;47(4):487-495. http://www.pubmedcentral.nih.gov/articlerender.fcgi?artid=2011337&tool=pmcentrez&rendertype=abstract. Accessed June 29, 2015.

16. Yan H. Thymidine kinase 1 as a diagnostic tumor marker is of moderate value in cancer patients: A meta-analysis. *Biomed Reports*. 2013;1(4):629-637. doi:10.3892/br.2013.114

17. O'Neill KL, Zhang F, Li H, Fuja DG, Murray BK. Thymidine kinase 1--a prognostic and

diagnostic indicator in ALL and AML patients. *Leuk Off J Leuk Soc Am Leuk Res Fund, UK*. 2007;21(3):560-563. doi:10.1038/sj.leu.2404536

18. Wu B-J, Li W-P, Qian C, Ding W, Zhou Z-W, Jiang H. Increased serum level of thymidine kinase 1 correlates with metastatic site in patients with malignant melanoma. *Tumour Biol*. 2013;34(2):643-648. doi:10.1007/s13277-012-0591-0

19. He Q, Zou L, Zhang PA, Lui JX, Skog S, Fornander T. The clinical significance of thymidine kinase 1 measurement in serum of breast cancer patients using anti-TK1 antibody. *Int J Biol Markers*. 2000;15(2):139-146. http://www.ncbi.nlm.nih.gov/pubmed/10883887. Accessed November 11, 2016.

20. Alegre MM, Robison RA, O'Neill KL. Thymidine kinase 1 upregulation is an early event in breast tumor formation. *J Oncol*. 2012;2012:575647. doi:10.1155/2012/575647

21. Svobodova S, Topolcan O, Holubec L, et al. Prognostic importance of thymidine kinase in colorectal and breast cancer. In: *Anticancer Research*. Vol 27. International Institute of Anticancer Research; 2007:1907-1909. http://www.ncbi.nlm.nih.gov/pubmed/17649793. Accessed June 6, 2017.

22. Zhang J, Jia Q, Zou S, et al. Thymidine kinase 1: A proliferation marker for determining prognosis and monitoring the surgical outcome of primary bladder carcinoma patients. *Oncol Rep*. 2006;15(2):455-461. http://www.spandidos-publications.com/or/15/2/455/abstract. Accessed February 9, 2016.

23. Thymidine kinase and cancer monitoring. *Cancer Lett*. 2012;316(1):6-10. doi:10.1016/J.CANLET.2011.10.025

24. O'Neill KL, Hoper M, Odling-Smee GW. Can thymidine kinase levels in breast tumors predict disease recurrence? *JNCI J Natl Cancer Inst*. 1992;84(23):1825-1828. doi:10.1093/jnci/84.23.1825

25. Konoplev SN, Fritsche HA, O'Brien S, et al. High Serum Thymidine Kinase 1 Level Predicts Poorer Survival in Patients With Chronic Lymphocytic Leukemia. *Am J Clin Pathol*. 2010;134(3):472-477. doi:10.1309/AJCPHMYT93HUIZKW

26. Zhou J, He E, Skog S. The proliferation marker thymidine kinase 1 in clinical use. *Mol Clin Oncol*. 2013;1(1):18-28. doi:10.3892/mco.2012.19

27. Munch-Petersen B. Reversible tetramerization of human TK1 to the high catalytic efficient form is induced by pyrophosphate, in addition to tripolyphosphates, or high enzyme concentration. *FEBS J*. 2009;276(2):571-580. doi:10.1111/j.1742-4658.2008.06804.x

28. Alegre MM, Weyant MJMJ, Bennet DT, et al. Serum Detection of Thymidine Kinase 1 as a Means of Early Detection of Lung Cancer. *Anticancer Res*. 2014;34(5):2145-2151. http://ar.iiarjournals.org/content/34/5/2145.short. Accessed February 13, 2015.

29. Fujiwaki R, Hata K, Moriyama M, et al. Clinical value of thymidine kinase in patients with cervical carcinoma. *Oncology*. 2001;61(1):47-54. doi:55352 [pii]

30. Luo P, He E, Eriksson S, et al. Thymidine kinase activity in serum of renal cell carcinoma patients is a useful prognostic marker. *Eur J Cancer Prev*. 2009;18(3):220-224. doi:10.1097/CEJ.0b013e328329d817

31. Alegre MM, Robison RA, O'Neill KL. Thymidine Kinase 1: A Universal Marker for Cancer. *Cancer Clin Oncol*. 2013;2(1):p159. doi:10.5539/cco.v2n1p159

32. Dunleavy K, Pittaluga S, Shovlin M, et al. Low-intensity therapy in adults with Burkitt's lymphoma. *N Engl J Med*. 2013;369(20):1915-1925. doi:10.1056/NEJMoa1308392

33. Thomas DA, Faderl S, O'Brien S, et al. Chemoimmunotherapy with hyper-CVAD plus rituximab for the treatment of adult Burkitt and Burkitt-type lymphoma or acute lymphoblastic leukemia. *Cancer*. 2006;106(7):1569-1580. doi:10.1002/cncr.21776

34. Molyneux EM, Rochford R, Griffin B, et al. Burkitt's lymphoma. *Lancet*. 2012;379(9822):1234-1244. doi:10.1016/S0140-6736(11)61177-X

35. Hesseling P, Broadhead R, Mansvelt E, et al. The 2000 Burkitt lymphoma trial in Malawi. *Pediatr Blood Cancer*. 2005;44(3):245-250. doi:10.1002/pbc.20254

36. Gerrard M, Cairo MS, Weston C, et al. Excellent survival following two courses of COPAD chemotherapy in children and adolescents with resected localized B-cell non-Hodgkin's lymphoma: results of the FAB/LMB 96 international study. *Br J Haematol*. 2008;141(6):840-847. doi:10.1111/j.1365-2141.2008.07144.x

37. Hunger SP, Mullighan CG. Acute Lymphoblastic Leukemia in Children. *N Engl J Med*. October 2015. doi:10.1056/NEJMra1400972

38. Inaba H, Greaves M, Mullighan CG. Acute lymphoblastic leukaemia. *Lancet*. 2013;381(9881):1943-1955. doi:10.1016/S0140-6736(12)62187-4

39. Ribera J-M. Acute Lymphoblastic Leukemia. In: *HIV-Associated Hematological Malignancies*. Cham: Springer International Publishing; 2016:145-151. doi:10.1007/978-3-319-26857-6_11

40. Zhang F, Shao X, Li H, Robison JG, Murray BK, O'Neill KL. A monoclonal antibody specific for human thymidine kinase 1. *Hybridoma*. 2001;20(1):25-34. doi:10.1089/027245701300060382

41. O'Neill KL. Monoclonal antibodies to thymidine kinase 1 and uses in diagnostic and therapeutic applications. 1997;(3).

42. O'Neill K. Anti-Cancer Activity of an Anti-Thymidine Kinase Monoclonal Antibody. *US Pat App 12/767,489*. 2010;(54). https://www.google.com/patents/US20100266495. Accessed May 30, 2017.

43. O'Neill KL, Abram WP, McKenna PG. Serum thymidine kinase levels in cancer patients. *Ir J Med Sci*. 1986;155(8):272-274. doi:10.1007/BF02939884

44. Lee LS, Cheng Y-C. Human deoxythymidine kinase II: substrate specificity and kinetic behavior of the cytoplasmic and mitochondrial isozymes derived from blast cells of acute myelocytic leukemia. *Biochemistry*. 1976;15(17):3686-3690. http://pubs.acs.org/doi/pdf/10.1021/bi00662a007. Accessed May 30, 2017.

45. Milner AE, Grand RJ, Waters CM, Gregory CD. Apoptosis in Burkitt lymphoma cells is

driven by c-myc. *Oncogene*. 1993;8(12):3385-3391. http://www.ncbi.nlm.nih.gov/pubmed/8247541. Accessed August 8, 2016.

46. - AD, - PJ, - HY, et al. - Surface molecule CD229 represents a target for the treatment of multiple myeloma. - *Bone Marrow TransplantationConference 36th Annu Meet Eur Gr Blood Marrow Transplantation, EBMT 2010 Vienna AustriaConference Start 20100321 Conf End 20100324Conference Publ (var.pagings)45 (pp S(TRUNCATED*. 2011;96(10). doi:- http://dx.doi.org/10.1038/bmt.2010.41

47. Vinayagam A, Stelzl U, Foulle R, et al. A directed protein interaction network for investigating intracellular signal transduction. *Sci Signal*. 2011;4(189):rs8. doi:10.1126/scisignal.2001699

48. Stelzl U, Worm U, Lalowski M, et al. A human protein-protein interaction network: A resource for annotating the proteome. *Cell*. 2005;122(6):957-968. doi:10.1016/j.cell.2005.08.029

49. Wang J, Huo K, Ma L, et al. Toward an understanding of the protein interaction network of the human liver. *Mol Syst Biol*. 2011;7(1). http://msb.embopress.org/content/7/1/536.abstract.

50. Stewart BW, Wild CP. *World Cancer Report 2014*.; 2014. doi:9283204298

51. Torre LA, Bray F, Siegel RL, Ferlay J, Lortet-Tieulent J, Jemal A. Global cancer statistics, 2012. *CA Cancer J Clin*. 2015;65(2):87-108. doi:10.3322/caac.21262 [doi]

52. Siegel RL, Miller KD, Jemal A. Cancer statistics, 2016. *CA Cancer J Clin*. 2016;66(1):7-30. doi:10.3322/caac.21332

53. Pepe MS, Etzioni R, Feng Z, et al. Phases of biomarker development for early detection of cancer. *J Natl Cancer Inst*. 2001;93(14):1054-1061. doi:11459866

54. Dalton WS, Friend SH. Cancer Biomarkers-An Invitation to the Table. *Science (80-)*. 2006;312(5777):1165-1168. doi:10.1126/science.1125948

55. Zhang F, Li H, Pendleton AR, et al. Thymidine kinase 1 immunoassay: a potential marker for breast cancer. *Cancer Detect Prev*. 2001;25(1):8-15. http://www.ncbi.nlm.nih.gov/pubmed/11270425. Accessed November 11, 2016.

56. Wang Y, Jiang X, Dong S, et al. Serum TK1 is a more reliable marker than CEA and AFP for cancer screening in a study of 56,286 people. *Cancer Biomarkers*. 2016;16(4):529-536. doi:10.3233/CBM-160594

57. Kumar JK, Aronsson AC, Pilko G, et al. A clinical evaluation of the TK 210 ELISA in sera from breast cancer patients demonstrates high sensitivity and specificity in all stages of disease. *Tumor Biol*. 2016;37(9):11937-11945. doi:10.1007/s13277-016-5024-z

58. Chang K, Creighton CJ, Davis C, et al. The Cancer Genome Atlas Pan-Cancer analysis project. *Nat Genet*. 2013;45(10):1113-1120. doi:10.1038/ng.2764

59. Liao Y, Smyth GK, Shi W. featureCounts: an efficient general purpose program for assigning sequence reads to genomic features. *Bioinformatics*. 2014;30(7):923-930. doi:10.1093/bioinformatics/btt656

60. Rahman M, Jackson LK, Johnson WE, Li DY, Bild AH, Piccolo SR. Alternative preprocessing of RNA-Sequencing data in The Cancer Genome Atlas leads to improved analysis results. *Bioinformatics*. 2015;31(22):3666-3672. doi:10.1093/bioinformatics/btv377

61. R Core Team. A language and environment for statistical computing. R foundation for statistical computing. 2014. http://www.r-project.org/.

62. Wickham H. *Ggplot2: Elegant Graphics for Data Analysis*. Vol 35. New York, NY: Springer New York; 2009. doi:10.1007/978-0-387-98141-3

63. Schneider CA, Rasband WS, Eliceiri KW. NIH Image to ImageJ: 25 years of image analysis. *Nat Methods*. 2012;9(7):671-675. doi:10.1038/nmeth.2089

64. Wong WM, Wright NA. Cell proliferation in gastrointestinal mucosa. *J Clin Pathol*. 1999;52(5):321-333. doi:10.1136/jcp.52.5.321

65. Leon G, MacDonagh L, Finn SP, Cuffe S, Barr MP. Cancer stem cells in drug resistant lung cancer: Targeting cell surface markers and signaling pathways. *Pharmacol Ther*. 2016;158:71-90. doi:10.1016/j.pharmthera.2015.12.001

66. Kibbelaar RE, Moolenaar KEC, Michalides RJAM, et al. Neural cell adhesion molecule expression, neuroendocrine differentiation and prognosis in lung carcinoma. *Eur J Cancer*. 1991;27(4):431-435. doi:10.1016/0277-5379(91)90379-R

67. Lawson DA, Bhakta NR, Kessenbrock K, et al. Single-cell analysis reveals a stem-cell program in human metastatic breast cancer cells. *Nature*. 2015;526(7571):131-135. doi:10.1038/nature15260

68. Sahlberg SH, Spiegelberg D, Glimelius B, Stenerlöw B, Nestor M. Evaluation of Cancer Stem Cell Markers CD133, CD44, CD24: Association with AKT Isoforms and Radiation Resistance in Colon Cancer Cells. Yeudall A, ed. *PLoS One*. 2014;9(4):e94621. doi:10.1371/journal.pone.0094621

69. Weagel EG, Meng W, Townsend MH, et al. Biomarker analysis and clinical relevance of thymidine kinase 1 on the cell membrane of Burkitt's lymphoma and acute lymphoblastic leukemia. *Onco Targets Ther*. 2017;10:1-13.

70. Pegram M, Slamon D. Biological rationale for HER2/neu (c-erbB2) as a target for monoclonal antibody therapy. *Semin Oncol*. 2000;27(5 Suppl 9):13-19. http://www.ncbi.nlm.nih.gov/pubmed/11049052. Accessed May 3, 2018.

71. English DP, Roque DM, Santin AD. HER2 expression beyond breast cancer: therapeutic implications for gynecologic malignancies. *Mol Diagn Ther*. 2013;17(2):85-99. doi:10.1007/s40291-013-0024-9

72. Magnifico A, Albano L, Campaner S, et al. Tumor-initiating cells of HER2-positive carcinoma cell lines express the highest oncoprotein levels and are sensitive to trastuzumab. *Clin Cancer Res*. 2009;15(6):2010-2021. doi:10.1158/1078-0432.CCR-08-1327

73. Sartore-Bianchi A, Trusolino L, Martino C, et al. Dual-targeted therapy with trastuzumab

and lapatinib in treatment-refractory, KRAS codon 12/13 wild-type, HER2-positive metastatic colorectal cancer (HERACLES): a proof-of-concept, multicentre, open-label, phase 2 trial. *Lancet Oncol*. 2016;17(6):738-746. doi:10.1016/S1470-2045(16)00150-9

74. Seol H, Lee HJ, Choi Y, et al. Intratumoral heterogeneity of HER2 gene amplification in breast cancer: its clinicopathological significance. *Mod Pathol*. 2012;25(7):938-948. doi:10.1038/modpathol.2012.36

75. Ram S, Kim D, Ober RJ, Ward ES. The level of HER2 expression is a predictor of antibody-HER2 trafficking behavior in cancer cells. *MAbs*. 2014;6(5):1211-1219. doi:10.4161/mabs.29865

76. Cunningham MP, Thomas H, Fan Z, Modjtahedi H. Responses of Human Colorectal Tumor Cells to Treatment with the Anti–Epidermal Growth Factor Receptor Monoclonal Antibody ICR62 Used Alone and in Combination with the EGFR Tyrosine Kinase Inhibitor Gefitinib. *Cancer Res*. 2006;66(15):7708-7715. doi:10.1158/0008-5472.CAN-06-1000

77. Hathaway HJ, Butler KS, Adolphi NL, et al. Detection of breast cancer cells using targeted magnetic nanoparticles and ultra-sensitive magnetic field sensors. *Breast Cancer Res*. 2011;13(5). file:///C:/Users/Evita Weagel/Downloads/bcr3050.pdf. Accessed May 3, 2018.

78. Mutahir Z, Clausen AR, Andersson K-M, Wisen SM, Munch-Petersen B, Piškur J. Thymidine kinase 1 regulatory fine-tuning through tetramer formation. *FEBS J*. 2013;280(6):1531-1541. doi:10.1111/febs.12154

79. Weagel EG, Burrup W, Kovtun R, et al. Membrane expression of thymidine kinase 1 and potential clinical relevance in lung, breast, and colorectal malignancies. *Cancer Cell Int*. 2018.

80. American Cancer Society. *Cancer Facts & Figures 2015*.; 2015.

81. Hoyert DL, Xu J. *National Vital Statistics Reports Deaths : Preliminary Data for 2011*. Vol 61.; 2012.

82. American Cancer Society. Cancer Facts & Figures. *Cancer Facts Fig*. 2014. http://www.cancer.org/research/cancerfactsstatistics/cancerfactsfigures2014/index. Accessed May 8, 2014.

83. Steidl C, Lee T, Shah S. Tumor-associated macrophages and survival in classic Hodgkin's lymphoma. *N Engl J Med*. 2010;362(10):875-885. http://www.nejm.org/doi/full/10.1056/NEJMoa0905680. Accessed November 26, 2012.

84. Kurahara H, Shinchi H, Mataki Y, et al. Significance of M2-polarized tumor-associated macrophage in pancreatic cancer. *J Surg Res*. 2011;167(2):e211-9. doi:10.1016/j.jss.2009.05.026

85. Eiró N, Vizoso FJ. Inflammation and cancer. *World J Gastrointest Surg*. 2012;4(3):62-72. doi:10.4240/wjgs.v4.i3.62

86. Lewis C, Leek R. Cytokine regulation of angiogenesis in breast cancer: the role of tumor-associated macrophages. *J Leukoc …*. 1995;57(May):747-751. http://www.jleukbio.org/content/57/5/747.short. Accessed August 19, 2014.

87. Kelly PM, Davison RS, Bliss E, McGee JO. Macrophages in human breast disease: a quantitative immunohistochemical study. *Br J Cancer*. 1988;57(2):174-177. http://www.pubmedcentral.nih.gov/articlerender.fcgi?artid=2246436&tool=pmcentrez&rendertype=abstract. Accessed August 19, 2014.

88. Porta C, Rimoldi M, Raes G, et al. Tolerance and M2 (alternative) macrophage polarization are related processes orchestrated by p50 nuclear factor kappaB. *Proc Natl Acad Sci U S A*. 2009;106(35):14978-14983. doi:10.1073/pnas.0809784106

89. Mantovani A, Biswas SK, Galdiero MR, Sica A, Locati M. Macrophage plasticity and polarization in tissue repair and remodelling. *J Pathol*. 2013;229(2):176-185. doi:10.1002/path.4133

90. Sica A, Mantovani A. Macrophage plasticity and polarization: in vivo veritas. *J Clin Invest*. 2012;122(3):787-796. doi:10.1172/JCI59643DS1

91. Anderson CF, Mosser DM. A novel phenotype for an activated macrophage: the type 2 activated macrophage. *J Leukoc Biol*. 2002;72(1):101-106. http://www.ncbi.nlm.nih.gov/pubmed/12101268.

92. Ghassabeh GH, De Baetselier P, Brys L, et al. Identification of a common gene signature for type II cytokine-associated myeloid cells elicited in vivo in different pathologic conditions. *Blood*. 2006;108(2):575-583. doi:10.1182/blood-2005-04-1485

93. Liao X, Sharma N, Kapadia F. Krüppel-like factor 4 regulates macrophage polarization. *J Clin Invest*. 2011;121(7). doi:10.1172/JCI45444DS1

94. Davis MJ, Tsang TM, Qiu Y, et al. Macrophage M1/M2 polarization dynamically adapts to changes in cytokine microenvironments in Cryptococcus neoformans infection. *MBio*. 2013;4(3):e00264-13. doi:10.1128/mBio.00264-13

95. Mantovani A, Sozzani S, Locati M, Allavena P, Sica A. Macrophage polarization: tumor-associated macrophages as a paradigm for polarized M2 mononuclear phagocytes. *Trends Immunol*. 2002;23(11):549-555. http://www.ncbi.nlm.nih.gov/pubmed/12401408.

96. Forssell J, Oberg A, Henriksson ML, Stenling R, Jung A, Palmqvist R. High macrophage infiltration along the tumor front correlates with improved survival in colon cancer. *Clin cancer Res*. 2007;13(5):1472-1479. doi:10.1158/1078-0432.CCR-06-2073

97. Edin S, Wikberg ML, Dahlin AM, et al. The distribution of macrophages with a m1 or m2 phenotype in relation to prognosis and the molecular characteristics of colorectal cancer. *PLoS One*. 2012;7(10):e47045. doi:10.1371/journal.pone.0047045

98. Hao N-B, Lü M-H, Fan Y-H, Cao Y-L, Zhang Z-R, Yang S-M. Macrophages in tumor microenvironments and the progression of tumors. *Clin Dev Immunol*. 2012;2012:948098. doi:10.1155/2012/948098

99. Sinha P, Clements VK, Ostrand-Rosenberg S. Reduction of myeloid-derived suppressor cells and induction of M1 macrophages facilitate the rejection of established metastatic disease. *J Immunol*. 2005;174(2):636-645. http://www.ncbi.nlm.nih.gov/pubmed/15634881.

100. Ma J, Liu L, Che G, Yu N, Dai F, You Z. The M1 form of tumor-associated macrophages in non-small cell lung cancer is positively associated with survival time. *BMC Cancer*. 2010;10:112. doi:10.1186/1471-2407-10-112

101. Ohri CM, Shikotra A, Green RH, Waller D a, Bradding P. Macrophages within NSCLC tumour islets are predominantly of a cytotoxic M1 phenotype associated with extended survival. *Eur Respir J*. 2009;33(1):118-126. doi:10.1183/09031936.00065708

102. Herbeuval J-P, Lambert C, Sabido O, et al. Macrophages from cancer patients: analysis of TRAIL, TRAIL receptors, and colon tumor cell apoptosis. *J Natl Cancer Inst*. 2003;95(8):611-621. http://www.ncbi.nlm.nih.gov/pubmed/12697854.

103. Bingle L, Brown NJ, Lewis CE. The role of tumour-associated macrophages in tumour progression: implications for new anticancer therapies. *J Pathol*. 2002;196(3):254-265. doi:10.1002/path.1027

104. Wong S-C, Puaux A-L, Chittezhath M, et al. Macrophage polarization to a unique phenotype driven by B cells. *Eur J Immunol*. 2010;40(8):2296-2307. doi:10.1002/eji.200940288

105. Urban JL, Shepard HM, Rothstein JL, Sugarman BJ, Schreiber H. Tumor necrosis factor: a potent effector molecule for tumor cell killing by activated macrophages. *Proc Natl Acad Sci U S A*. 1986;83(14):5233-5237. http://www.pubmedcentral.nih.gov/articlerender.fcgi?artid=323925&tool=pmcentrez&rendertype=abstract.

106. Hardison SE, Herrera G, Young ML, Hole CR, Wozniak KL, Wormley FL. Protective immunity against pulmonary cryptococcosis is associated with STAT1-mediated classical macrophage activation. *J Immunol*. 2012;189(8):4060-4068. doi:10.4049/jimmunol.1103455

107. Wang Y-C, He F, Feng F, et al. Notch signaling determines the M1 versus M2 polarization of macrophages in antitumor immune responses. *Cancer Res*. 2010;70(12):4840-4849. doi:10.1158/0008-5472.CAN-10-0269

108. Cai X, Yin Y, Li N, et al. Re-polarization of tumor-associated macrophages to pro-inflammatory M1 macrophages by microRNA-155. *J Mol Cell Biol*. 2012;4(5):341-343. doi:10.1093/jmcb/mjs044

109. Wei Y, Nazari-Jahantigh M, Chan L, et al. The microRNA-342-5p fosters inflammatory macrophage activation through an Akt1- and microRNA-155-dependent pathway during atherosclerosis. *Circulation*. 2013;127(15):1609-1619. doi:10.1161/CIRCULATIONAHA.112.000736

110. Squadrito ML, Etzrodt M, De Palma M, Pittet MJ. MicroRNA-mediated control of macrophages and its implications for cancer. *Trends Immunol*. 2013;34(7):350-359. doi:10.1016/j.it.2013.02.003

111. Guiducci C, Vicari AP, Sangaletti S, Trinchieri G, Colombo MP. Redirecting in vivo elicited tumor infiltrating macrophages and dendritic cells towards tumor rejection. *Cancer Res*. 2005;65(8):3437-3446. doi:10.1158/0008-5472.CAN-04-4262

112. Biswas SK, Gangi L, Paul S, et al. A distinct and unique transcriptional program expressed by tumor-associated macrophages (defective NF-kappaB and enhanced IRF-3/STAT1 activation). *Blood*. 2006;107(5):2112-2122. doi:10.1182/blood-2005-01-0428

113. Lin EY, Li J-F, Gnatovskiy L, et al. Macrophages regulate the angiogenic switch in a mouse model of breast cancer. *Cancer Res*. 2006;66(23):11238-11246. doi:10.1158/0008-5472.CAN-06-1278

114. Barros MHM, Hauck F, Dreyer JH, Kempkes B, Niedobitek G. Macrophage Polarisation: an Immunohistochemical Approach for Identifying M1 and M2 Macrophages. Idzko M, ed. *PLoS One*. 2013;8(11):e80908. doi:10.1371/journal.pone.0080908

115. Hagemann T, Wilson J, Burke F, et al. Ovarian cancer cells polarize macrophages toward a tumor-associated phenotype. *J Immunol*. 2006;176(8):5023-5032. http://www.ncbi.nlm.nih.gov/pubmed/16585599.

116. Mandal P, Pratt BT, Barnes M, McMullen MR, Nagy LE. Molecular mechanism for adiponectin-dependent M2 macrophage polarization: link between the metabolic and

innate immune activity of full-length adiponectin. *J Biol Chem*. 2011;286(15):13460-13469. doi:10.1074/jbc.M110.204644

117. Baccala R, Hoebe K, Kono DH, Beutler B, Theofilopoulos AN. TLR-dependent and TLR-independent pathways of type I interferon induction in systemic autoimmunity. *Nat Med*. 2007;13(5):543-551. doi:10.1038/nm1590

118. Hu Y, Zhang H, Lu Y, et al. Class A scavenger receptor attenuates myocardial infarction-induced cardiomyocyte necrosis through suppressing M1 macrophage subset polarization. *Basic Res Cardiol*. 2011;106(6):1311-1328. doi:10.1007/s00395-011-0204-x

119. Lawrence T, Natoli G. Transcriptional regulation of macrophage polarization: enabling diversity with identity. *Nat Rev Immunol*. 2011;11(11):750-761. doi:10.1038/nri3088

120. Banerjee S, Xie N, Cui H, et al. MicroRNA let-7c regulates macrophage polarization. *J Immunol*. 2013;190(12):6542-6549. doi:10.4049/jimmunol.1202496

121. Lodish HF, Zhou B, Liu G, Chen C-Z. Micromanagement of the immune system by microRNAs. *Nat Rev Immunol*. 2008;8(2):120-130. doi:10.1038/nri2252

122. Murray PJJ, Allen JEE, Biswas SKK, et al. Macrophage Activation and Polarization: Nomenclature and Experimental Guidelines. *Immunity*. 2014;41(1):14-20. doi:10.1016/j.immuni.2014.06.008

123. Mantovani A, Allavena P, Sica A, Balkwill F. Cancer-related inflammation. *Nature*. 2008;454(7203):436-444. doi:10.1038/nature07205

124. Cortez-Retamozo V, Etzrodt M, Newton A, et al. Origins of tumor-associated macrophages and neutrophils. *Proc Natl Acad Sci U S A*. 2012;109(7):2491-2496. doi:10.1073/pnas.1113744109

125. Smith HO, Stephens ND, Qualls CR, et al. The clinical significance of inflammatory cytokines in primary cell culture in endometrial carcinoma. *Mol Oncol*. 2013;7(1):41-54. doi:10.1016/j.molonc.2012.07.002

126. Hercus TR, Thomas D, Guthridge MA, et al. The granulocyte-macrophage colony-stimulating factor receptor: linking its structure to cell signaling and its role in disease. *Blood*. 2009;114(7):1289-1298. doi:10.1182/blood-2008-12-164004

127. West RB, Rubin BP, Miller MA, et al. A landscape effect in tenosynovial giant-cell tumor from activation of CSF1 expression by a translocation in a minority of tumor cells. *Proc Natl Acad Sci U S A*. 2006;103(3):690-695. doi:10.1073/pnas.0507321103

128. Lin EY, Pollard JW. Tumor-associated macrophages press the angiogenic switch in breast cancer. *Cancer Res*. 2007;67(11):5064-5066. doi:10.1158/0008-5472.CAN-07-0912

129. Dalton HJ, Armaiz-Pena GN, Gonzalez-Villasana V, Lopez-Berestein G, Bar-Eli M, Sood AK. Monocyte subpopulations in angiogenesis. *Cancer Res*. 2014;74(5):1287-1293. doi:10.1158/0008-5472.CAN-13-2825

130. Hagemann T, Lawrence T, McNeish I, et al. "Re-educating" tumor-associated macrophages by targeting NF-kappaB. *J Exp Med*. 2008;205(6):1261-1268. doi:10.1084/jem.20080108

131. Saccani A, Schioppa T, Porta C, et al. p50 nuclear factor-kappaB overexpression in tumor-associated macrophages inhibits M1 inflammatory responses and antitumor resistance. *Cancer Res*. 2006;66(23):11432-11440. doi:10.1158/0008-5472.CAN-06-1867

132. Gazzaniga S, Bravo AI, Guglielmotti A, et al. Targeting tumor-associated macrophages and inhibition of MCP-1 reduce angiogenesis and tumor growth in a human melanoma xenograft. *J Invest Dermatol*. 2007;127(8):2031-2041. doi:10.1038/sj.jid.5700827

133. Luo Y, Zhou H, Krueger J. Targeting tumor-associated macrophages as a novel strategy against breast cancer. *J Clin Invest*. 2006;116(8):2132-2141. doi:10.1172/JCI27648.2132

134. Zeisberger SM, Odermatt B, Marty C, Zehnder-Fjällman a HM, Ballmer-Hofer K, Schwendener R a. Clodronate-liposome-mediated depletion of tumour-associated macrophages: a new and highly effective antiangiogenic therapy approach. *Br J Cancer*. 2006;95(3):272-281. doi:10.1038/sj.bjc.6603240

135. Shaw RJ. Glucose metabolism and cancer. *Curr Opin Cell Biol*. 2006;18(6):598-608. doi:10.1016/j.ceb.2006.10.005

136. Bettencourt-Dias M, Giet R, Sinka R, et al. Genome-wide survey of protein kinases required for cell cycle progression. *Nature*. 2004;432(7020):980-987. doi:10.1038/nature03160

137. Wolf A, Agnihotri S, Micallef J, et al. Hexokinase 2 is a key mediator of aerobic glycolysis and promotes tumor growth in human glioblastoma multiforme. *J Exp Med*. 2011;208(2):313-326. doi:10.1084/jem.20101470

138. Geschwind JH, Vali M, Wahl R. Effects of 3 - bromopyruvate (hexokinase 2 inhibitor) on glucose uptake in lewis rats using 2-(F-18) fluoro-2-deoxy-d-glucose. In: *2006 Gastrointestinal Cancers Symposium*. ; 2006:12-14.

139. Blagih J, Jones RG. Polarizing macrophages through reprogramming of glucose metabolism. *Cell Metab*. 2012;15(6):793-795. doi:10.1016/j.cmet.2012.05.008

140. Haschemi A, Kosma P, Gille L, et al. The sedoheptulose kinase CARKL directs macrophage polarization through control of glucose metabolism. *Cell Metab*. 2012;15(6):813-826. doi:10.1016/j.cmet.2012.04.023

141. Arranz A, Doxaki C, Vergadi E, et al. Akt1 and Akt2 protein kinases differentially contribute to macrophage polarization. *Proc Natl Acad Sci U S A*. 2012;109(24):9517-9522. doi:10.1073/pnas.1119038109

142. Jones RG, Thompson CB. Revving the engine: signal transduction fuels T cell activation. *Immunity*. 2007;27(2):173-178. doi:10.1016/j.immuni.2007.07.008

143. Shu CJ, Guo S, Kim YJ, et al. Visualization of a primary anti-tumor immune response by positron emission tomography. *Proc Natl Acad Sci U S A*. 2005;102(48):17412-17417. doi:10.1073/pnas.0508698102

144. Van Ginderachter JA, Movahedi K, Hassanzadeh Ghassabeh G, et al. Classical and alternative activation of mononuclear phagocytes: Picking the best of both worlds for

tumor promotion. *Immunobiology*. 2006;211(6):487-501. http://www.sciencedirect.com/science/article/pii/S0171298506000829. Accessed January 22, 2014.

145. Mills CD, Shearer J, Evans R, Caldwell MD. Macrophage arginine metabolism and the inhibition or stimulation of cancer. *J Immunol*. 1992;149(8):2709-2714. http://www.ncbi.nlm.nih.gov/pubmed/1401910.

146. Ji Y, Sun S, Xu A, et al. Activation of natural killer T cells promotes M2 Macrophage polarization in adipose tissue and improves systemic glucose tolerance via interleukin-4 (IL-4)/STAT6 protein signaling axis in obesity. *J Biol Chem*. 2012;287(17):13561-13571. doi:10.1074/jbc.M112.350066

147. Andreesen R, Scheibenbogen C, Brugger W. Adoptive transfer of tumor cytotoxic macrophages generated in vitro from circulating blood monocytes: a new approach to cancer immunotherapy. *Cancer Res*. 1990:7450-7456. http://cancerres.aacrjournals.org/content/50/23/7450.short. Accessed November 28, 2012.

148. Korbelik M, Naraparaju VR, Yamamoto N. Macrophage-directed immunotherapy as adjuvant to photodynamic therapy of cancer. *Br J Cancer*. 1997;75(2):202-207. http://www.pubmedcentral.nih.gov/articlerender.fcgi?artid=2063270&tool=pmcentrez&rendertype=abstract.

149. Ellem KAO, Rourke MGEO, Johnson GR, et al. A case report: immune responses and clinical course of the first human use of granulocyte/macrophage-colony-stimulating-factor-transduced autologous melanoma. *Cancer Immunol Immunother*. 1997:10-20. http://www.springerlink.com/index/JQ4EB21E4C7ADMT7.pdf. Accessed November 28, 2012.

150. Hill H, Jr TC, Sabel M. Immunotherapy with Interleukin 12 and Granulocyte-Macrophage Colony-stimulating Factor-encapsulated Microspheres Coinduction of Innate and Adaptive Antitumor. *Cancer Res*. 2002. http://cancerres.aacrjournals.org/content/62/24/7254.short. Accessed November 28, 2012.

151. Gast G de, Klümpen H. immunotherapy with subcutaneous granulocyte macrophage colony-stimulating factor, low-dose interleukin 2, and interferon Î± in progressive metastatic melanoma. *Clin cancer Res*. 2000. http://clincancerres.aacrjournals.org/content/6/4/1267.short. Accessed November 28, 2012.

152. Lokshin A, Mayotte JJE, Levitt MML. Mechanism of Interferon Beta-Induced Squamous Differentiation and Programmed Cell Death in Human Non-Small-Cell Lung Cancer Cell Lines. *J Natl Cancer Inst*. 1995;87:206-212. http://jnci.oxfordjournals.org/content/87/3/206.short. Accessed November 28, 2012.

153. Johns T, Mackay IIR, Johns ATG, et al. Antiproliferative potencies of interferons on melanoma cell lines and xenografts: higher efficacy of interferon Î². *J Natl Cancer Inst*. 1992;(type II):1185-1190. http://jnci.oxfordjournals.org/content/84/15/1185. Accessed November 28, 2012.

154. Qin X-Q, Runkel L, Deck C, DeDios C, Barsoum J. Interferon-beta induces S phase accumulation selectively in human transformed cells. *J Interf Cytokine Res*. 1997;17(6):355-367. doi:10.1089/jir.1997.17.355

155. Zhang F, Lu W, Dong Z. Tumor-infiltrating macrophages are involved in suppressing growth and metastasis of human prostate cancer cells by INF-β gene therapy in nude mice. *Clin cancer Res*. 2002:2942-2951. http://clincancerres.aacrjournals.org/content/8/9/2942.short. Accessed November 28, 2012.

156. Simpson KD, Templeton DJ, Cross J V. Macrophage Migration Inhibitory Factor Promotes Tumor Growth and Metastasis by Inducing Myeloid-Derived Suppressor Cells in the Tumor Microenvironment. *J Immunol*. November 2012. doi:10.4049/jimmunol.1201161

157. Sanford DE, Belt BA, Panni RZ, et al. Inflammatory monocyte mobilization decreases patient survival in pancreatic cancer: a role for targeting the CCL2/CCR2 axis. *Clin Cancer Res*. 2013;19(13):3404-3415. doi:10.1158/1078-0432.CCR-13-0525

158. Schmall A, Al-Tamari HM, Herold S, et al. Macrophage and Cancer Cell Crosstalk via CCR2 and CX3CR1 is a Fundamental Mechanism Driving Lung Cancer. *Am J Respir Crit Care Med*. December 2014. doi:10.1164/rccm.201406-1137OC

159. Kimura YN, Watari K, Fotovati A, et al. Inflammatory stimuli from macrophages and cancer cells synergistically promote tumor growth and angiogenesis. *Cancer Sci*. 2007;98(12):2009-2018. doi:10.1111/j.1349-7006.2007.00633.x

160. Chen H, Li P, Yin Y, et al. The promotion of type 1 T helper cell responses to cationic polymers in vivo via toll-like receptor-4 mediated IL-12 secretion. *Biomaterials*. 2010;31(32):8172-8180. doi:10.1016/j.biomaterials.2010.07.056

161. Rogers TL, Holen I. Tumour macrophages as potential targets of bisphosphonates. *J Transl Med*. 2011;9(1):177. doi:10.1186/1479-5876-9-177

162. Junankar S, Shay G, Jurczyluk J, et al. Real-time intravital imaging establishes tumor-associated macrophages as the extraskeletal target of bisphosphonate action in cancer. *Cancer Discov*. 2015;5(1):35-42. doi:10.1158/2159-8290.CD-14-0621

163. Huang Z, Yang Y, Jiang Y, et al. Anti-tumor immune responses of tumor-associated macrophages via toll-like receptor 4 triggered by cationic polymers. *Biomaterials*. 2013;34(3):746-755. doi:10.1016/j.biomaterials.2012.09.062

164. Michel O, Nagy A. Dose-response relationship to inhaled endotoxin in normal subjects. *Am J Respir Crit Care Med*. 1997;156(4 Pt 1):1157-1164. http://www.atsjournals.org/doi/abs/10.1164/ajrccm.156.4.97-02002. Accessed September 12, 2013.

165. Apostolaki M, Armaka M, Victoratos P, Kollias G. Cellular Mechanisms of TNF Function in Models of Inflammation and Autoimmunity - Karger Publishers. Molecular and Cellular Mechanisms. http://www.karger.com/Article/Abstract/289195. Published 2010. Accessed September 12, 2013.

166. Kolb W, Granger G. Lymphocyte in vitro cytotoxicity: characterization of human lymphotoxin. *Proc Natl Acad Sci U S A*. 1968:1250-1255.

http://www.ncbi.nlm.nih.gov/pmc/articles/PMC225248/. Accessed September 12, 2013.

167. National Vital Statistics Reports. http://www.cdc.gov/nchs/data/nvsr/nvsr61/nvsr61_06.pdf. Accessed June 12, 2013.

168. Boland C, Ricciardiello L. How many mutations does it take to make a tumor? *Proc Natl ...*. 1999;96(26):14675-14677. http://www.pubmedcentral.nih.gov/articlerender.fcgi?artid=33954&tool=pmcentrez&rendertype=abstract. Accessed August 24, 2012.

169. Hanahan D, Weinberg R. The Hallmarks of Cancer. *Cell*. 2000;100:57-70.

170. Reya T, Morrison SJ, Clarke MF, Weissman IL. Stem cells, cancer, and cancer stem cells. *Nature*. 2001;414(6859):105-111. doi:10.1038/35102167

171. Anand P, Kunnumakkara AB, Kunnumakara AB, et al. Cancer is a preventable disease that requires major lifestyle changes. *Pharm Res*. 2008;25(9):2097-2116. doi:10.1007/s11095-008-9661-9

172. Adly A. Oxidative stress and disease: An updated review. *Res J Immunol*. 2010. http://www.doaj.org/doaj?func=abstract&id=636059. Accessed August 24, 2012.

173. Gupta SC, Hevia D, Patchva S, Park B, Koh W, Aggarwal BB. Upsides and downsides of reactive oxygen species for cancer: the roles of reactive oxygen species in tumorigenesis, prevention, and therapy. *Antioxid Redox Signal*. 2012;16(11):1295-1322. doi:10.1089/ars.2011.4414

174. Thannickal VJ, Fanburg BL. Reactive oxygen species in cell signaling. *Am J Physiol Lung Cell Mol Physiol*. 2000;279(6):L1005-28. http://www.ncbi.nlm.nih.gov/pubmed/11076791.

175. Ji LL, Dickman JR, Kang C, Koenig R. Exercise-induced hormesis may help healthy aging. *Dose Response*. 2010;8(1):73-79. doi:10.2203/dose-response.09-048.Ji

176. Forman HJ, Fukuto JM, Torres M. Redox signaling: thiol chemistry defines which

reactive oxygen and nitrogen species can act as second messengers. *Am J Physiol Cell Physiol*. 2004;287(2):C246-56. doi:10.1152/ajpcell.00516.2003

177. Lee YJ, Shacter E. Oxidative stress inhibits apoptosis in human lymphoma cells. *J Biol Chem*. 1999;274(28):19792-19798. http://www.ncbi.nlm.nih.gov/pubmed/10391922.

178. Spector A. Review: Oxidative Stress and Disease. *J Ocul Pharmacol Ther*. 2000;16(2):193-201.

179. Childs, A., Jacobs, C., Kaminski, T., Halliwell, B., Leeuwenburgh C. Supplementation with vitamin C and N-acetyl-cysteine increases oxidative stress in humans after an acute muscle injury induced by eccentric exercise. *Free Radic Biol …*. 2001;31(6):745-753. http://www.sciencedirect.com/science/article/pii/S0891584901006402. Accessed August 24, 2012.

180. Leeuwenburgh C, Heinecke JW. Oxidative stress and antioxidants in exercise. *Curr Med Chem*. 2001;8(7):829-838. http://www.ncbi.nlm.nih.gov/pubmed/11375753.

181. MacIntyre D, Reid W. Different effects of strenuous eccentric exercise on the accumulation of neutrophils in muscle in women and men. *Eur J …*. 2000;81(1-2):47-53. doi:10.1007/PL00013796

182. Hilbert JE, Sforzo GA, Swensen T. Effects of massage on delayed-onset muscle soreness. *Br J Sports Med*. 2003;73(4):261-265. http://www.ncbi.nlm.nih.gov/pubmed/18847018.

183. Evans P, Halliwell B. Micronutrients: oxidant/antioxidant status. *Br J Nutr*. 2007;85(S2):S67. doi:10.1049/BJN2000296

184. Wang X, Tomso DJ, Chorley BN, et al. Identification of polymorphic antioxidant response elements in the human genome. *Hum Mol Genet*. 2007;16(10):1188-1200. doi:10.1093/hmg/ddm066

185. Honzel D, Carter SG, Redman K a, Schauss AG, Endres JR, Jensen GS. Comparison of chemical and cell-based antioxidant methods for evaluation of foods and natural products: generating multifaceted data by parallel testing using erythrocytes and polymorphonuclear

cells. *J Agric Food Chem*. 2008;56(18):8319-8325. doi:10.1021/jf800401d

186. Wilson JX. Regulation of vitamin C transport. *Annu Rev Nutr*. 2005;25:105-125. doi:10.1146/annurev.nutr.25.050304.092647

187. Rumsey S, Levine M. Absorption, transport, and disposition of ascorbic acid in humans. *J Nutr Biochem*. 1998;2863(98):116-130. http://www.sciencedirect.com/science/article/pii/S0955286398000023. Accessed August 24, 2012.

188. Block G. Vitamin C and cancer prevention: the epidemiologic evidence. *Am J Clin Nutr*. 1991;53(1 Suppl):270S-282S. http://www.ncbi.nlm.nih.gov/pubmed/1985398. Accessed August 24, 2012.

189. Chan ACAC. Partners in defense, vitamin E and vitamin C. *Can J Physiol Pharmacol*. 1993;71:725-731. http://www.nrcresearchpress.com/doi/abs/10.1139/y93-109. Accessed August 24, 2012.

190. Ju J, Picinich SC, Yang Z, et al. Cancer-preventive activities of tocopherols and tocotrienols. *Carcinogenesis*. 2010;31(4):533-542. doi:10.1093/carcin/bgp205

191. Yang CS, Suh N, Kong A-NT. Does vitamin E prevent or promote cancer? *Cancer Prev Res (Phila)*. 2012;5(5):701-705. doi:10.1158/1940-6207.CAPR-12-0045

192. Hagen TM, Aw TY, Jones DP. Glutathione uptake and protection against oxidative injury in isolated kidney cells. *Kidney Int*. 1988;34(1):74-81. http://www.ncbi.nlm.nih.gov/pubmed/3172638.

193. Ortega A, Mena S, Estrela J. Glutathione in Cancer Cell Death. *Cancers (Basel)*. 2011;3(1):1285-1310. doi:10.3390/cancers3011285

194. Balendiran, G.K., Dabur, R., Fraser D. The role of glutathione in cancer. *Cell Biochem Funct*. 2004;(August):343-352. doi:10.1027/cbf.1149

195. Goraça A, Huk-Kolega H, Piechota A, Kleniewska P, Ciejka E, Skibska B. Lipoic acid–

biological activity and therapeutic potential. *Pharmacol ...*. 2011;63(4):849-858. http://www.ncbi.nlm.nih.gov/pubmed/22001972. Accessed August 24, 2012.

196. Ramachandran L, Nair CKK. Protection against genotoxic damages following whole body gamma radiation exposure in mice by lipoic acid. *Mutat Res*. 2011;724(1-2):52-58. doi:10.1016/j.mrgentox.2011.06.002

197. Packer L. Alpha-Lipoic acid: a metabolic antioxidant which regulates NF-ÎºB signal transduction and protects against oxidative injury. *Drug Metab Rev*. 1998;30(2):245-275. http://informahealthcare.com/doi/abs/10.3109/03602539808996311. Accessed August 24, 2012.

198. Vig-Varga E, Benson E a, Limbil TL, Allison BM, Goebl MG, Harrington M a. Alpha-lipoic acid modulates ovarian surface epithelial cell growth. *Gynecol Oncol*. 2006;103(1):45-52. doi:10.1016/j.ygyno.2006.01.060

199. Na MH, Seo EY, Kim WK. Effects of alpha-lipoic acid on cell proliferation and apoptosis in MDA-MB-231 human breast cells. *Nutr Res Pract*. 2009;3(4):265-271. doi:10.4162/nrp.2009.3.4.265

200. Pack R a, Hardy K, Madigan MC, Hunt NH. Differential effects of the antioxidant alpha-lipoic acid on the proliferation of mitogen-stimulated peripheral blood lymphocytes and leukaemic T cells. *Mol Immunol*. 2002;38(10):733-745. http://www.ncbi.nlm.nih.gov/pubmed/11841833.

201. Jang M, Cai L, Udeani GO, et al. Cancer Chemopreventive Activity of Resveratrol, a Natural Product Derived from Grapes. *Science (80-)*. 1997;275(5297):218-220. doi:10.1126/science.275.5297.218

202. Jannin B, Menzel M, Berlot J-P, Delmas D, Lançon A, Latruffe N. Transport of resveratrol, a cancer chemopreventive agent, to cellular targets: plasmatic protein binding and cell uptake. *Biochem Pharmacol*. 2004;68(6):1113-1118. doi:10.1016/j.bcp.2004.04.028

203. Kitada M, Kume S, Imaizumi N, Koya D. Resveratrol improves oxidative stress and

protects against diabetic nephropathy through normalization of Mn-SOD dysfunction in AMPK/SIRT1-independent pathway. *Diabetes*. 2011;60(2):634-643. doi:10.2337/db10-0386

204. Huang D, Ou B, Hampsch-Woodill M, Flanagan J a, Prior RL. High-throughput assay of oxygen radical absorbance capacity (ORAC) using a multichannel liquid handling system coupled with a microplate fluorescence reader in 96-well format. *J Agric Food Chem*. 2002;50(16):4437-4444. http://www.ncbi.nlm.nih.gov/pubmed/12137457.

205. Garrett AR, Murray BK, Robison RA, O'Neill KL. Advanced Protocols in Oxidative Stress II. Armstrong D, ed. 2010;594(12):251-262. doi:10.1007/978-1-60761-411-1

206. Gupta-Elera G, Garrett AR, Martinez A, Robison RA, O'Neill KL. The antioxidant properties of the cherimoya (Annona cherimola) fruit. *Food Res Int*. 2011;44(7):2205-2209. doi:10.1016/j.foodres.2010.10.038

207. Packer L, Suzuki YJ. Vitamin E and alpha-lipoate: Role in antioxidant recycling and activation of the NF-κB transcription factor. *Mol Aspects Med*. 1993;14(3):229-239.